Ultrafast Dynamics and Phase Changes

in Phase Change Materials Triggered by Femtosecond Laser

QINFANG WANG

(M. Eng., South China University of Technology, P. R. China
B.Eng., Huazhong University of Science & Technology, P .R. China)

A THESIS SUBMITTED

FOR THE DEGREE OF DOCTOR OF PHILOSOPHY

DEPARTMENT OF ELECTRICAL & COMPUTER ENGINEERING

NATIONAL UNIVERSITY OF SINGAPORE

2005

Acknowledgements

There are many people whom I have interacted and worked with during my study at the Department of Electrical and Computer Engineering at National University of Singapore and Data Storage Institute that have influenced me tremendously and without whom I would not be in the program.

First of all, I would like to express my most sincere appreciation to my supervisor, Prof. Chong Tow Chong, for giving me this wonderful opportunity to work on such an interesting and challenging project. I am extremely grateful for all the support and guidance which he has extended to me throughout the project. It has been a very enlightening and rewarding experience working under his supervision.

My deepest thankfulness also goes out to Dr. Shi Luping, my co-supervisor for his patience in guiding me throughout the project and his invaluable suggestions and discussions that have given me new inspirations.

My whole-hearted thanks go to National University of Singapore and Data Storage Institute for their financial support through the Research Scholarship during my pursuit my Ph. D degree at National University of Singapore. I would also like to thank Data Storage Institute and National University of Singapore for their staff and resources during my study here.

Special thanks must also go to the many wonderful staff and research scholars at Data

Storage Institute and National University of Singapore. I am deeply indebted to Dr Miao Xiangshui, Dr Hong Minghui, Tan Pik Kee, Dr Zhao Rong, Dr Hu Xiang, Dr Huang Sumei, Dr Li Jianming, Research Engineers, Yi Kaijun, Yao Haibiao, Lim Kian Guan, Meng Hao etc. for their vast amount of help and discussions. I would also like to thank many research scholars Wang Zenbo, Chen Guoxin, Lan Bing, Lin Ying, Yang Hongxin, Wei Xiaoqian etc. for their help and encouragement.

Table of Contents

Summary

Phase change optical disk is one important type of rewritable optical disk available nowadays. It takes advantage of the fact that Phase change materials have different optical indices in their crystalline and amorphous states, leading to different reflectivity. Data transfer rate is one of key issues in optical data storage and is highly dependent on the crystalline and amorphous phase transition time. Femtosecond laser is very attractive for optical data storage. If femtosecond laser can induce reversible phase transition in phase change media, it may greatly increase date transfer rate.

This study investigated the interaction of femtosecond laser with phase change optical data storage media. The static experiment setup was employed to determine whether a single femtosecond laser pulse could induce amorphous or crystalline mark in phase change media or not. In order to investigate the nature of electronic and structural changes induced by femtosecond laser pulse, a time resolved microscopy with femtosecond resolution and micrometer spatial resolution was developed to measure transient surface change after femtosecond laser irradiation. Because optical band gaps of phase change media are fundamental for understanding the mechanism of carrier excitation and relaxation after laser irradiation, they were calculated with refractive index which was measured with Steag etaoptic ETA-RT quality control systems for compact disc production.

Refractive index measurement indicates that GeSbTe and AgInSbTe has an indirect

optical band gap approximately 0.6~0.7 eV. The static experiment shows that ultrafast crystalline and amorphous phase transformations triggered by femtosecond laser pulse in GeSbTe films could be achieved by proper control of the heat flow conditions imposed by film thickness. In thick films such as those of 100 nm thickness, crystalline to amorphous and amorphous to crystalline phase transitions triggered by femtosecond laser were observed. Using time resolved microscope, it was observed that a transient non-equilibrium state of the excited material in phase change media after femtosecond laser irradiation was formed in picoseconds time scale.

Our experiments show that even a single femtosecond pulse can induce and erase an amorphous mark in GeSbTe films. An electronically induced non-thermal phase transition is suggested to be the mechanism of these ultrafast phase transitions. Our results might provide the possibility of achieving a data transfer rate higher than 1 Tbit/s.

List of Figures

List of Tables

Chapter 1 Introduction

1.1 Optical data storage

We are in an information age. The demand for high performance, low cost and nonvolatile information systems is ever-increasing. Genarally speaking, there are three major types of storage technology, i.e., solid-state memory, magnetic data storage and optical data storage. Each of them has its own advantages and disadvantages.

Solid state memories, which have high-speed and compact size, are mainly used as internal memories, while magnetic and optical storage devices are typically used as secondary storage device for computer systems. Hard disk drives, which are the primary type of magnetic storage devices, have high cost-performance and high growth rate in area density. They have been and remain the device of choice for secondary storage device in computer systems. Optical storage devices, since the first introduction of audio compact disk player in the early 1980's [1], have undergone numerous progress in read-only optical data storage such as Compact Disc-Read Only Memory (CD-ROM), Laser Disk (LD), Digital Versital Disk (DVD)-Video, DVD-ROM, DVD-Randon Access Memory (RAM), DVD-Recordable (R) and Blue-ray Disk (BD)-ROM. Due to their unique feature of large capacity, long life-time,

removability, low cost and non-contact data retrieval [2], optical discs are widely used in multimedia to store digitized audio, video, animation and images.

Several kinds of write-once optical discs have been developed during the past two decades, namely WORM (Write Once Read Many), CD-R and DVD-R. These types of disks are mainly used for archival purposes to store permanent information, such as medical record, legal document. However, these kinds of disks can be written only once.

To meet the rewritable requirement, several types of rewritable optical disks, such as CD- Rewritable (RW) and DVD-RAM has been introduced. Because the data can be rewritten many times, rewritable optical discs can be used as the peripheral data storage device in computer systems.

There are mainly two kinds of techniques in the rewritable optical discs. One is magneto-optical (MO) recording [3] which is based on small polarization rotations of light reflected from different directions (upward or downward) of magnetic domains to distinguish recorded data bits. Another one is phase-change recording (PC) which takes advantage of the fact that PC materials have different optical indices in their crystalline and amorphous states, leading to different reflectivities. Over the last decade, the race between the technology of MO recording and PC recording has spurred the technological advancement of rewritable optical disc.

In today's consumer market, DVD uses PC technology, while mini-disk (MD) uses MO technology. PC technology has many advantages that make it attractive. PC

technology [1] [2] needs an optical head with few components, which makes the alignment easy and a compact integrated optical head practical. PC technology also has higher carrier-to-noise ratio (CNR) than MO technology because the magnitude of the PC signal is several orders higher than that of MO signal. Furthermore, direct overwrite can be achieved by laser modulation in PC technology. And PC disc drivers are compatible with existing CD-ROMs and CD-Rs because they are all based on the reflective difference of amorphous and crystalline phase of the PC media. Table 1.1 summarizes the characteristics of two technologies as compared to CD-ROM [1][2][3]. It is apparent that PC technology is playing more and more important role in optical data storage.

Table 1-1 Technology comparisons of CD, phase-change and MO disks

Term	CD Disk	Phase-change Disk	MO Disk
Read/write head	Optical head	Optical head	Optical head and Magnetic head
Write mechanism	Emboss-Pit	Amorphous mark	Magnetization domain
Reading mechanism	Diffraction	Refraction index change	Polarization Change
Signal Detection	Reflectivity change	Reflectivity change	Kerr Rotation change
Normalized Signal Amplitude to CD-ROM	1.0	¼	1/80
Disk track structure	λ/4 emboss-pit	λ/8 pre-groove λ/4 emboss-pit	λ/8 pre-groove λ/4 emboss-pit
Substrate materials	Polycarbonate	Polycarbonate	Polycarbonate
Reflection layer	Al-alloy	Al-alloy	Al-alloy
Active layer		GeSbTe	TbFeCo
Dielectric layer		ZnS-SiO2	SiN
Function	Read-only	Overwrite	Overwrite

In PC optical disk, recording and erasing are achieved by the crystallographic structural changes of thin films heated by a laser pulse. The reproduction of recorded information takes the advantage of the fact that PC materials have different optical indices in their crystalline and amorphous states, leading to different reflectivities.

Density, data transfer rate and overwrite cycle are the three most important parameters in PC optical data storage. Recording density is related to mark size. The smaller the mark size, the higher the recoding density. There are many methods to increase the recording density such as short wavelength, large numerical aperture (NA), mark edge recording, land and groove recording, dual layers recording, multilevel recording, near-field recording and super resolution near-field system (Super-Rens).

The maximum data transfer rate that can be achieved in PC optical data storage is highly dependent on the phase transition speed of phase change materials. By increasing the linear velocity of the disc and reducing the laser pulse duration, the dwell time of the laser spot decreases, leading to a shorter energy deposition time for phase transitions.

Overwrite cycle is related to PC materials and structure. Repeated melting, crystallization and amorphization of PC media result in material segregation, stress buildup, microcrack formation etc. These factors tend to reduce the data reliability and cyclability of PC media.

1.2 Motivation of the project

With the increasing usage of multimedia, PC rewritable optical discs are becoming more and more popular nowadays due to their CD and DVD compatibility. Many effects have been done to increase density, data transfer rate and overwrite cycle. This project will focus on the data transfer rate, which is highly related to phase transition time of phase change media.

In conventional phase change optical disk, recording and erasing are achieved by laser pulses emitted from semiconductor laser diodes with nanosecond duration that thermally induce crystallographic structural changes in the phase change media, thus limiting the data transfer rate to megabyte per second. Furthermore, thermal diffusion is one of the fundamental limitations in the conventional phase change optical disk which uses rather long pulse duration of 10 ns to 60 ns. Thermal diffusion will not only make the mark size wider than laser spot size which reduces recording density, but also deform the disk layer.

A short pulse is believed to be very promising for optical data storage due to its efficient delivery of optical power and extreme suppression of the thermal diffusion effect. Intense femtosecond (10^{-15} s) laser can excite a dense electron-hole population in semiconductors, which causes the materials in the most extreme non-equilibrium conditions and gives rise to novel and unusual phase transitions. Nonthermal phase transitions induced by femtosecond pulse have been reported in many materials such as Si [5][6][7], GaAs [8][10][11][12][13], GeSb [14], InSb [15]. If femtosecond pulse

can induce crystalline to amorphous and amorphous to crystalline phase transitions in phase change media, it might greatly increase data transfer rate to terabyte per second. Motivated by its potential prospect in phase-change optical data storage, considerable effort has been contributed to the interaction of short laser pulse with phase-change media for both fundamental studies and application [13][16][17][18][19][20][21][22] [23][24]. Electron diffraction [16][17][22] clearly shows that nano-, pico-, and femtosecond pulses above a certain threshold fluence (F_{cr}) transform amorphous GeSb permanently to a stable crystalline phase. F_{cr} exceeds the fluence F_m required for melting, and for fluence between F_{cr} and F_m, the material reamorphizes on solidification. Jolis ***et. al.,*** [18] investigated the threshold crystallization energy density of amorphous GeSb films as a function of the laser pulse duration in the range from 170 fs to 8 ns. They found that enhanced crystallization occurs for pulse shorter than 800 fs and proposed that the crystallization mechanism is electronically enhanced crystallization for pulse shorter than 800 fs. K. Sokolowski-Tinten [8] used time resolved imaging to study structural transformations induced by intense 100 fs laser pulses in amorphous GeSb films and found the formation of a transient nonequilibrium state of the excited material within 300 fs. Callan [13] used time-resolved measurement of the spectral dielectric function to investigate femtosecond laser induced phase transition in amorphous GeSb and proposed an ultrafast phase transition from amorphous phase to another disorder state within 200 fs after excitation by intense femtosecond pulse. Ohta and co-workers [24] first studied the interaction of femtosecond laser pulse with ternary alloy of GeSbTe. They reported that single 120 fs laser pulse could induce an amorphous mark at crystalline

background accurately in the laser spot without the crystalline edge in GeTe-Sb_2Te_3-Sb sandwich structure. However, whether femtosecond pulse can induce crystalline to amorphous phase transition in other phase change materials or amorphous to crystalline phase transition in phase change materials or not has never been investigated yet.

Furthermore, it is also very important to understand the mechanism of the phase transitions in phase change media in order to increase data transfer rate. Fundamental physical and chemical processes involving hot carriers, such as carrier and lattice dynamics, occur on timescales of femtosecond to picosecond. Femtosecond laser can afford high temporal resolution for observation and study of these fundamental processes. Thus the focus of this thesis is the interaction of femtosecond laser with phase change media.

1.3 Objectives

The present study focused on the interaction of femtosecond laser with PC media. The main objectives were:

- To investigate the possibility of ultrafast phase transitions in GeSbTe media triggered by single femtosecond pulse with a self-built static experiment setup.
- To study the mechanism of the ultrafast phase transformations in GeSbTe by real time measurement of transient reflective intensity with time-resolved microscopy[25] which has femtosecond time and micrometer space resolution.

- To study the interaction of femtosecond laser with superlattice-like structure to elucidate the phase transitions triggered by femtosecond pulse and reveal the mechanism of the ultrafast phase transformations.

These three topics are very important to PC optical data storage. The static experiments will show whether femtoseond pulse can induce any phase transition in PC media or not. The real time reflective intensity measurements will be important for understanding how the energy is transferred from photon to carriers, and then from carriers to lattice. It may also reveal the mechanism of the ultrafast phase transitions such as whether it is thermal or non-thermal. It can be used to improve data transfer rate of optical data storage via designing the PC media composition and multilayer structure to shorten the phase transition time. Our study could provide possible access to achieve 1 terabyte per second date transfer rate.

1.4 Organization of the thesis

The second chapter of this thesis will begin with a brief introduction to the development of phase change optical data storage followed by a discussion of the media used in phase change optical data storage. The principle of phase change optical data storage will be demonstrated. And the techniques and prospects of phase change optical data storage will be presented in the end of the chapter.

Chapters 3-6 are the core of the thesis. Our femtosecond laser system will be introduced in the beginning of chapter 3. Then the two experimemtal setups will be

presented. Chapter 4 will describe femtosecond pulse induced phase transitions in phase change media and chapter 5 will present the ultrafast dymanics in phase change media triggered by femtosecond pulse. Whether single femtosecond pulse can induce ultrafast phase transition in superlattice-like phase change media will be investigated in chapter 6.

This thesis will end up with a summary of all the results obtained and the potential future work.

Chapter 2 Phase change optical data storage

With the increasing usage of multimedia, phase-change optical disks are becoming more and more popular. In this chapter, the principle of phase change optical data storage will be introduced first, followed by the development of phase change optical data storage media. Then the two widely used phase change media will be discussion. The typical phase change disk structure and key performance parameters will also be presented. The chapter ends up with an outlook of the future trends in phase change optical data storage.

2.1 Principle of phase change optical data storage

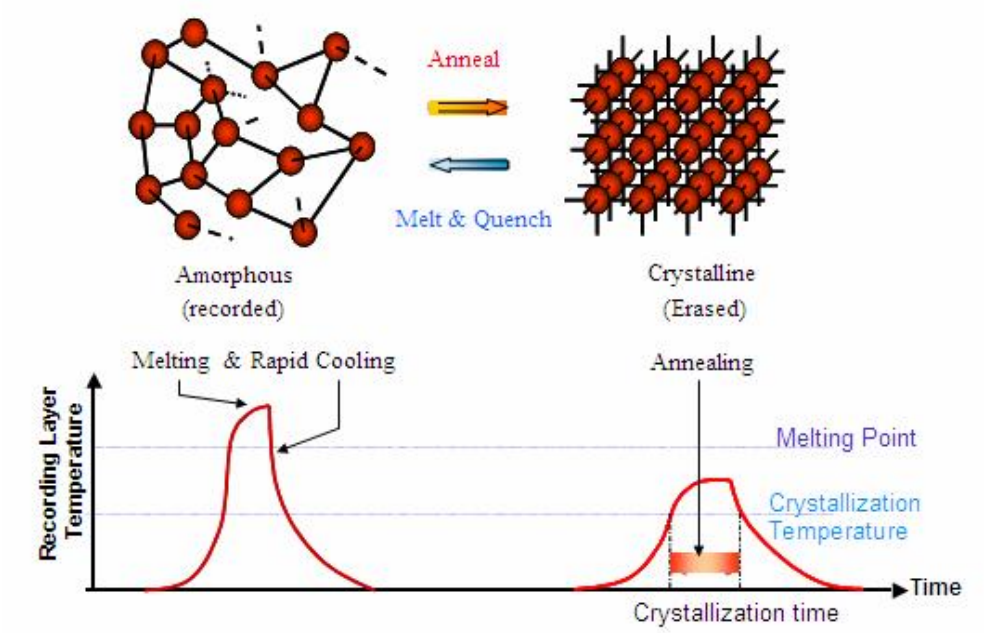

Figure 2.1 Principle of phase-change recording and temperature profile of the recording layer in writing and erasing process.

The principle of phase change optical data storage [27] is based on the concept that some physical property of microscopic area of recording layer on disc surface is altered due to crystallographic structure changes when the films are irradiated by laser pulses. The reproduction of the recorded information takes the advantage of difference in reflectivity due to the difference in refractive index between two phases (Figure 2.1).

Although there may be two types of phase changes: one is between amorphous and crystalline phases and another is between two different crystalline phases, the materials used in phase-change optical disks are only the amorphous-crystalline type.

Before recording data on the phase change optical discs, the as-deposited amorphous films have to be initialized to the crystalline state. In the writing process (Figure 2.1), the amorphous state is achieved by heating the phase change thin films with sufficient laser power to melt the material over its melting point and then being rapidly quenched to room temperature. As the atoms in melting state are in disordered state and the cooling rate of the area irradiated by laser pulses is very high, the time is not sufficient for the atoms to be arranged into order structure; thus amorphous mark are formed. The absolute minimum quenching rates required for amorphization are different for various materials, ranging from 10^7 to 10^{11} deg/s.

In the erasing process (Figure 2.1), the crystalline phase is realized by annealing the phase change films at the temperature between crystallization temperature T_c and melting point T_m with a medium power laser irradiation. During the irradiation period, the atoms of phase-change media are rearranged into the ordered structure; thus amorphous region can be changed to the crystalline state.

The phase-changes in the phase-change optical discs are accomplished by using the irradiation of laser light, which typically have a diameter in the order of 1 μm. When a laser beam having a 1 μm diameter traces on the recording thin films at a linear velocity of 10 m/s, as shown in Figure 2.2 (a) irradiation time of a point on the films is only 100 ns. Hence, the energy deposition time is within this time duration. The recorded mark of optical disc is normally smaller than the laser beam size, this is because of the Gaussian distribution of the laser beam. Figure 2.2 (b) shows the gaussain distribution of laser beam.

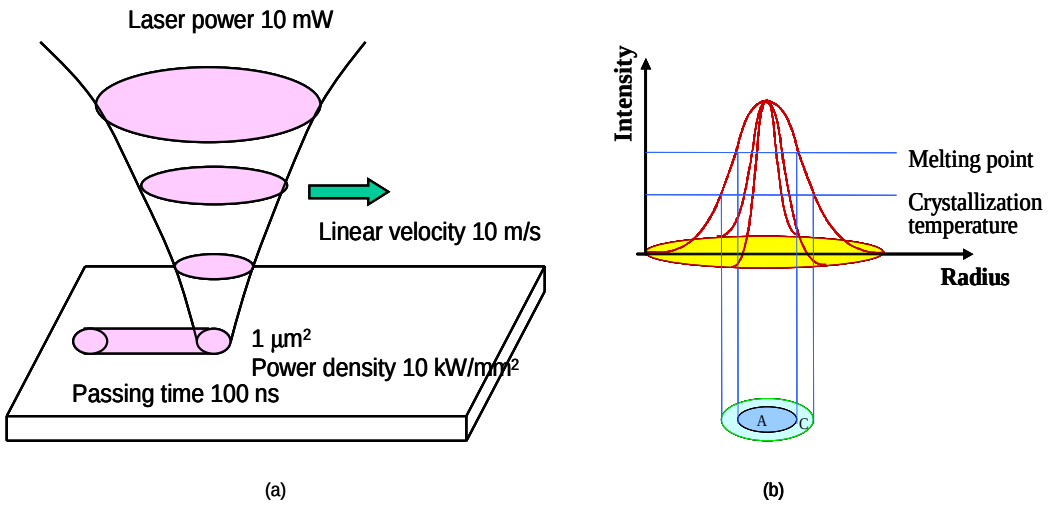

Figure 2.2 (a) Schematic representation of optical recording. (b) Gaussian beam distribution of laser beam in optical recording (A refers to amorphous phase and C refers to crystalline phase).

Assuming that the laser power is 10 mW, the power density of the light spot is up to the order of 10 kW/mm^2. It is possible to shorten the energy deposition time for amorphizion, because the amorphizion is achieved by the melting and quenching process. However, the crystallization process requires a time duration determined by the physical characters of the material because during crystallization the atoms or molecules are re-arranged. In other words, each material has its own crystallization speed. Consequently, the materials

for phase-change optical disks are required to have not only the high thermal stability of the amorphous state but also a high crystallization speed to enable that the rearrangement process of atoms can be realized within the energy deposition time of 100 ns.

The direct overwriting is a common performance in magnetic recording. However, it is an issue for optical recording due to heating mode technology in current optical recording.

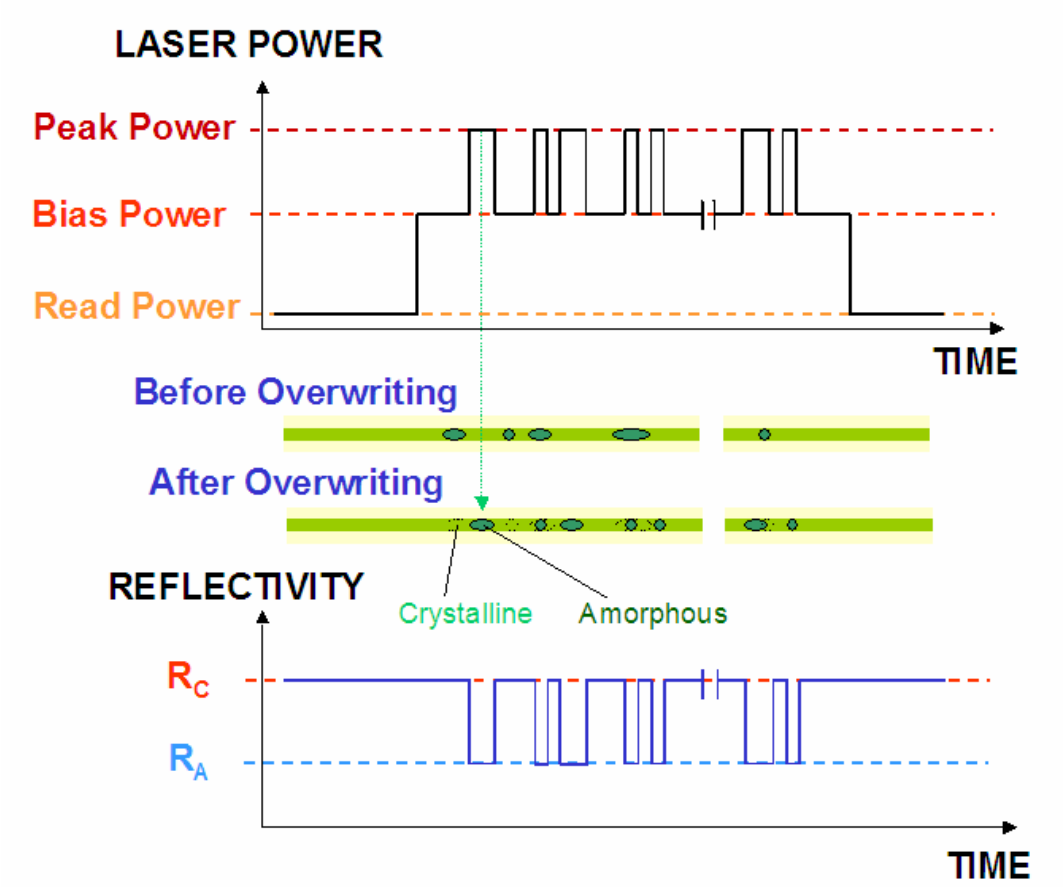

Figure 2.3 Overwriting methods of phase-change optical recording.

If a thin film material has sufficiently high crystallization speed and the atoms can be rearranged with a short duration time of the laser beam, the direct overwriting can be

accomplished by laser power modulation between a peak recording power level and a bias erasing level as shown in Figure 2.3 [28]. Before overwriting, there are some amorphous or recorded spots on the track. When peak power laser is applied, it raises the temperature to above the melting point and quenches rapidly so that an amorphous mark is written on the same track. These amorphous marks are formed on the original spots of either amorphous mark or crystalline phase. When the bias power laser is applied, it heats up the phase-change media to a temperature between the crystallization temperature and the melting point so that crystalline phase is formed. This overwrite method shows that no matter whether the phase is amorphous or crystalline before overwriting, films irradiated with the peak power become amorphous phase, and those irradiated with bias power are changed to crystallize phase.

2.2 Development of phase change optical data storage media

Phase change (PC) optical disk is one important type of rewritable (RW) optical disk available nowadays. When selecting a suitable material for the erasable phase-change recording layer, there are several important factors that must be considered:

1) Optical constants. The material must be chosen such that it has enough absorption that shifts in the visible or near-infrared region with phase transitions. Hence, metals and insulators are eliminated, leaving only semiconductors. Amorphous semiconductors [29] which have limited long-range periodic order possess optical

behaviors that are far from their crystalline counterparts.

2) Melting point. Because the material must be melted by laser power, the melting point cannot be too high. However, if it is too low, self-crystallization may occur, resulting in the amorphous phase unstable at room temperature. Hence, the materials are limited to those with melting points in the range of 500~1000 °C and glass transition temperature about 1/2 to 2/3 of the corresponding melting point.
3) Crystallization speed. The faster the speed at which the phase-change material crystallizes, the shorter the erasing time. To achieve rapid crystallization, the materials should have: (a) large atomic mobility in the amorphous and supercooled states and (b) short atomic diffusion distance from the atomic location in the amorphous state to the lattice sites of the crystalline state. Atomic mobility is controlled by the viscosity of the supercooled liquid. Generally speaking, a weak bond indicates a low viscosity force among atoms, which increases atom mobility and crystallization speed.
4) Read/write cyclability. The materials should be transformed between amorphous and crystalline phase for many times. Usually, the materials without phase separation during the reversible phase transitions should have good read/write cyclability.

Research on phase change optical data storage media began many years ago. In 1968, S. R. Ovshinsky [30] discovered a rapid and reversible transition between a highly resistive (disorder structure) and conductive state (order structure) in chalcogenide materials due to the reversible phase transition between amorphous and crystalline phase induced by an electric field. This order-disorder memory phenomenon was later called as “Ovonic

memory".

Soon later, a laser optical memory phenomenon in chalcogenide materials was observed by Feinleib [31]. High speed and reversible phase transitions between amorphous and crystalline phase could be triggered by short laser pulse in $Te_{81}Ge_{15}Sb_2S_2$ composition material, which led to a sharp change in optical reflection and transmission because of different refractive index of amorphous and crystalline phases.

In developing the phase change optical data storage medium, the main issues are the stability of the film materials, the stability of the reversible cycle characteristics and overwrite function. Because amorphous chalcogenide materials are not stable at room temperature due to the rather low glass transformation, for example, the glass transformation of tellurium is ~10 °C [32], the search of potential materials for phase change optical data storage had mostly been based on one approach: alloy chalcogenide materials with other elements to achieve desired properties. A familiar example of this approach is doping Ge and As with Te [33][34] to increase the stability of the amorphous phase at room temperature and to determine their feasibility as phase change optical storage media. However, these media showed limited reversibility as only 10-20 write/erase cycles were achieved. This poor reversibility was due to the irreversible formation of a phase mixture comprising of telluric microcrystals and amorphous chalcogenide glass as well as to an irreversible destruction of the filmsby hole formation. Furthermore, the light energy required to obtain a definite degree of crystallization changed as the number of cycles increased [34]. This aging effect further limited the usage of these media as phase change optical data storage media.

Bell [35] suggested that hole formation could be restrained by encapsulation with a capping layer. He demonstrated 50 write/erase cycles of pure tellurium films without any hole formation or impairment of the optical signal.

Great progress was made in 1983 by Clemens [36]. By using low-doped Te films ($Te_{96.8}As_{3.0}Ge_{0.2}$) with thick capping layers, he realized a reversible optical storage with over $4x10^4$ possible write/erase cycles. In the same year, Takenaga et al. [37] claimed 10^6 write/erase cycles on a disk with 55 dB carrier-to-noise ratio (CNR) using a tellurium-oxide-based active layer. The amorphization was easily achieved and the data stability was longer than 1 year. However, the erasion time was longer than 1 us and the observed optical property changes were mainly due to the segregation of Te from TeO_2 matrix [37] which had an adverse effect on the reversibility of the TeO_x based optical recording media. Furthermore, Te segregation from TeO_2 matrix caused nucleation and crystal growth, resulting in undesirable effect on the read back signal after recording.

In 1985, Chen et al. [39] demonstrated for the first time that as-deposited amorphous $Te_{87}Ge_8Sn_5$ films could be optically switched between the crystalline and amorphous states more than 10^6 times. The reversibility was not limited by phase segregation, but by ablation. The medium had high crystallization temperature and hence long data retention time. But for optical data storage application, the minimum erasure time should be reduced and the crystallization temperature should be further increased. One year later, Chen [40] investigated the laser induced and heating induced crystallization of $Te_{1-x}Ge_x$. They found that films with compound compositions, Te and GeTe, can be crystallized using laser pulses of less than 100 ns duration. Furthermore, GeTe had a crystallization

temperature of 170 °C, which implied long-term data stability. They argued that choice of compound materials which did not require phase separation upon crystallization could results in sub-100 ns erase speeds. If the compound materials have high glass transition temperatures and sufficiently high melting temperature, the fast-switching capability, from the amorphous to the crystalline state and backward, can be achieved simultaneously with long-term data (amorphous phase) stability. This allowed a much simple optical head with single-laser beam to be used for both writing and erasing and the feasibility of the phase change optical recording system was greatly enhanced.

In 1991, Yamada [40] found that stoichiometric compositions on the GeTe-Sb_2Te_3 pseudobinary line, $GeSb_2Te_4$ and $Ge_2Sb_2Te_5$, were good candidates for PC media in optical data storage. They had large optical contrast between the amorphous and crystalline phases. When sandwiched by heat-conductive ZnS layers, these materials can be transformed rapidly and reversiblely between the amorphous and crystalline phases by laser irradiation with very short duration, less than 50 ns. The quick amorphization is due to extremely high cooling speed of the sandwiched films: ~10^6 deg/s, which permits the molten materials to solidify while keeping the atomic distribution of the liquid state. The fast crystallization is attribute to their two-step crystallization processes [42][43][44]. When the amorphous phase of stoichiometric compositions on the GeTe- Sb_2Te_3 pseudobinary line is crystallized into a stable hexagonal (HEX) structure at high temperature, it first transforms into a metastable face-centered cubic (FCC) structure at lower temperature. The metastable FCC structure has a high symmetric isotropic structure similar to that of amorphous structure and crystallization from amorphous to FCC structure occurs without phase separation of the stoichiometric compositions.

Atoms need to travel only short distance from the amorphous phase to FCC crystalline lattice. This allows the fast crystallization of stoichiometric compositions on the GeTe-Sb_2Te_3 pseudobinary line from amorphous to FCC crystalline phase.

AgInSbTe system was first proposed in 1992 by Iwasaki *et al.* [45] as a completely erasable phase change material. This material has many advantages, especially in pulse width modulation recording, such as high erasability and high controllability of mark length. They suggested that the narrow widths of the written marks and no large crystalline grains in the periphery of the written marks were the major causes for the high erasability. Thus AgInSbTe based PC media could also be used in high density rewritable disc systems [46].

Other significant developments in phase change media include that In-Se-Tl media reported by T. Nishida [47] in 1987 had a short crystallization time of 0.2us and In_3SbTe_2 presented by Maeda [48] in 1988 had reversible cycles above 10^5. All of these media are good candidates for phase change optical data storage with high-speed erasing and long-term data stability. Furthermore, all these media can be overwritten directly with a single laser beam.

2.3 Media widely used in phase change optical data storage

Many materials, such as In-Sb, Ag-Zn, In-Sb,Ge-Sb-Te, Ge-Te-Sn, Sb-Se-Te, Ga-SeTe, In-Sb-Te, Ag-In-Sb-Te etc, have been reported to be potential candidates for phase-

change optical data storage [49]. Among all kinds of phase-change materials, stoichiometric compositions along GeTe-Sb_2Te_3 pseudo-binary line (here referred to as GeSbTe) and quaternary AgInSbTe alloys are widely used in phase change optical data storage. GeSbTe materials possess both the stability of the amorphous states and the high crystallization speed [41]. Rescent research [50] showed that crystallization and amorphization processes in GeSbTe do not required the rapture of strong covalent bonds and the transition is diffusionless. The reversed transformations could achieve easily because te sublattice is partially preserved and the local structure around Sb is conserved.

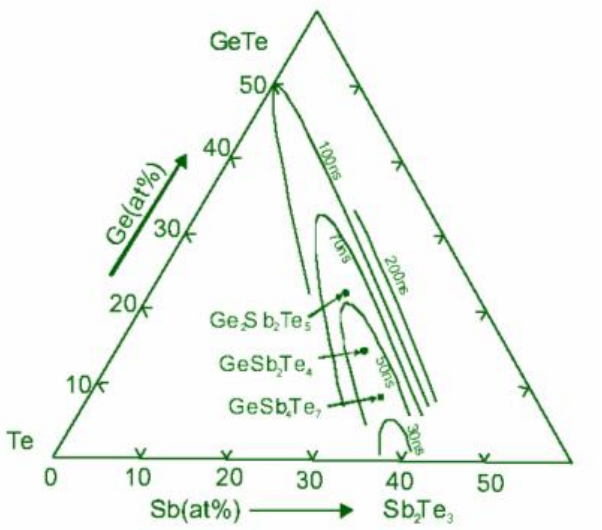

Figure 2.4 Composition dependence of the minimum laser-irradiation duration to cause crystallization in 100nm thick Ge-Sb-Te films sandwiched between 100nm and 200nm thick ZnS layer.

Figure 2.4 gives an indication of the minimum laser pulse duration required for crystallization of various compositions in the GeSbTe system [41]. These compositions show good overwriting characteristics. Because no phase separation occurs at stoichiometric compositions, compositional deviations are minimized as phase changes

are cycled. The properties of these compounds are shown in Table 2-1 [51].

Table 2-1 Properties of pseudobinary GeTe-Sb_2Te_3

Composition	Crystallization temperature (°C)	Activation energy (eV)	Melting point (°C)
$Ge_2Sb_2Te_5$	142	2.23	616
$GeSb_2Te_4$	131	1.82	614
$GeSb_4Te_7$	123	1.52	607

Quaternary AgInSbTe alloys [45][52][53] are also widely used in phase change optical data storage because they can be completely erased and the mark length can be easily controlled. AgInSbTe alloys also have low jitter [52][53] which can be attributed to the mechanism by which amorphous marks are erased, i.e., via growth of the crystalline edge towards the mark center, resulting in marks with well-defined edges. The nature of this re-crystallization process also has an effect on the time required to erase marks of different size: the minimum laser pulse duration required to erase amorphous marks decreases with decreasing mark size. As a result, the maximum data rate of a particular AgInSbTe recording stack increases with decreasing laser spot size.

2.4 Disk Structure of Phase-change Optical Disk

Figure 2.5 shows the typical structure of a phase-change optical disk of quadra-layered thin films on the polycarbonate substrate. The phase change layer is sandwiched by two dielectric protective layers made of Zn-SiO_2, and a reflective layer made of Al alloy. The design of the individual layer thickness and the choice of material used are very important in the manufacture of phase-change optical disks due to the following reasons:

- Optically, the layers are required to have large absorption efficiency of laser light and large signal amplitude corresponding to the reflectivity difference between the amorphous and crystalline states.
- Thermally, heating efficiency and rapid quenching condition for amorphization have to be balanced and met by the disk structure design.
- Mechanically, the disk should withstand the thermal stress caused by the repeated heating and quenching cycles [54].

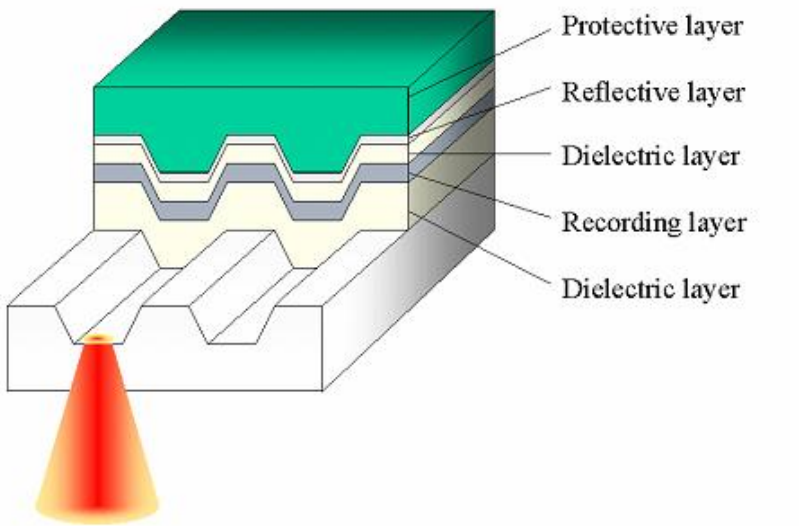

Figure 2.5 The structure of a typical phase-change optical disk.

The protective dielectric layers and reflective layer have following functions:

- Mechanical protection against humidity and prevention of thermal damage to the substrate.
- Optical enhancement of reflectivity difference between amorphous and crystalline phases.

- Controlling thermal condition during the recording and erasing processing.

For the reflective layer, the material should have properties that allow it to act as a mechanically protective layer and as a reflector. As a heat sink, it prevents thermal damage of the substrate as well as promotes rapid cooling of the phase-change layer by quenching it into the amorphous state during writing cycles. It also acts as a reflector of the laser light so as to achieve high sensitivity for measurements to attain the necessary CNR value.

The dielectric layer is made of the ZnS-SiO_2 compound. ZnS has a large refractive index of 2.4 which permits better laser spot size resolution while its high melting point of 1700 °C ensures that it is not melted by the laser heat. SiO_2 is added into ZnS to make an amorphous like structure with smaller grain size and to decrease its internal stress and reduce degradation on heating cycles of phase-change recording. ZnS-SiO_2 does not show grain growth phenomena even after 700 °C annealing and is therefore a thermally stable protective layer for phase-change optical disks, which allows millions of read/write cycles of phase change layer.

The lower layer is designed to be relatively thick to impede heat diffusion from the phase-change layer to the substrate. This is because the heat dissipated from the recording layer must not be allowed to damage the substrate, which has a lower tolerance for heat. In addition, this layer provides anti-reflection and also functions to couple more laser lights into the active layer to ensure sufficient quantity of heat in the recording spot of the films during writing.

The upper layer is designed to be relatively thinner to allow the heat generated from the recording layer to dissipate through it quickly to the top metallic layer in order to achieve a rapid cooling effect. Thus, a thin layer improves the writing characteristics as the temperature of the melted recording spot can be decreased rapidly after writing, which allows the written spot to amorphize quickly.

A rapid quenching structure has been proposed to withstand the thermal stress caused by the repeated heating and quenching cycles. In this rapid quenching structure, the phase-change, as well as the dielectric layer between the reflective and phase-change layer are deliberately made thin. This will allow the thermal energy produced in the recording phase-change layer to be diffused rapidly, leading to less damage to the other layers.

As a result, it was reported that a million cycles of overwrite has been achieved [54]. The life spans of the phase-change optical disks have also been investigated and have been found to be sufficiently long for practical use. From an accelerated aging test, the life spans were estimated to be more than 60 years in the environment of 32 °C and 80% relative humidity.

Consequently, the degradation of the protective layer during heating cycle of phase-change recording is fairly reduced, enabling the possibility of overwriting cycles in the order of millions of times.

2.5 Techniques for phase-change optical data storage

Numerous technologies have been introduced to improve the performance of the phase-

change optical data storage: (1) to achieve higher recording density [55]; (2) to increase the data transfer rate; (3) to achieve long overwrite cycle. Advancement has been made in the area of optical system, coding/modulation, disc structure, and signal processing scheme. Many kinds of methods have been proposed, such as land/groove recording, shorter laser wavelength recording, near-field phase-change optical recording, multilevel phase-change recording and super-resolution near-field (super-RENS) phase-change optical recording, dual layers recording etc. The most promising techniques will be discussed in the following section.

2.5.1 Land/Groove Recording

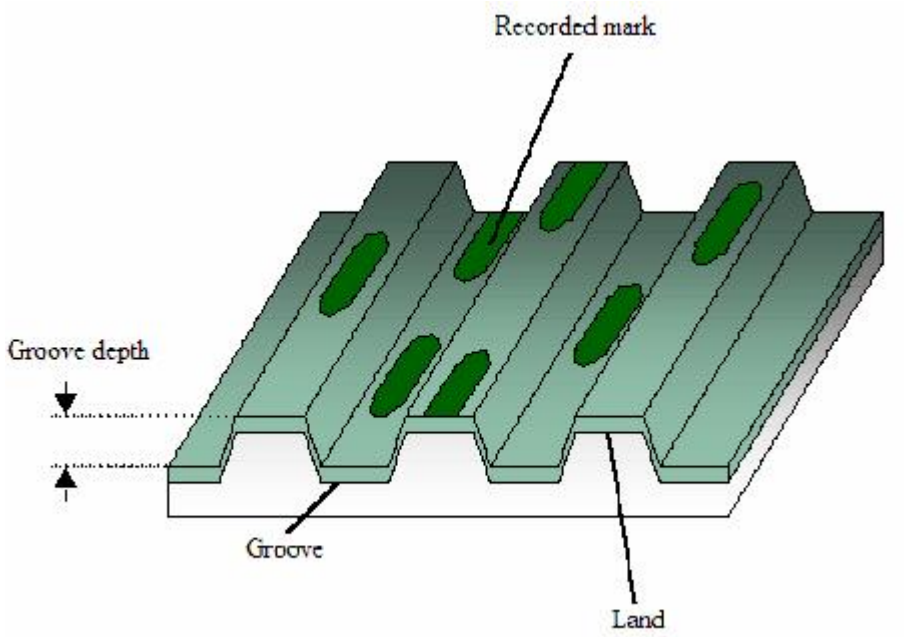

Figure 2.6 Schematically show the land and groove recording method.

In the early rewritable phase-change discs, marks were recorded only on the grooves, whereas the lands served as the guides for tracking and the suppression of heat flow from

the adjacent groove tracks. Recording on both the land and groove area is one of the simplest methods for doubling the track density [56][58], as shown in Figure 2.6. Both the land and groove have similar widths and are available for recording. The advantages of this recording method are as follows:

- Doubling track density with conventional optical heads and drivers
- Compatible to conventional disk fabrication process.

However, this track density doubling leads to the problem of two forms of interference between adjacent tracks, namely optical cross-talk and thermal cross-erasure [59]. The former occurs as a result of the interference of light reflected from both the land and groove areas during reading. The latter arises due to excessive heat flowing from the laser-irradiated area, for example, the groove area to the land area, resulting in an existing spot there to be erased.

2.5.2 Shorter Wavelength Recording

Optical pick-up systems with coherent light sources of short wavelength and high numerical-aperture (NA) objectives are essential to improve resolution because the light beam spot size is determined by the diffraction limit which is approximately $0.6\lambda/NA$.

Currently GaN blue laser diodes [60][61][62] with the wavelength of 405 nm, an output power over 50 nW and a lifetime over 3000 h are available and used for phase-change optical data storage. The numerical aperture is 0.85. The cover layer is 0.1 mm and the substrate is 1.1 mm. The data bit length is 103 nm, which gives rise to approximately 27

GB of formatted user capacity for a single side 120 mm-diameter disk.

The storage capacity can be further increased by using shorter wavelength lasers or objective lenses with a higher NA, or a combination of both. The development of shorter wavelength laser light or objective lenses with a higher NA will be inevitable in the pursuit of high-density recording in the near future. For a better understanding of the respective characteristics of the three important phase-change media (CD, DVD and BD), it will be instructive to compare them as shown in Table 2-2.

Table 2-2 Technology Comparison of CD, DVD and BD

	CD	DVD	BD
λ (nm)	780	650	405
NA	0.45	0.65	0.85
Cover (mm)	1.2	0.6	0.1
Capacity (MB)	650	4.7	27
Data rate (Mb/s)	1.2	11.2	36

2.5.3 Near-field Phase-change Optical Data Storage

The data density of the optical recording disc is mainly dependent on the light beam spot size. In conventional optical recording system, the beam spot size, which is fundamentally limited by the optical diffraction limit, can be reduced by using a light source with shorter wavelength or an objective lens with larger NA. Currently, a Blu-ray DVD disc has a high storage capacity of 27 GB. But further capacity expansion is restricted by the NA of objective lens and the availability of short wavelength light source.

Near-field optical technique is one of the promising candidates showing a possibility for realizing ultra-high density over the diffraction limit. This method is based on the usage of an optical near-field generated from a sub-wavelength aperture. The near-field optical system, which makes use of the solid immersion lens (SIL), is very attractive for ultra-density optical data storage. It can obtain a 360 nm optical spot size with 830 nm light [63] and reading and writing of data are achieved at a density of 3.8×10^8 bits/cm^2 with a data rate of 3.3×10^6 bits/s. Using a SIL made from n=1.83 glass, it achieves a 317 nm spot size with 780 nm light and a 125 nm focused spot size with blue light [64]. If the objective lens is mounted on a slider in the near field optics, similar to the magnetic head in a hard disk, a single-layer capacity of 60–100GB might be possible with numerical aperture of 1.4 or even 2.

Another approach which goes beyond the optical diffraction limits and realizes ultra high-density optical data storage is super-resolution near-field structure (super-RENS). As first proposed by Tominaga *et al.,* [65] in 1998, it employed a thin mask layer (Sb) and modified the distance between the mask layer and recording layer to integrate optical near-field and super-resolution techniques into one disk. A small aperture produced in the mask layer can operate as an optical near-field probe similar to a scanning near-field optical microscope (SNOM) in the readout process. Super-RENS is a new technique for recording and retrieving small marks beyond the optical diffraction limit, rather than by using a laser with shorter wavelength or an objective lens with higher numerical aperture (NA).

Later, a new mask material was proposed and light scattering-mode super-RENS (LSC super-RENS) was realized by adopting a silver oxide (AgO_x) films instead of Sb [66].

The recording layer is $Ge_2Sb_2Te_5$ phase-change film, whose crystallization temperature (~ 433 K) is close to the decomposition temperature of the AgO_x mask layer (around 433 - 473 K). During the readout process, silver oxide thin layers thermally decomposed into silver particles which were used to work as a light scattering center and produced an optical near-field around the scattering center. The scattering center worked as an aperture-less probe in LSC super-RENS and could retrieve recording marks beyond the optical diffraction limit in super-RENS. But the recorded marks are unstable during the readout process because the distance between recording layer and mask layer is about 50 nm. This problem can be solved by introducing thermal shield layer [66].

Recently, the same group observed a huge signal enhancement in a super-resolution near-field structure disk with a platinum-oxide layer as the mask layer and GeSbTe as the phase change layer because 200 nm bubble pits were formed in good separation and 20 nm platinum particles precipitated inside [67]. The CNR of 200-nm-mark trains reached 46.1 dB, and 42.3 dB was obtained even at 150 nm mark trains using the same optical system as that of a digital versatile disk (a 635 nm wavelength red laser system). With AgInSbTe as active layer, the CNR of over 47 dB for 100 nm mark length signals (over 43 dB for 80 nm mark length signals) was obtained [68]. By using a new structure of $ZnS\text{-}SiO_2$ inserted PtO_x layers for blue laser system, they obtained CNR of above 33 dB at the 37.5 nm mark which is equivalent to 100 GB capacity with 0.32 μm track pitch [69].

The researchers in our group proposed a new super-resolution near-field optical disk with an additional localized surface plasmon coupling layer and observed the recording marks

as small as 31 nm at the wavelength of 650 nm [70]. With a thermal shield layer, the observable smallest marks were 16 nm at the wavelength of 405 nm [71]. These results represent a potential for a much higher-density storage using the red laser system and a sub-terabyte optical storage using the blue laser system.

2.5.4 Multilevel Phase-change Recording

Multilevel data storage is very attractive due to its increasing disc capacity as well as data transfer rate [72][73]. Many attempts have been made to realize multilevel recording in optical disc recording. By controlling the pulse power amplitude, multi-level reflection modulation recording can be realized. Different levels of input power give rise to different reflection levels. The combination of size effect and partial crystallization effect was proposed as main reasons to cause the multi-level reflection. The feasibility of 8 levels [74] and 12 levels [75] multilevel technology on a red laser DVD rewritable base has been demonstrated. Proof of feasibility has also been demonstrated on a blue-laser tester using a 0.6mm substrate and 0.60NA lens [76] and a blue-laser tester with 0.85NA lens using media with 0.1mm cover [77]. Hieslmair et al [78] reported over 34 GB rewritable multi-level recording using blue laser with 0.85 NA lens and 0.1 mm cover layer.

2.6 Future development of optical data storage

In the era of the Internet, massive amounts of information and multimedia can be easily accessed in every corner of the world. The demand for larger storage capacities of ever

smaller devices, lower cost and faster storage media is ever increasing.

Current phase change optical data storage technologies offer unparalleled capacity and reliability for long-term data storage and archive applications. Today, the rewritable phase-change optical disks in the form of DVD-RAM 4.7 GB have been very popular. Recently, the 3rd generation optical disks, blue-ray disks (BD), are coming into market. Sony Electronics, well established in the professional storage market, released at CNETAsia News on April 8 2003 that the 1st generation of BD capable of storing up to 23 GB on a single recording side with dual recording layers. The 2nd generation BD with capacity of 50 GB and 3rd generation BD with capacity of 100 GB will be available in 2005 and 2007, respectively. These technologies all use small marks to store bits of information.

The pusuit of optical disk with larger storage capacities and faster data transfer rate will continue. To further increase the storage capacity, the data should be recorded in even smaller mark by using shorter wavelength lasers or objective lenses with a higher NA, or a combination of both, or near field technology. However, there is strong evidence that optical data storage are approaching fundamental limits that may be difficult to overcome as the ever-smaller regions that store bits of information become harder to access.

Researchers are seeking options for the next generation optical data storage. An intriguing approach is Mansuripur's unique proposal [79]. Many problems of current data storage are due to that the data-blocks are confined and the read/write head is mobile. If the read/write head is fixed and the data-blocks can move freely between read/write head, what will happen? M. Mansuripur presented this approach for the new generation

data storage [79][80][81]. In his vision, the mimicking of the biological systems and individual molecules which are mobile are used to storage information. The individual nanometer sized molecules - strung together in a flexible macromolecular chain - will represent the 0's and 1's of binary information. The read/write head is fixed within an integrated chip so that a large number of read/write heads could operate in parallel and the heads and parking spots would be constructed (layer upon layer) in a truly 3-dimensional fashion. In this scheme, the storage capacity of the 10^6 parking spots will be 10^{12} bytes/cm^2 and 10^{15} bytes/cm^3 in a three-dimensional design based on 10 μm thick layers. However, whether this scheme could be realized or not is not clear yet.

Increase of rotation speed is always used to achieve high data transfer rate in optical diak. To obtain the same storage capacity at higher rotation speed as that at lower rotation speed, the laser pulse duration should be reduced to achieve the same mark size. However, there may exist minimum laser pulse duration for phase transition of phase change media to occur. Although Ohta [24] reported that single 120 fs laser pulse could induce crystalline to amorphous phase transition in 20 nm $Ge_2Sb_2Te_5$ films, short laser pulse, such as femtosecon or picosecond, may not trigger crystalline to amorphous phase transition in phase change media. Our study focused on the interaction of femtosecond laser with phase change media to investigate whether femtosecond pulse can induce any phase transitions in phase change materials or not. It may provide the posibility to increase data transfer rate for future application.

Chapter 3 Experimental tools and setups

Intense femtosecond laser pulses excite a dense electron-hole plasma in a semiconductor, which causes the material in extremely nonequilibrium condition and leads to novel structural transitions [5][6][7][8][9][10][11][12][13][13][15]. Femtosecond pulses also have high temporal resolution which allows investigating the dynamics of the laser-induced transitions. Motivated in part by potential applications in materials processing, optical switching and optoelectronic devices, considerable effort has been contributed in the past two decades to observing high-density carriers dynamics and understanding atomic motion during subpicosecond laser-induced phase transitions.

The experiments described in the next three chapters in this thesis were carried out using the Spectra-physics femtosecond laser system. In this chapter, the laser system will be introduced first. A cw Argon ion laser pumps a mode-locker Ti: sapphire laser. The Spitfire amplifies pulses from the mode-locked laser at the repetition rate of 1-1000 Hz. Then the details of our two experiment setup will be presented. This chapter ends with a critical assessment of the experimental method, presenting its strengths and limitations and offering proposals for future improvement.

3.1 Femtosecond laser system

Figure 3.1 shows the Spectra-physics femtosecond laser system. The Millennia laser

pumps a cw mode-locked Ti: Sapphire laser, producing the ultrashort pulses (100~130 fs) with approximately 500 mW power at the wavelength of 800 nm and repetition rate of 82 MHz. The Spitfire which is pumped by a frequency doubled Evolution Nd: YLF laser, stretches, amplifies and then recompresses these short pulses to achieve a power of 600 mW at the repetition rate of 0~1000 Hz. The pulse shape of the laser beam is Gaussian.

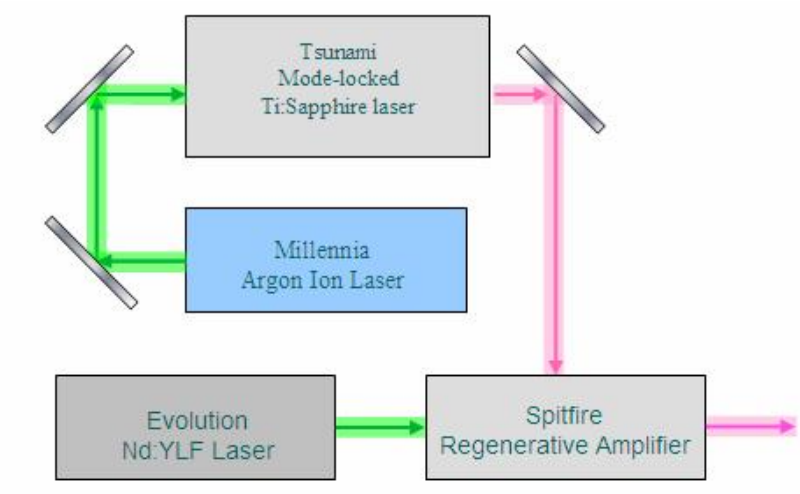

Figure 3.1 Spectra-physics femtosecond laser system.

As laser pulse duration shrinks in length, the measurement becomes very important because the short pulse is easy to be broadened. In our experiments, Femtochrome FR-103MN Autocorrelater was used to measure the pulse duration of Tsunami femtosecond laser at the frequency of 82 MHz and Newport Video FROG was used to realtime measure the pulse duration of Spitfire Regenerative Amplifier at the frequency of 1000 Hz. The measurement results are shown in Figure 3.2 and Figure 3.3, respectively.

The calibration factor of Femtochrome FR-103MN Autocorrelater in our measurement is 6.67 fs/μs. The conversion factor of the autocorrelation trace to the pulse width for

Gaussian beam is 0.707.

Figure 3.2 shows that the FWHM (full width half maximum) autocorrelation trace is 15.704 μs. The FWHM pulse width of Tsunami femtosecond laser is equal to 15.704x6.67x0.707=74.87 fs. And Figure 3.3 shows that the pulse duration of Spitfire Regenerative Amplifier is 108.09 fs.

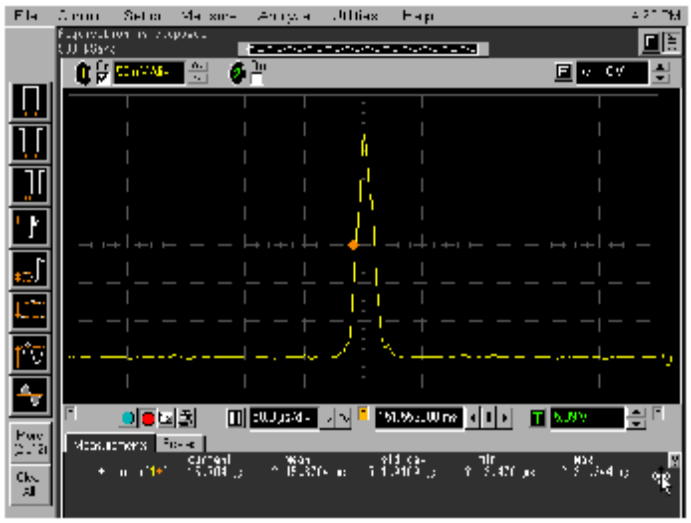

Figure 3.2 Measurement result of Tsunami femtosecond laser.

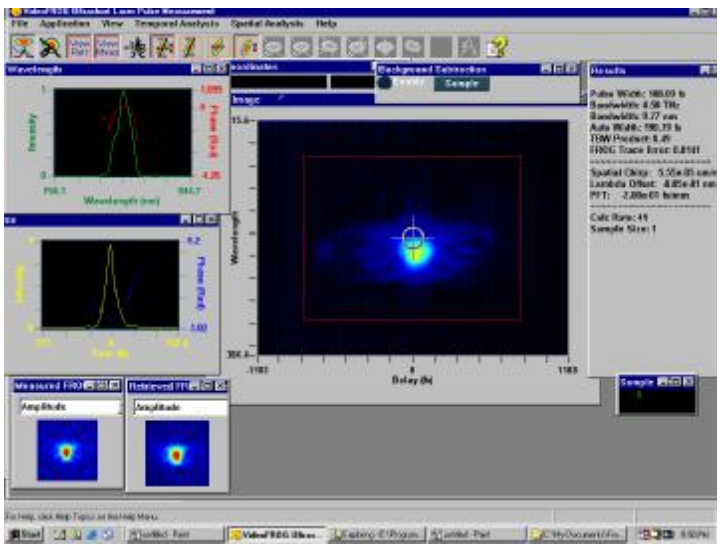

Figure 3.3 Measurement result of Spitfire Regenerative Amplifier.

3.2 Static Experiment Setup

The static experiment setup is used to investigate whether single femtosecond pulse can induce any phase transition in phase change materials or not. The setup is shown in Figure 3.4. The 100 fs pulses at the wavelength of 800 nm from the Sapphire amplifier passing through a fixed attenuator, an adjustable attenuator and a shutter is focused by an objective lens and is normal incidence on a sample. The stage, which holds the sample and the shutter, is controlled by a computer to ensure the number of pulses irradiated on the same place of the sample. Because ultra-short optical pulses can be easily broadened and distorted by common optical components, all the optical components in this setup are specially required for femtosecond application to reducing the broadening effects. For example, all the mirrors used in the setup have special dielectric coating which can sustain high chirp power of femtosecond pulses and produce less than 18% widening of pulse duration.

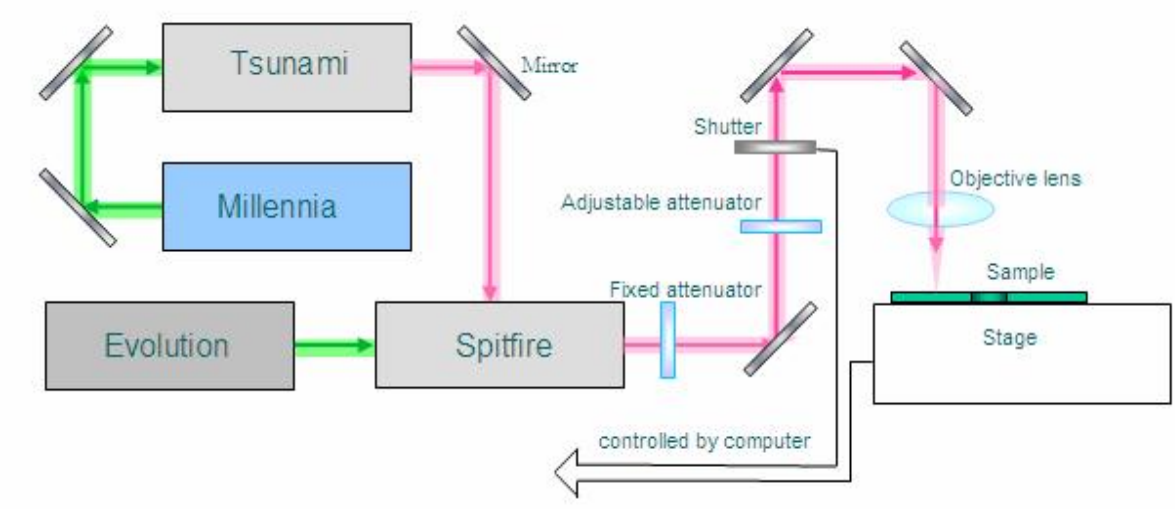

Figure 3.4 Static experiment setup.

The static experiment setup can only indicated whether single femtosecond pulse can induce any phase transition in phase change material or not. To investigate the mechanism of the phase transformations triggered by femtosecond pulse, pump-probe experiment setup should be employed.

3.3 Pump-probe Experiment Setup

The common way to study the process of the changes in a material is to measure a parameter over time. For example, as a material is heated, its temperature can be recorded by measuring the amount of light emitted as a function of time, this can be down as follows:

1) Open the shutter of a camera for a short time and measure the amount of light emitted.
2) Repeat several times while the material is heated, tracking the time of each shutter opening
3) Draw the measured light energy as function of time.

However, this method cannot be used in fast processes when the open time of the shutter is longer than that for the entire process to finish. A technique called strobe photography , which is usually used to measure fast moving objects and requires a dark room, can solved this problem. It works as follows:

1) Open the camera shutter. No light enters to shine the camera film.
2) Emit a flash of light to illuminate the fast moving object of interest.

3) After this, close the shutter.

Although the shutter is open for a long time, the material is only exposed when the flash is on. Hence the moving object is observed only for this length of time. This method can reach higher time resolution than standard photography because the flash of light can be made much shorter than the shutter open times.

With sub-nanosecond pulses, the strobe photography is called pump-probe technique. One laser beam, termed pump beam, starts to induce changes in the material. After a certain time delay, a second weaker beam, called probe beam, interrogates the area of the sample that is changing. A detector or camera is used to measure the light that is reflected, transmitted, converted to second-harmonic frequency, or whatever. The delay between the pump beam and probe beam is varied by changing the distance that the probe beam passes through. Thus the optical property of the material can be measured for different delay time to reveal how the material changes in response to the excitation by the pump beam.

Indeed, now there are light pulses of femtosecond [84][85] or attosecond [86][87][88][89][90][91]. With this kind of pulses, time resolution of femtosecond or attosecond timescale can be reached.

In our experiment, ultrafast time-resolved microscopy [26] was employed to investigate the mechanism of the phase transformations in phase change media induced by femtosecond pulse, as shown in

Figure 3.5. A single shot of 100 fs, P-polarized pulse at 800 nm was produced by a

regenerative amplifier, Ti:sapphire, which is pumped by the mode-lock femtosecond laser (Spectra physics). A 50% beam splitter divided this output into a pump beam, which was focused at normal incidence onto a sample surface (spot diameter ~250 μm), and a second beam, served as a probe beam and replaced the standard illumination of an optical microscopy, was focused at near 45° incidence to a spot of approximately 1000 μm diameter overlapping and illuminating the area excited by the pump beam, as shown in Figure 3.6. A magnified image of the excited surface region was recorded at a given pump-probe time delay by collecting the specularly reflected light with a CCD camera.

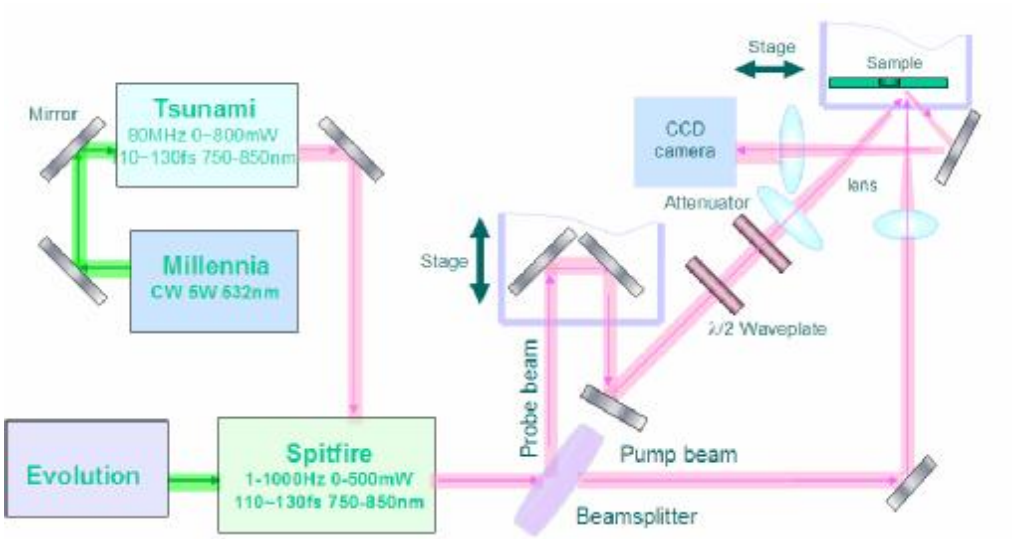

Figure 3.5 Time-resolved microscopy

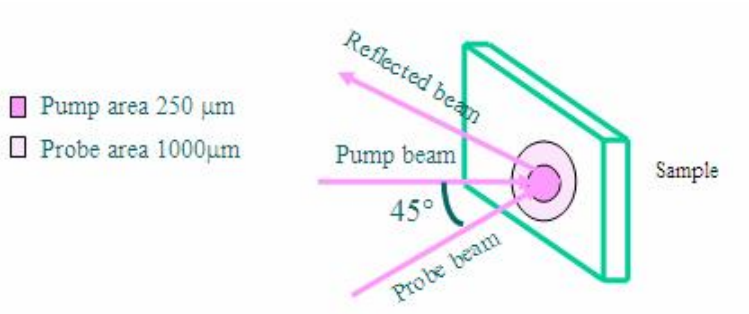

Figure 3.6 Schematically show the pump beam and probe bean overlap on the sample.

The same as previous setup, all the optical components in this setup are specially required for femtosecond applications to reducing broadening effects. All the mirrors used in the setup have special dielectric coating which can sustain high chirp power of femtosecond pulses and produce less than 18% widening of pulse duration. The large angle between the pump and probe beam isolates the CCD camera from the strayed pump light. To obtain a single shot image, the shutter of CCD camera is opened for longer time than the time for single fire to ensure the exposure by single pulse, but slightly shorter than the time between two successive laser pulses to prevent double exposure. The λ/2 waveplate is used to ensure that the polarizations of the pump beam and probe beam are orthogonal in order to reduce their coherent interaction near zero delay [92]. The time delay between the pump and probe can be varied with the computer controlled delay stage, which has the resolution of 0.010 μm. For 1 fs optical delay, the stage moves 0.15 μm. The pulse duration of our laser system is about 110 fs, as measured before, which is lower than the resolution of the stage. Thus the temporal resolution of the setup is determined by the duration of laser pulse, not by the stage.

In this setup, the key point is to determine the point of zero delay, where the pump beam and probe beam travel equal distance to reach the sample at the same time. The images of CCD camera was used to determine the zero point. When the probe beam reaches the sample before the pump beam, the image of pump-probe beam should be the same as that of probe beam. If the pump beam arrives at the sample before probe beam, the image of pump-probe beam should be different from that of probe beam because the probe beam detects the surface which has already changed by the pump beam. The turning point

between the same image and different image is the zero point we are looking for.

Since a single femtosecond pulse could induce a permanent structural change in the irradiated area, the sample was moved 2000 μm after each laser shot by a compute-controlled stage. Consequently, each laser shot interrogated a fresh region of the sample. Furthermore, the probe beam was attenuated much weaker than the pump beam to avoid any phase transition that might be induced by the probe beam.

3.4 Critical assessment of the experimental method

Before proceeding to describe our results of phase transitions and ultrafast dynamics in phase change media induced by femtosecond pulse, I would like to compare our method with other methods for investigating ultrafast dynamics.

Femtosecond microscopy [26] was used to measure the reflectivity intensity change to investigate the utrafast dynamics in phase change media. It has many advantages over the traditional pump-probe technique, in which the probe beam is focused more tightly than the pump beam in order to monitor a uniformly excited region: the probed surface area is about 10 times smaller than the focused area of the pump beam on the sample. Thus the traditional pump-probe technique provides a space-integrated information over an inhomogeneously excited area which may mask the details of optical properties evilution of the surface. Time resolved microscopy, similar to the traditional pump-probe technique, also has femtosecond time and micrometer spatial resolution. But unlike the traditional pump-probe technique, the focused probe beam in time resolved microscopy

is approximately 4 times larger than the focused area of the pump beam on the sample. Thus it avoids special averaging effects and provides a richer body of information on the time and fluence dependence of the phase transition process. In particular, the Gaussian intensity distribution of the focused pump pulse results in a continuous variation of the excitation conditions across the sample surface. A single snapshot picture of the illuminated area contains information over an extended range of fluence. And femtosecond microscopy is the only method which obverses the variation of material response across a pumped region. The disadvantage is that it only measures the reflectivity intensity at a single frequency.

Two other techniques are good alternatives for the investigation of materials under intense femtosecond laser excitation of sufficient intensity to trigger ultrafast phase changes. They provide information which complements the data produced by our technique. One technique is the measurement of spectral dielectric function, which have been employed by Mazur's group at Harvard University in many experiments to study ablation, melting and resolidification in various materials [10][11][12][13][13]. Their experiments clearly indicate the phase of material, telling us whether it is a metal, semiconductor or insulator, or whether it is in order or disordered state. Furthermore, for crystalline materials, the spectral dielectric function probes much of the band structure and thus enables one to track many aspects of the electron dynamics in one experiment. For these reasons, the technique clearly provides more information than time-resolved measurements of reflectivity, or the dielectric function at only one frequency. The trade-off is that this method cannot measure as precisely as those using just a single frequency.

Another technique, time-resolved X-ray diffraction, promises to give more insight in the field of ultrafast dynamics. As we known, ultrashort visible pulses have been used for more than two decades to optically pump and dynamically probe a wide array of atomic, molecular, solid-state, and plasma systems, including extreme states of materials normally found only in experiments triggered by excitation of ultrashort pulses. In these experiments, however, the visible light used to probe the ensuing dynamics cannot resolve the features in atomic-scale because it interacts predominately with valence and free electrons and not with the deeper lying core electrons and nuclei that most directly indicate the structure. Hard x-ray radiation, with wavelengths comparable with interatomic distances, is well suited to measure structure and atomic rearrangement and can measure structural dynamics in the interior of samples that are not transparent to ordinary light. Rescently, subpicosecond sources of hard x-rays have been developed using optical femtosecond pulses [94][95][96][97]. In the past several years, several groups used such pulses to carry out time-resolved visible-pump, x-ray diffraction probe experiments on materials after excitation by the femtosecond optical pulse [98][99][100] [101][102][103][104][105]. In those experiments, milli-angstrom changes in lattice spacing were measured with picosecond temporal resolution. These X-ray techniques are still in their infancy. But with time, they will provide the definitive means to study ultrafast structural dynamics in solids and other materials. In combination with optical measurements, which primarily detect electronic changes, X-ray data could provide a complete picture of ultrafast electronic and lattice dynamics in solids.

Chapter 4 Phase transitions in phase change media induced by femtosecond laser

Great progress has been made in phase change optical data storage recently. Phase change optical data storage has become a mature technology for rewritable data storage system. Ternary GeSbTe alloy and quaternary AgInSbTe alloy are two materials that are widely used in phase change optical disk. In conventional optical data storage, however, recording and erasing are achieved by laser pulses emitted from semiconductor laser diodes with nanosecond duration that thermally induces crystallographic structural changes in the phase change media. Thermal diffusion is one of the fundamental limitations in the conventional optical data storage which uses rather long pulse widths of 10 ns to 60 ns. It will not only make the mark size wider than laser spot size but also deform the disk.

Recently, the interaction of intense ultrafast laser pulses such as femtosecond (10^{-15} s) laser with phase change media has drawn much attention. It is believed that femtosecond pulse is very promising for phase change optical data storage because of its efficient delivery of optical power, enhancement of the cooling rate and suppression of the thermal diffusion effects. Intense femtosecond pulse can excite a dense electron-hole plasma in semiconductors, which causes the materials in the most extreme non-equilibrium conditions and gives rise to novel and unusual phase transitions.

Femtosecond pulse induced nonthermal phase transitions, in which phase transitions occur before free carrier and lattice reach thermal equilibrium, have been reported in many materials such as Si [5][6][7], GaAs [8][10][11][12][13], GeSb [13], InSb [15] etc. If femtosecond pulse can induce crystalline to amorphous and amorphous to crystalline phase transitions in phase change media, it might greatly increase data transfer rate to terabyte per second. Ohta *et al.* [24] first presented that single 120 fs laser pulse can induce an amorphous mark without the crystalline edge in GeTe-Sb_2Te_3-Sb sandwich structure at crystalline background. Nevertheless, whether single femtosecond laser pulse can induce amorphous to crystalline phase transition in phase change media or not has never been reported. This chapter focuses on our study of the phase transitions in phase change media triggered by femtosecond laser.

This chapter will start with the measurement of refractive index of phase change media, with which the optical band gap of phase change media is calculated and the sample structure is designed. Then our experiment results using static experiment setup will be presented. This chapter ends with a summary.

4.1 Characterization of optical properties of phase change media

The refractive index ($h = n + ik$) determines all the linear optical phenomena in a material, such as light propagation in a media, light reflection and transmission at an interface. The imaginary part of the refractive index, also called the extinction

coefficient, determines the absorption coefficient. The relationship between the absorption coefficient and light energy can be used to calculate the optical band gap of the material [26], which is very important to clarify the excitation mechanism of the material after light irradiation. Thus it is very important to know the refractive index of phase change media.

In this thesis, the reflective index is measured with Steag etaoptic ETA-RT quality control systems for compact disc production. The sample used to measure the refractive index is 0.6 mm polycarbonate substrate/ 100 nm ZnS-SiO_2 / phase change layer /100nm ZnS-SiO_2. The two dielectric layers which sandwich the phase change media have following functions:

1) Protect the phase change layer from contamination and oxidation;
2) Make the as-deposited phase change media easy to be changed to crystalline phase with the initializer.

The samples were fabricated using a Balzers Cube sputtering system, which is guided by windows-based software. The system has four independent process chambers and three sputtering power sources (two DC and one RF). The phase change layers were sputtered using the DC magnetron sputtering method. The $(ZnS)_{80}(SiO_2)_{20}$ dielectric layers were sputtered by the RF sputtering method. The distance between the target and substrate is 4 cm, the chamber background pressure is below $1.2x10^{-7}$ mbar, and the sputtering pressure of Ar gas is approximately $4.5\text{-}5.5x10^{-3}$ mbar. The as-deposited samples were at amorphous background and could be changed to crystalline background by the ShibaSoKu optical disk initializer.

The refractive index of 0.6 mm polycarbonate substrate and 100 nm ZnS-SiO_2 dielectric layer were first measured in order to obtain acceptable deviation (>10^{-7}) in fitting refractive index of phase change layer. Here the detailed measurement of refractive index and calculation of optical band gap of 20 nm amorphous $Ge_2Sb_2Te_5$ films will be presented.

Figure 4.1 and Figure 4.2 are the measured spectral reflectance and transmittance of 20nm amorphous $Ge_2Sb_2Te_5$ films sandwiched by two 100 nm dielectric layers on 0.6 mm polycarbonate substrate, respectively.

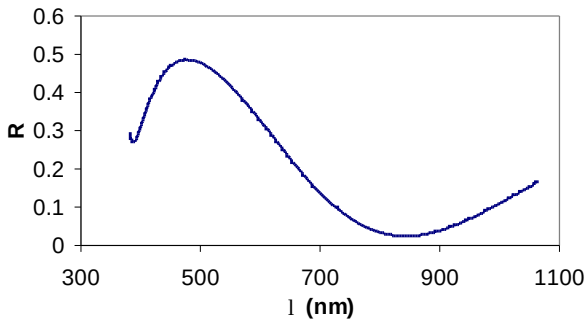

Figure 4.1 Spectral reflectance of 20 nm $Ge_2Sb_2Te_5$ films at as-deposited background sandwiched by two 100 nm dielectric layers on 0.6 mm polycarbonate substrate.

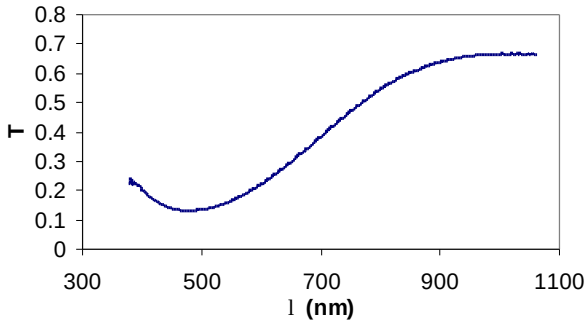

Figure 4.2 Spectral transmittance of 20 mm $Ge_2Sb_2Te_5$ films at as-deposited background sandwiched by two 100 nm dielectric layers on 0.6 nm polycarbonate substrate.

The refractive index of 20 nm amorphous $Ge_2Sb_2Te_5$ films was fited with its spectral reflectance and transmittance, already measured refractive index of 0.6 mm polycarbonate substrate and 100 nm ZnS-SiO_2 dielectric layer, as shown in Figure 4.3. The result was confirmed with ellipsometer measurement.

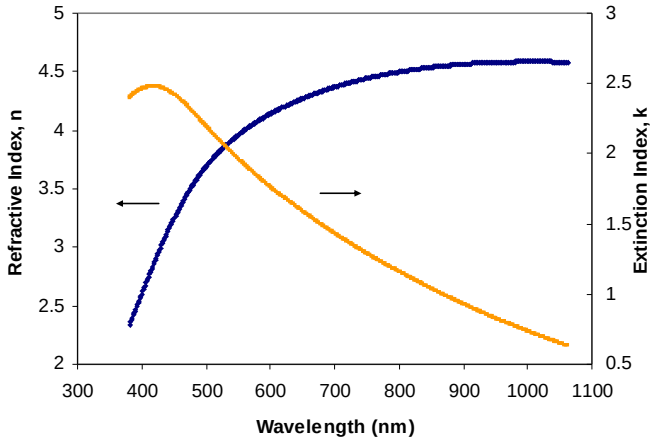

Figure 4.3 Refractive index of 20 nm amorphous $Ge_2Sb_2Te_5$ films.

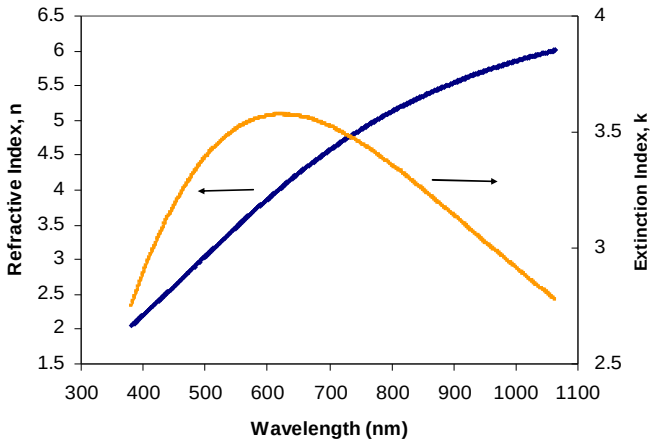

Figure 4.4 Refractive index of 20 nm crystalline $Ge_2Sb_2Te_5$ films.

With the same method, the refractive indexes of $Ge_2Sb_2Te_5$ films at different conditions and other phase change media were also measured, as shown in following Figure 5.5-

5.21.

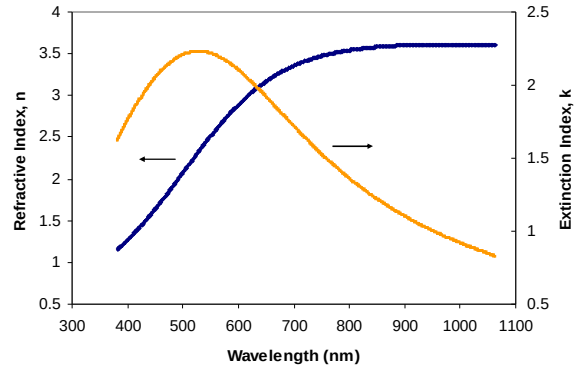

Figure 4.5 Refractive index of 100 nm amorphous $Ge_2Sb_2Te_5$ films.

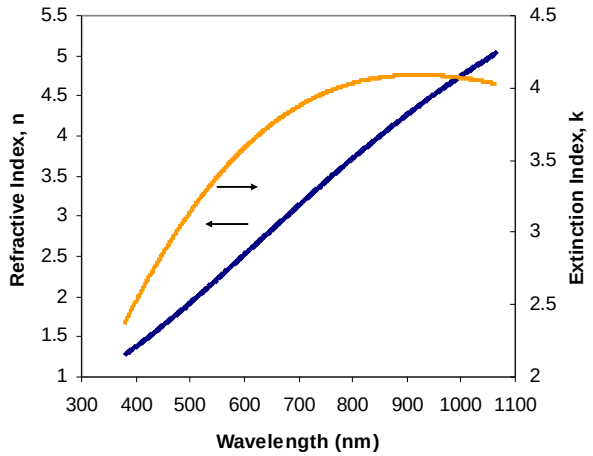

Figure 4.6 Refractive index of 100 nm crystalline $Ge_2Sb_2Te_5$ films.

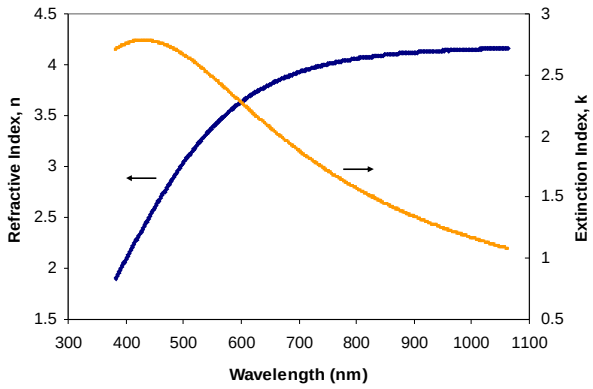

Figure 4.7 Refractive index of 20 nm amorphous $Ge_1Sb_2Te_4$ films.

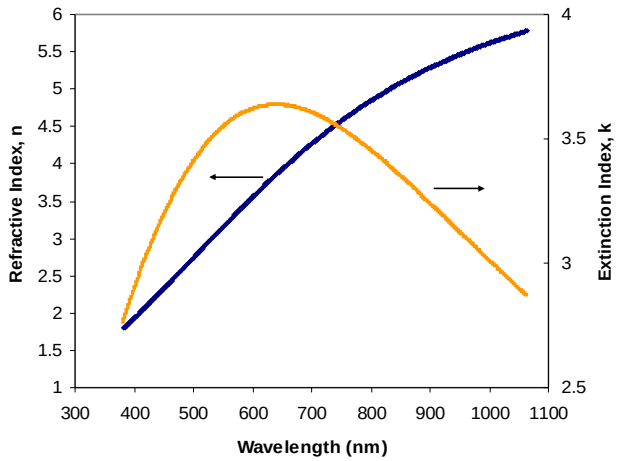

Figure 4.8 Refractive index of 20 nm crystalline $Ge_1Sb_2Te_4$ films.

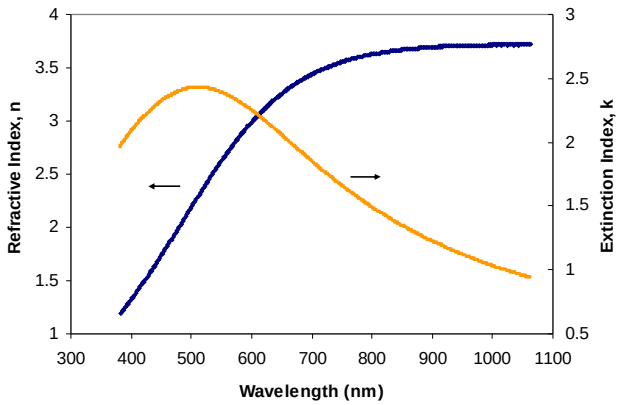

Figure 4.9 Refractive index of 100 nm amorphous $Ge_1Sb_2Te_4$ films.

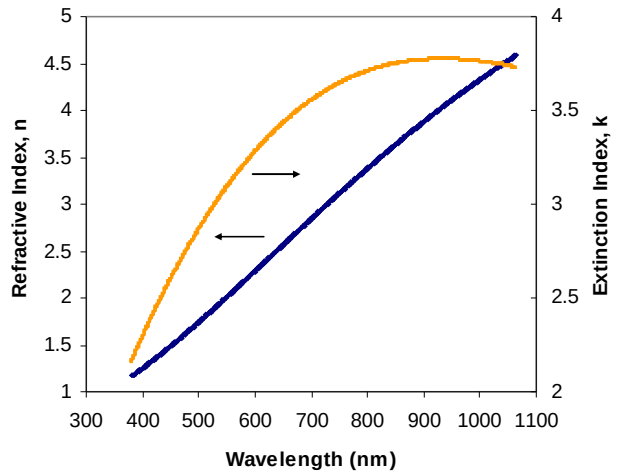

Figure 4.10 Refractive index of 100 nm crystalline $Ge_1Sb_2Te_4$ films.

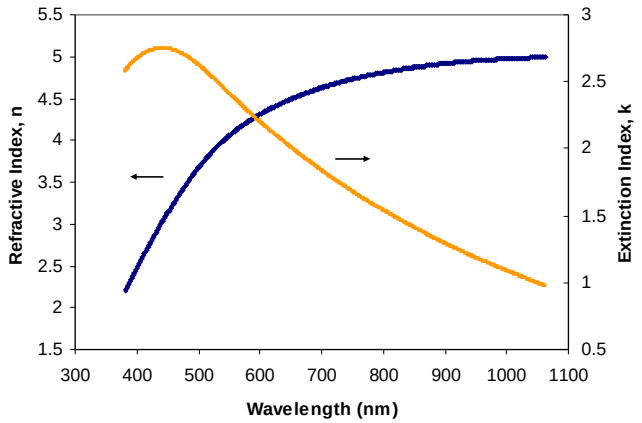

Figure 4.11 Refractive index of 20 nm amorphous $Ge_1Sb_4Te_7$ films.

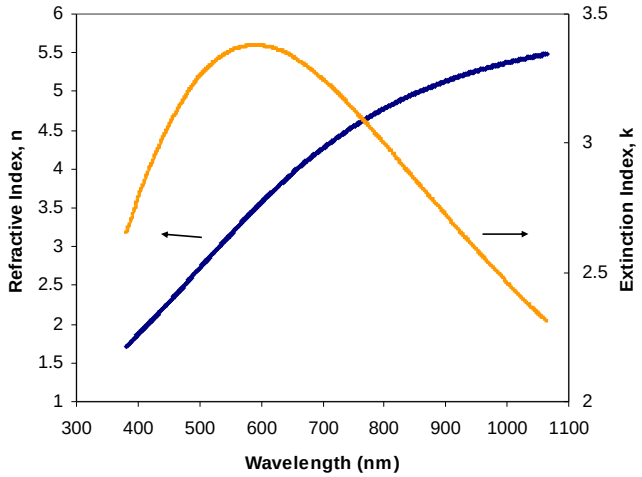

Figure 4.12 Refractive index of 20 nm crystalline $Ge_1Sb_4Te_7$ films.

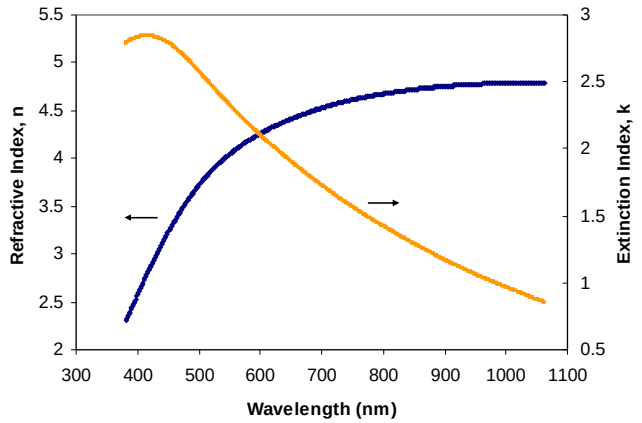

Figure 4.13 Refractive index of 100 nm amorphous $Ge_1Sb_4Te_7$ films.

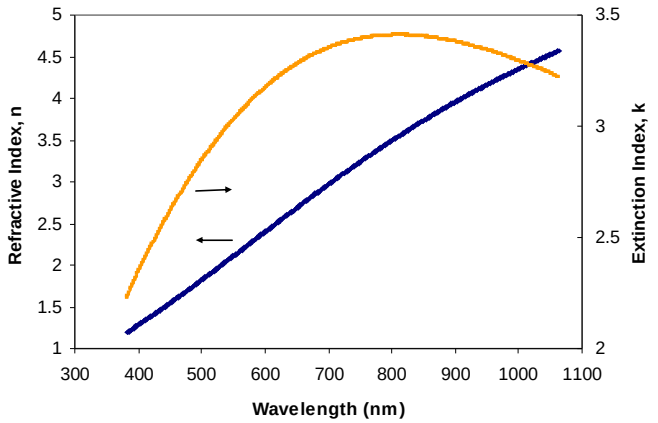

Figure 4.14 Refractive index of 100 nm crystalline $Ge_1Sb_4Te_7$ films.

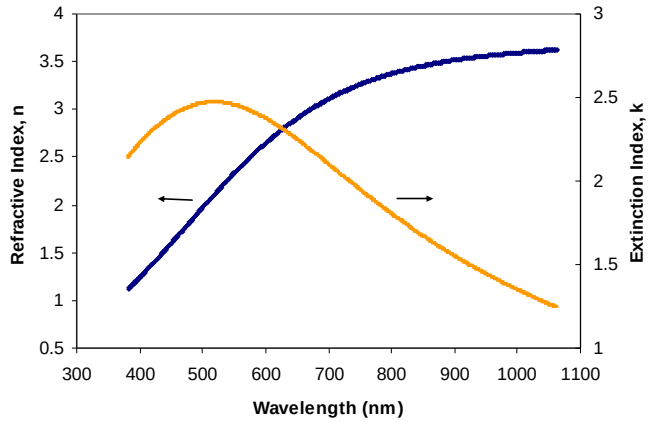

Figure 4.15 Refractive index of 20 nm amorphous $Ag_5In_5Sb_{30}Te_{60}$ films.

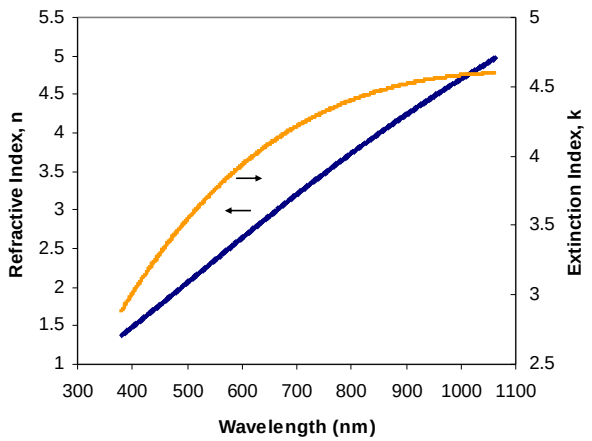

Figure 4.16 Refractive index of 20 nm crystalline $Ag_5In_5Sb_{30}Te_{60}$ films.

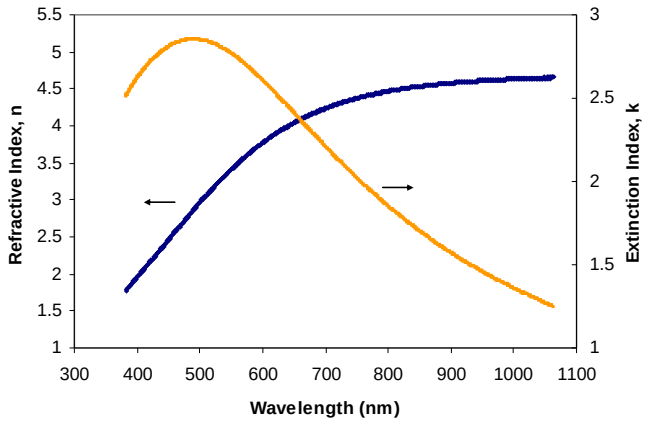

Figure 4.17 Refractive index of 100 nm amorphous $Ag_5In_5Sb_{30}Te_{60}$ films.

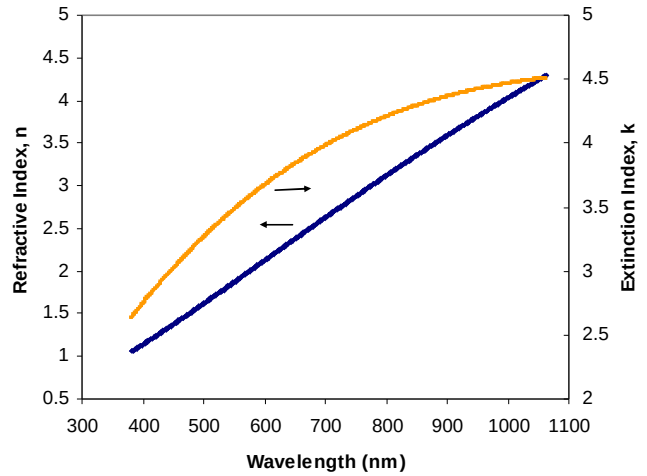

Figure 4.18 Refractive index of 100 nm crystalline $Ag_5In_5Sb_{30}Te_{60}$ films.

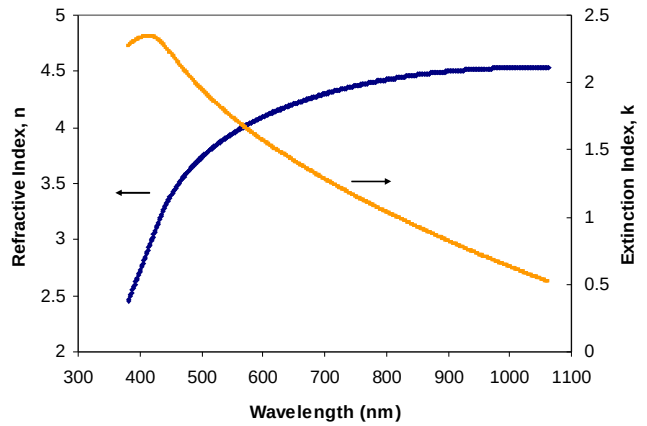

Figure 4.19 Refractive index of 100 nm GeTe amorphous films.

The quantum theory of semiconductor, as initially developed, was based completely on the presence of long-range order and on the periodicity of the crystalline structures. It used to be believed that amorphous solids could not have band structures and could not be regarded as semiconductors due to lack of long range periodicity. Later, however, it was found that chalcogenide glasses can also act as semiconductors [106] with an optical energy bandgap [26]. The covalent interatomic bonds give rise to the usual bonding (valence) and anti-bonding (conduction) bands.

The absorption coefficient a can be calculated according to the following expression:

$$a = 4pk / l \tag{4-1}$$

where k is the imaginary part of the refractive index, also called extinction coefficient.

According to Tauc [29], amorphous semiconductors have three distinct regions in the absorption edge spectrum: the weak absorption tail which originates from defects and impurities, the exponential edge region which is strongly related to the structural randomness of the system, and the high absorption region which determines the optical energy bandgap.

In the exponential edge region, where $1 < a < 10^4 cm^{-1}$, the absorption coefficient is governed by the equation:

$$a = a_0 \exp(hg / E_e) \tag{4-2}$$

Where α_0 is a constant, $h\gamma$ is the energy of incident photons and E_e is the slope of the

exponential edge region.

In the high absorption region, where $a > 10^4 cm^{-1}$, the parabolic relation can be expressed:

$$ahg = B(hg - E_0)^n \tag{4-3}$$

Where B is a parameter that depends on the transition probability, E_0 is the band gap, and n is an index which can be assumed to values of 2, 3, 1/2 and 3/2 depending on the nature of the electronic transition responsible for the absorption. For example, n equals 1/2 for allowed direct transition and equals to 2 for allowed indirectly transition. Thus the type of transition and the energy of transition can be determind via plotting a graph of $(ahg)^{1/n}$ against hg .

In our experiments, the absorption coefficients of phase change media at amorphous background were larger than 10^4 cm^{-1}. It belonged to high absorption region. Figure 4.20 is $(ahg)^{1/2}$ and $(ahg)^2$ as a function of photon energy (hg) for 20 nm amorphous $Ge_2Sb_2Te_5$ film. It shows that $(ahg)^{1/2}$ has a linear function to the photon energy (hg) at low energy region, indicating an allowed indirect transition. Its interception with (hg) is the indirect transition optical band gap, which is about 0.66 eV. Our result that 20 nm as-deposited $Ge_2Sb_2Te_5$ films has indirect optical band gap of 0.66 eV is consistent with that of Pirovano's that amorphous GeSbTe has an indirect optical energy bandgap of 0.7 eV [107].

The optical band gaps of 100 nm amorphous $Ge_2Sb_2Te_5$ films and other phase change

materials at amorphous background were also calculated with their measured refractive media. They all have indirect optical band gap around 0.6~0.7 eV, as listed in Table 4-1

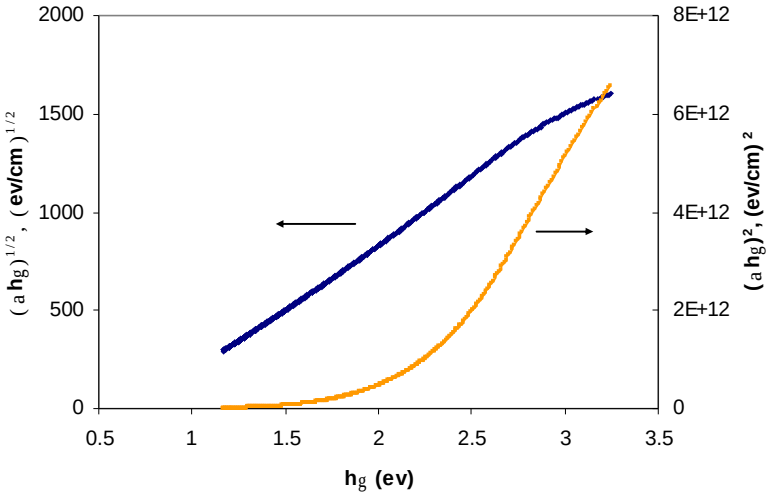

Figure 4.20 Dependence of $(ahg)^{1/2}$ and $(ahg)^2$ on photon energy (hg) for 20 nm amorphous $Ge_2Sb_2Te_5$ films.

Table 4-1 Optical band gap of some phase change media at amorphous background calculated with the measured refractive index

Material	Thickness(nm)	Transition type	Optical band gap(eV)
$Ge_1Sb_4Te_7$	20	Indirect	0.63
	100	Indirect	0.67
$Ge_1Sb_2Te_4$	20	Indirect	0.61
	100	Indirect	0.68
$Ge_2Sb_2Te_5$	20	Indirect	0.66
	100	Indirect	0.70
$Ag_5In_5Sb_{30}Te_{60}$	20	Indirect	0.57
	100	Indirect	0.60
GeTe	100	Indirect	0.73

4.2 Sample structure design

Previously measured refractive index of phase change media with our in-house-developed Phase Change Optical Disk Design (PCODD) software [25] were used to

design the multilayer structures in order to achieve good optical contrast between amorphous and crystalline phases at wide range of film thickness of phase change media. The wavelength of 800 nm which was our experiment condition was seleted. The sample structure was designd as following: the phase change layer was sandwiched by two dielectric layers on 0.6 mm polycarbonate substrate. The two dielectric layers have following functions:

1) Protect the phase change layer from contamination and oxidation;
2) Make the as-deposited phase change media easy to be changed to crystalline phase with the initializer;
3) Achieve good optical contrast between amorphous and crystalline phase at the desired wavelength.

The simulation results of $Ge_2Sb_2Te_5$ films in Figure 4.21 show that the sample structure, 0.6 mm polycarbonate substrate/ 120 nm $(ZnS)_{80}(SiO_2)_{20}$ / $Ge_2Sb_2Te_5$ / 92 nm $(ZnS)_{80}(SiO_2)_{20}$/ air, has high modulation reflectivity at the wavelength of 800 nm for a wide range of thickness.This sample structure was chosen for $Ge_2Sb_2Te_5$ films and other phase change materials for comparison between them. The simulation results (not show here) also show they have high modulation reflectivity at the wavelength of 800 nm for a wide range of thickness.

After design the sample structure, the samples were fabricated with a Balzers Cube sputtering system. The as-deposited samples could be changed to crystalline phase with the initializer. After the preparation of samples, they were irradiated by femtosecond pulse to investigate whether femtosecond pulse could induce any phase transitions in

phase change media or not.

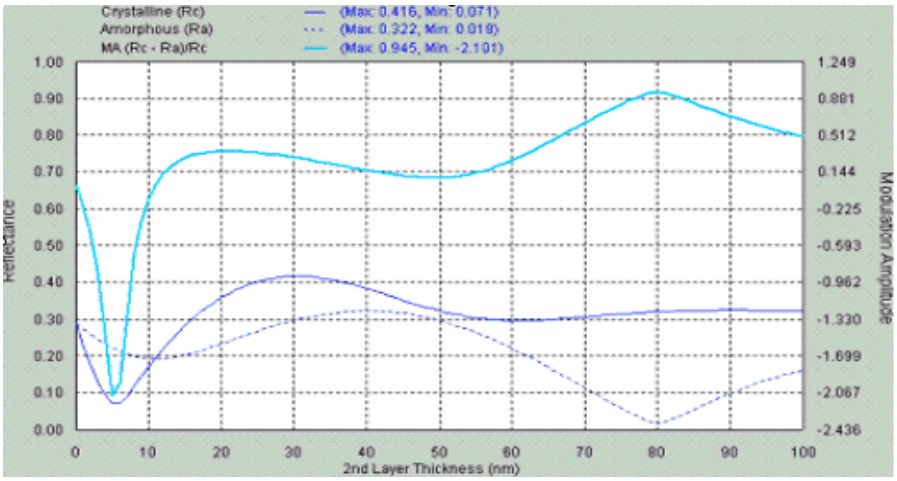

Figure 4.21 Simulation result of 0.6 mm polycarbonate substrate/ 120 nm $(ZnS)_{80}(SiO2)_{20}$ / 0~100 nm $Ge_2Sb_2Te_5$ / 92 nm $(ZnS)_{80}(SiO2)_{20}$/ air at the wavelength of 800 nm.

4.3 Phase transitions in phase change media induced by femtosecond pulse

The static experiment setup described in Chapter 3 is used to investigate whether femtosecond pulse can induce any phase transitions in phase change media or not. After femtosecond laser irradiation, the samples were observed with an optical microscope (OM).

Before our experiment, the Steag etaoptic ETA-RT quality control systems for compact disc production was employed to measure the absorption of phase change media in our designed structure at the normal incidence of 800 nm, assording to to following formula [108]:

$$A+T+R=1 \quad (4\text{-}4)$$

where A, T and R are absorption, transmittance and reflectance, respectively. The absorption of some phase change media in our designed structure at the normal incidence of 800 nm is listed in Table 4-2. It can be used to calculate the energy absorbed by the phase change media after normal incidence to 800 nm light.

Table 4-2 Absorption of some phase change media in our designed structure at the normal incidence of 800 nm.

Material	Thickness(nm)	Phase	Absorption
$Ge_1Sb_2Te_4$	20	amorphous	0.5
		crystalline	0.66
	100	amorphous	0.87
		crystalline	0.77
$Ge_2Sb_2Te_5$	20	amorphous	0.46
		crystalline	0.66
	100	amorphous	0.88
		crystalline	0.79
$Ag_5In_5Sb_{30}Te_{60}$	100	amorphous	0.89
		crystalline	0.72
SLL*	100	amorphous	0.86
		crystalline	0.76

*SLL: Superlattice-like sample consisting of alternatice layers of GeTe with the thickness of 2 nm and Sb_2Te_3 with thickness of 3 nm. Total layers are 20.

4.3.1 Experiment results

Figure 4.22 and Figure 4.23 are OM images of 20 nm $Ge_2Sb_2Te_5$ films after single femtosecond pulse irradiation at crystalline and amorphous background, respectively. They clearly indicate that single femtosecond pulse (~100 fs) can induce crystalline to amorphous phase transition in 20 nm $Ge_2Sb_2Te_5$ film, while amorphous to crystalline phase transition could not be achieved in 20 nm $Ge_2Sb_2Te_5$ film, as only over-burn marks are observed in Figure 4.23. A cw HeNe laser beam (λ =632.8 nm) was used to

measure the reflectivity change of amorphous marks induced by single femtosecond pulse and found that the detected intensity of amorphous mark induced by single femtosecond pulse was almost the same as that of the as-deposited amorphous, suggesting that even single femtosecond pulse can induce crystalline to amorphous phase transition in $Ge_2Sb_2Te_5$ films. Our result that single 100 fs pulse can induce crystalline to amorphous phase transition in 20 nm crystalline $Ge_2Sb_2Te_5$ films is consistent with that of Ohta's [24] that single 120 fs laser pulse could induce an amorphous mark in GeTe-Sb_2Te_3-Sb sandwich structure at crystalline background.

However, the results in 100 nm $Ge_2Sb_2Te_5$ films (Figure 4.24 and Figure 4.25) are quite different from those in 20 nm $Ge_2Sb_2Te_5$ films. Figure 4.24 and Figure 4.25 indicate that single femtosecond pulse can induce not only crystalline to amorphous phase transitions (Figure 4.24), but also amorphous to crystalline phase transition (Figure 4.25) in 100 nm $Ge_2Sb_2Te_5$ film. X-ray diffractometer (XRD) measurement was employed to investigate whether the marks in Figure 4.25 were cryatalline phase or not. The results are shown in Figure 4.26. The two peaks are Face center cube (FCC) (200) and (220), Our XRD result verified that amorphous to crystalline phase transition induced by single femtosecond pulse could be achieved in 100 nm $Ge_2Sb_2Te_5$ film. Amorphous to crystalline phase transition in 100 nm $Ge_2Sb_2Te_5$ films triggered by single femtosecond laser pulse, to our best knowledge, has never been reported before.

AFM was used to measure the profile of the over-burn crystalline mark and crystalline mark in 100 nm amorphous $Ge_2Sb_2Te_5$ films in Figure 4.25, as shown in Figure 4.27 and Figure 4.28, respectively. They clearly show the ejection of material in the over-burn mark, while no ablation occurs in the crystalline mark, confirming that the

crystalline mark observed with OM is due to phase transformation induced by single femtosecond pulse.

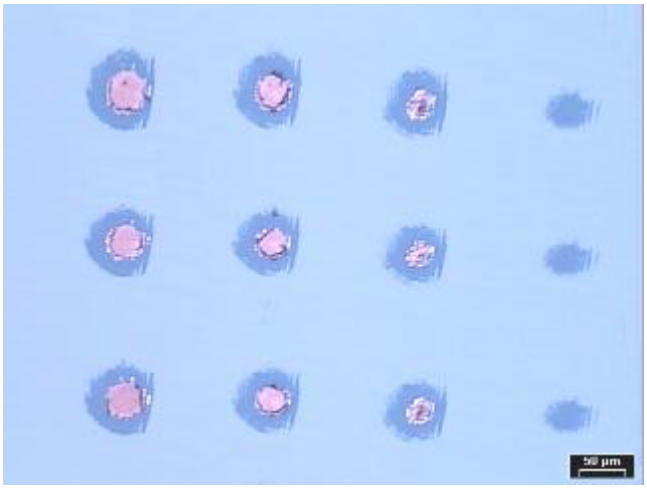

Figure 4.22 OM image of 20 nm $Ge_2Sb_2Te_5$ films at crystalline background after single femtosecond pulse irradiation. Pulse energy from left to right: 10 μJ, 8 μJ, 6 μJ and 4 μJ.

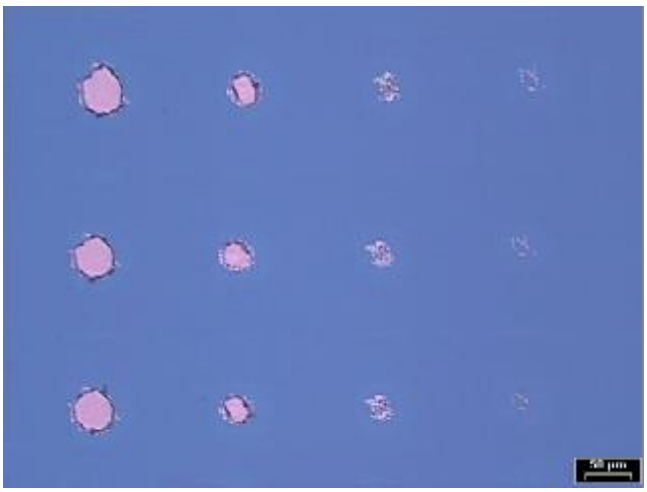

Figure 4.23 OM image of 20 nm $Ge_2Sb_2Te_5$ films at amorphous background after single femtosecond pulse irradiation. Pulse energy from left to right: 14 μJ, 12 μJ, 10 μJ and 8 μJ.

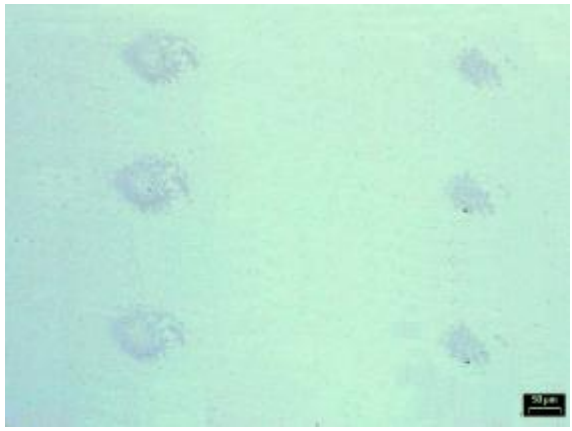

Figure 4.24 OM images of 100 nm $Ge_2Sb_2Te_5$ films at crystalline background after single femtosecond pulse irradiation. Pulse energy from left to right: 14 μJ and 12 μJ.

Figure 4.25 OM images of 100 nm $Ge_2Sb_2Te_5$ films at amorphous background after single femtosecond pulse irradiation. Pulse energy from left to right: 21 μJ and 18 μJ.

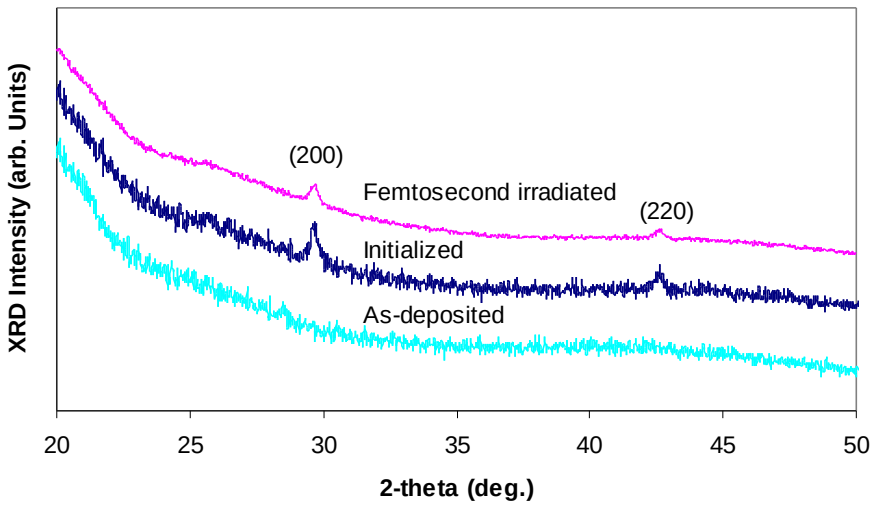

Figure 4.26 XRD patterns of 100 nm $Ge_2Sb_2Te_5$ films at as-deposited phase and after initialization and single 100fs laser irradiation.

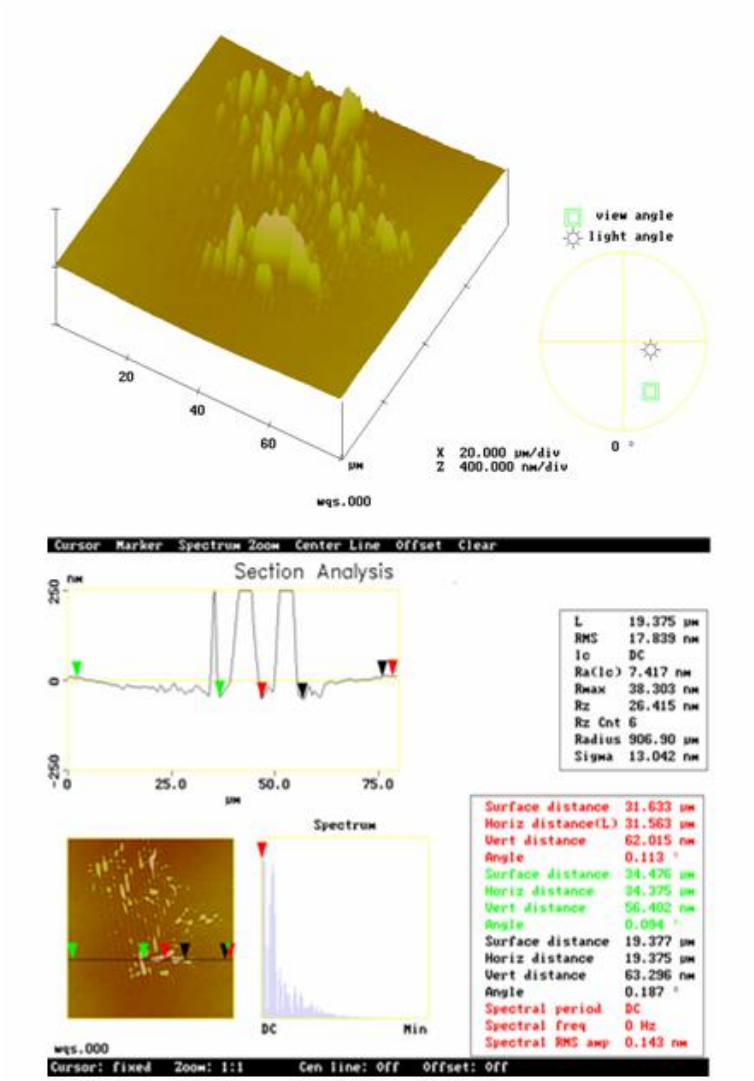

Figure 4.27 AFM profile and analysis of over-burn mark in 100 nm $Ge_2Sb_2Te_5$ films at amorphous background induced by single femtosecond pulse in Figure 4.25.

Experiments of irradiation by two femtosecond pulses were also performed in 100 nm $Ge_2Sb_2Te_5$ films to investigate whether the amorphous or crystalline mark induced by first femtosecond pulse can be erased or overwrite by second femtosecond pulse or not. The objective lens was defocused to make the marks large enough to be easily observed by OM. The results are shown in Figure 4.29 and Figure 4.30. The left mark in Figure 4.29 shows a crystalline mark induced by second pulse in the center surrounded by

amorphous mark triggered by the first pulse. It indicated that amorphous mark induced by the first femtosecond pulse can be erased by the second pulse. While the mark irradiated by two pulses in Figure 4.30 shows a different phase between crystalline and amorphous phase. It may suggest that writing in the crystalline mark induced by the first pulse is not complete by the second pulse.

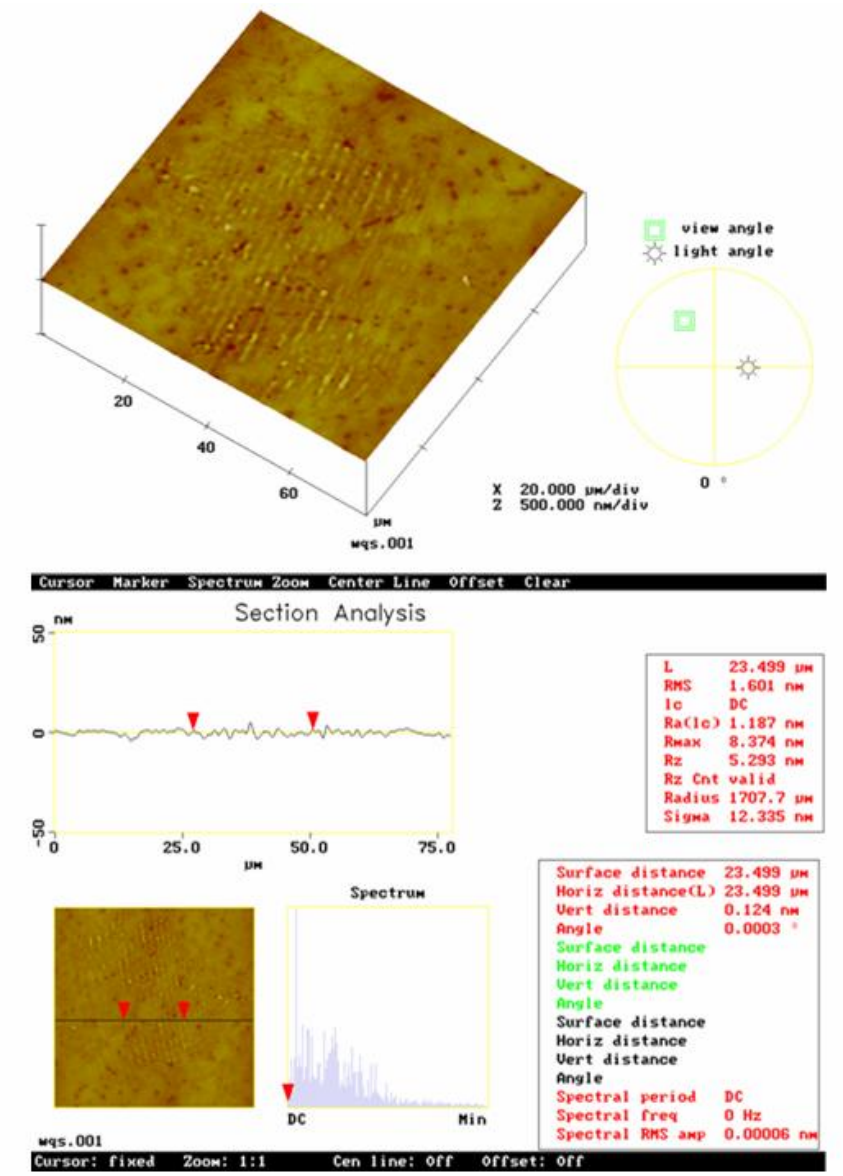

Figure 4.28 AFM profile and analysis of crystalline mark in 100 nm $Ge_2Sb_2Te_5$ films at amorphous background induced by single femtosecond pulse in Figure 4.25.

Figure 4.29 OM images of 100 nm $Ge_2Sb_2Te_5$ films at crystalline background after (left) single pulse irradiation at the energy of 24 μJ and (right) two pulses irradiation. First pulse energy: 24 μJ; Second pulse energy: 30 μJ.

Figure 4.30 OM images of 100 nm $Ge_2Sb_2Te_5$ films at amorphous background after (left) single pulse irradiation at the energy of 36 μJ and (right) two pulses irradiation. First pulse energy: 36 μJ; Second pulse energy: 21 μJ.

Our experiments clearly show that the results for 20 nm and 100 nm $Ge_2Sb_2Te_5$ films are different. Only amorphous mark could be induced by single femtosecond pulse in 20 nm $Ge_2Sb_2Te_5$ films, while single femtosecond pulse could triggered both amorphous and crystalline marks in 100 nm $Ge_2Sb_2Te_5$ films. What are the results of $Ge_2Sb_2Te_5$ films with thickness between 20 nm and 100 nm? 50 nm and 80 nm $Ge_2Sb_2Te_5$ films with the same structure as 20 nm and 100 nm were selected to be irradiated by single femtosecond pulse and the OM images are shown in Figure 4.31

and Figure 4.32, Figure 4.33 and Figure 4.34, respectively. Figure 4.31 and Figure 4.32 show that the results in 50 nm $Ge_2Sb_2Te_5$ films are similar to those in 20 nm $Ge_2Sb_2Te_5$ films. Single femtosecond pulse can induce crystalline to amorphous phase transition in 50 nm $Ge_2Sb_2Te_5$ films, while amorphous to crystalline phase transition cannot be triggered by single 100 fs pulse, as only over-burn marks are observed in Figure 4.32. Figure 4.33 and Figure 4.34 show that the results in 80 nm $Ge_2Sb_2Te_5$ films are similar to those in 100 nm $Ge_2Sb_2Te_5$ films. Single femtosecond pulse can induce not only crystalline to amorphous phase transitions but also amorphous to crystalline phase transition in 80 nm $Ge_2Sb_2Te_5$ films.

Next step, 60 nm and 70 nm $Ge_2Sb_2Te_5$ films with the same structure as previously were fabricated. After irradiated by single femtosecond pulse, the samples were observed with OM and the images are shown in Figure 4.35 and Figure 4.36, Figure 4.37 and Figure 4.38, respectively. Figure 4.35 and Figure 4.36 show that the results in 60 nm $Ge_2Sb_2Te_5$ films are similar to those in 20 nm and 50 nm $Ge_2Sb_2Te_5$ films. Single femtosecond pulse can induce crystalline to amorphous phase transition in 60 nm $Ge_2Sb_2Te_5$ films, while amorphous to crystalline phase transition cannot be triggered by single 100 fs pulse, as only over-burn marks are observed in Figure 4.36. Figure 4.37 and Figure 4.38 show that the results in 70 nm $Ge_2Sb_2Te_5$ films are similar to those in 80 nm and 100 nm $Ge_2Sb_2Te_5$ films. Single femtosecond pulse can induce not only crystalline to amorphous phase transitions but also amorphous to crystalline phase transition in 70 nm $Ge_2Sb_2Te_5$ films.

Finally, 65 nm $Ge_2Sb_2Te_5$ films with the same structure as before was prepared and shined by single femtosecond pulse. The OM images are shown inFigure 4.39 and

Figure 4.40. They show similar results to those in 70 nm, 80 nm and 100 nm $Ge_2Sb_2Te_5$ films. Single femtosecond pulse can induce both crystalline to amorphous phase transitions and amorphous to crystalline phase transitions in 65 nm $Ge_2Sb_2Te_5$ films.

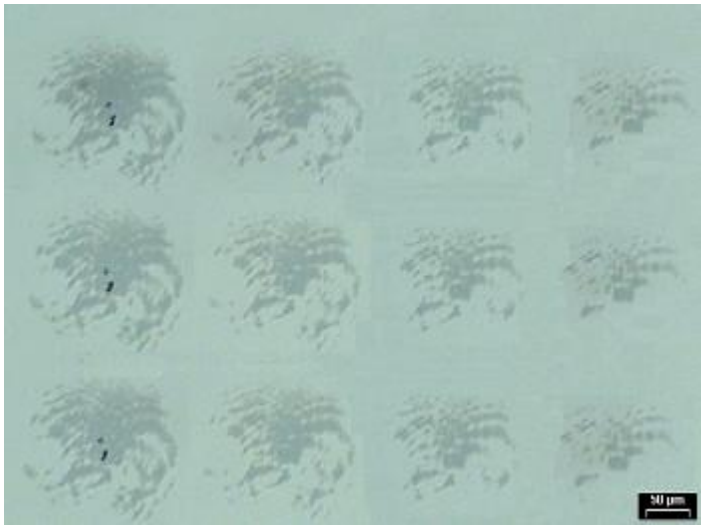

Figure 4.31 OM images of 50 nm $Ge_2Sb_2Te_5$ films at crystalline background after single femtosecond pulse irradiation. Pulse energy from left to right: 10 μJ, 9 μJ, 8 μJ and 7 μJ.

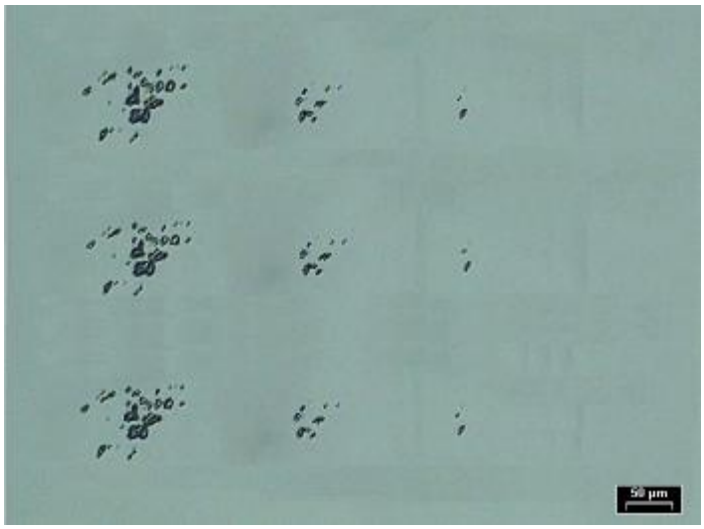

Figure 4.32 OM images of 50 nm $Ge_2Sb_2Te_5$ films at amorphous background after single femtosecond pulse irradiation. Pulse energy from left to right: 13 μJ, 12 μJ,10 μJ, and 9 μJ.

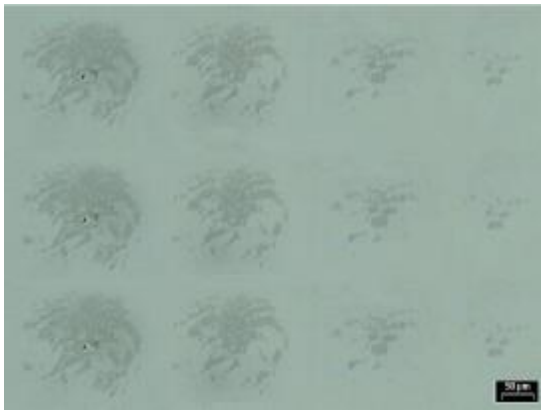

Figure 4.33 OM images of 80 nm $Ge_2Sb_2Te_5$ films at crystalline background after single femtosecond pulse irradiation. Pulse energy from left to right: 10 μJ, 9 μJ, 8 μJ and 7 μJ.

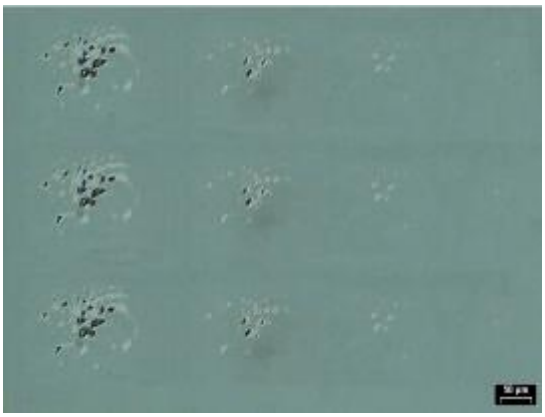

Figure 4.34 OM images of 80 nm $Ge_2Sb_2Te_5$ films at crystalline background after single femtosecond pulse irradiation. Pulse energy from left to right: 13 μJ, 12 μJ, 10 μJ and 9 μJ.

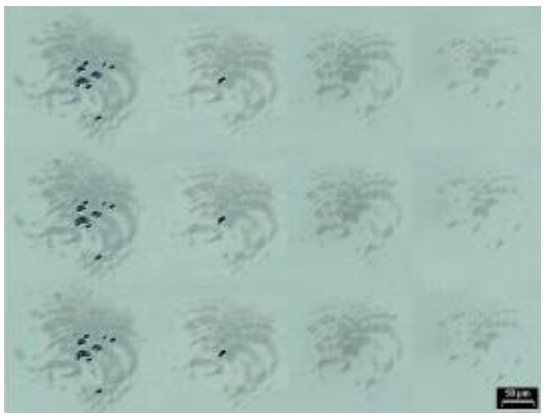

Figure 4.35 OM images of 60 nm $Ge_2Sb_2Te_5$ films at crystalline background after single femtosecond pulse irradiation. Pulse energy from left to right: 10 μJ, 9 μJ, 8 μJ and 7 μJ.

Figure 4.36 OM images of 60 nm $Ge_2Sb_2Te_5$ films at amorphous background after single femtosecond pulse irradiation. Pulse energy from left to right: 13 μJ, 12 μJ, 10 μJ, and 9 μJ.

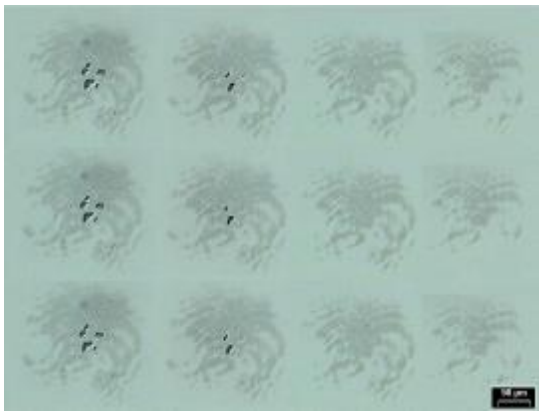

Figure 4.37 OM images of 70 nm $Ge_2Sb_2Te_5$ films at crystalline background after single femtosecond pulse irradiation. Pulse energy from left to right: 10 μJ, 9 μJ, 8 μJ and 7 μJ.

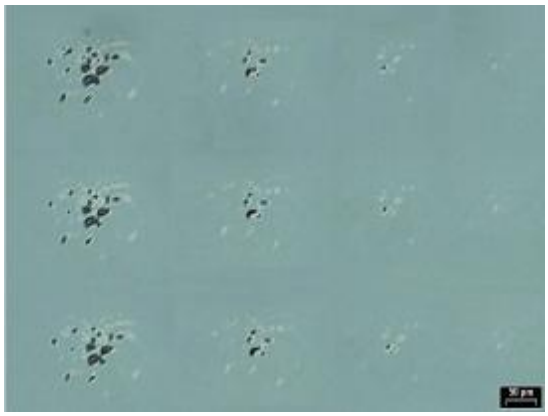

Figure 4.38 OM images of 70 nm $Ge_2Sb_2Te_5$ films at amorphous background after single femtosecond pulse irradiation. Pulse energy from left to right: 13 μJ, 12 μJ, 10 μJ, and 9 μJ.

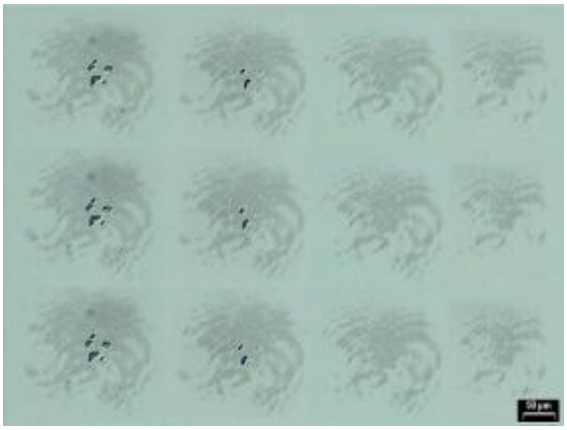

Figure 4.39 OM images of 65 nm $Ge_2Sb_2Te_5$ films at crystalline background after single femtosecond pulse irradiation. Pulse energy from left to right: 10 μJ, 9 μJ, 8 μJ and 7 μJ.

Figure 4.40 OM images of 65 nm $Ge_2Sb_2Te_5$ films at amorphous background after single femtosecond pulse irradiation. Pulse energy from left to right: 13 μJ, 12 μJ, 10 μJ, and 9 μJ.

The results in $Ge_1Sb_2Te_4$ films are similar to those in $Ge_2Sb_2Te_5$ films. For 20 nm $Ge_1Sb_2Te_4$ films, single femtosecond pulse can induce crystalline to amorphous phase transition (Figure 4.41). While amorphous to crystalline phase transition could not be achieved as only over-burn mark was observed in Figure 4.42. For 100 nm $Ge_1Sb_2Te_4$ films, single femtosecond pulse can induce not only crystalline to amorphous phase transitions (Figure 4.43), but also amorphous to crystalline phase transition (Figure 4.44)

in 100 nm $Ge_1Sb_2Te_4$ film. This amorphous phase to crystalline phase transition is also verified by X-ray diffractometer (XRD) measurement (Figure 4.45). The two peaks are FCC (200) and (220).

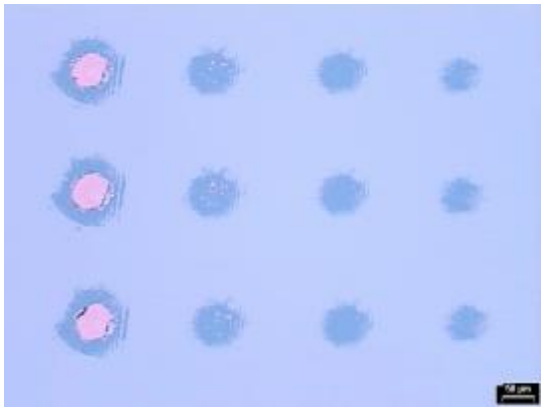

Figure 4.41 OM image of 20 nm $Ge_1Sb_2Te_4$ films at crystalline background after single femtosecond pulse irradiation. Pulse energy from left to right: 12 μJ, 10 μJ, 8 μJ and 6 μJ.

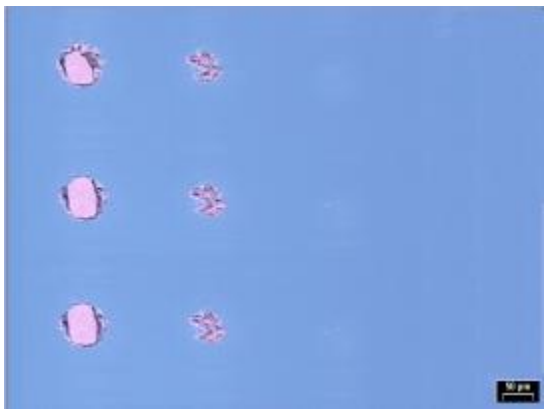

Figure 4.42 OM image of 20 nm $Ge_1Sb_2Te_4$ films at amorphous background after single femtosecond pulse irradiation. Pulse energy from left to right: 16 μJ, 14 μJ, 12 μJ and 10 μJ.

The results in 20 nm $Ag_5In_5Sb_{30}Te_{60}$ films (Figure 4.46 and Figure 4.47) are also similar to those in 20 nm GeSbTe films that single femtosecond pulse can induce amorphous marks at crystalline background and crystalline marks cannot be triggered

by single femtosecond pulse at amorphous background. However, the results in 100 nm $Ag_5In_5Sb_{30}Te_{60}$ films (Figure 4.48 and Figure 4.49) are quite different from those in 100 nm GeSbTe films. Although single femtosecond pulse can induce amorphous marks at crystalline background (Figure 4.48), amorphous to crystalline phase transition cannot be achieved by single femtosecond pulse as only over-burn marks are observed in Figure 4.49. One possible reason is that the crystallization mechanism of GeSbTe materials is nucleation dominated (nucleation rate is larger than growth rate), while AgInSbTe is growth dominated (growth rate is larger than nucleation rate).

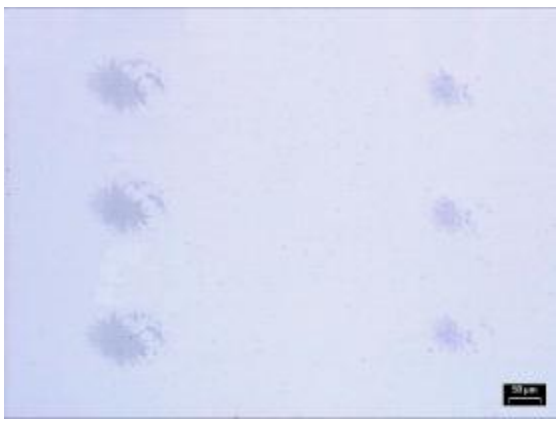

Figure 4.43 OM images of 100 nm $Ge_1Sb_2Te_4$ films at crystalline background after single femtosecond pulse irradiation. Pulse energy from left to right: 12 μJ and 10 μJ.

Figure 4.44 OM images of 100 nm $Ge_1Sb_2Te_4$ films at amorphous background after single femtosecond pulse irradiation. Pulse energy from left to right: 21 μJ and 18 μJ.

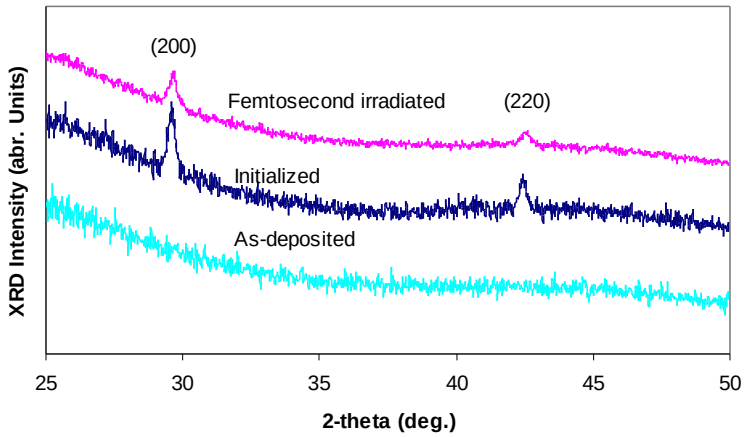

Figure 4.45 XRD patterns of 100 nm $Ge_1Sb_2Te_4$ films at as-deposited phase and after initialization and single 100fs laser irradiation.

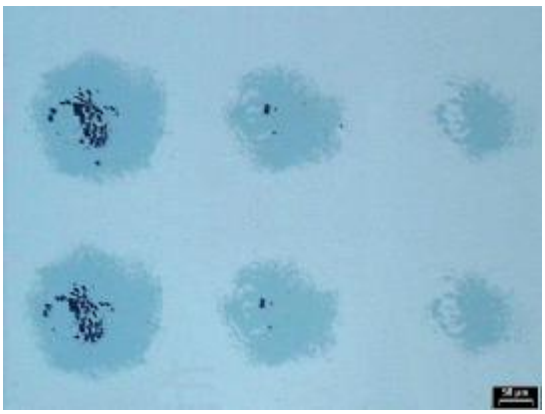

Figure 4.46 OM images of 20 nm $Ag_5In_5Sb_{30}Te_{60}$ films at crystalline background after single femtosecond pulse irradiation. Pulse energy from left to right: 10 μJ, 8 μJ and 6 μJ.

Figure 4.47 OM images of 20 nm $Ag_5In_5Sb_{30}Te_{60}$ films at amorphous background after single femtosecond pulse irradiation. Pulse energy from left to right: 12 μJ, 10 μJ and 8 μJ.

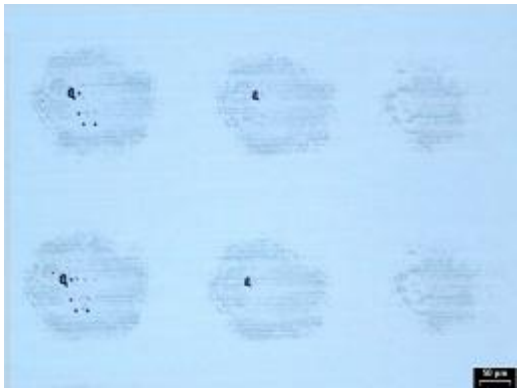

Figure 4.48 OM images of 100 nm $Ag_5In_5Sb_{30}Te_{60}$ films at crystalline background after single femtosecond pulse irradiation. Pulse energy from left to right: 16 μJ, 14 μJ and 12 μJ.

Figure 4.49 OM images of 100 nm $Ag_5In_5Sb_{30}Te_{60}$ films at amorphous background after single femtosecond pulse irradiation. Pulse energy from left to right: 16 μJ, 14 μJ and 12 μJ.

4.3.2 Discussions

Phase transitions triggered by ultrafast laser pulses on semiconductor surface have raised tremendous interests and controversy. Many experiments [5][6][7][9][15] and theoretical studies [109][110][111][112][113] suggest that exciting high-carrier densities (~10^{22} cm^{-3}) induced by intense femtosecond laser pulse in semiconductors can give rise to ultrafast nonthermal disordering on the femtosecond time scale. This ultrafast disordering is termed as nonthermal melting because the optical properties

of the disordering phase approach to those of melted phase, though disordering occurs before a significant amount of energy is transferred to the lattice by conventional electron-phonon interactions. Furthermore, excitation with pulses shorter than the longitudinal optical (LO) phonon emission time [13] in crystalline semiconductors may induce structural instability of the lattice, leading to the formation of a metastable transient phase with (semi) metallic character [13].

According to our previous measured refractive index of phase change media, the absorption depth of amorphous and crystalline phase change media at the wavelength of 800 nm is approximately 40 nm and 18 nm (Table 4-3), respectively.

Table 4-3 Absorption depth (α^{-1}) of some phase change media at the wavelength of 800 nm.

Material	Thickness(nm)	$a^{-1}_{amorphous}$ (nm)	$a^{-1}_{crystallines}$ (nm)
$Ge_1Sb_2Te_4$	20	40	18
	100	43	17
$Ge_2Sb_2Te_5$	20	45	19
	100	48	16
$Ag_5In_5Sb_{30}Te_{60}$	20	40	14
	100	37	15

Our experiments clearly show that single femtosecond pulse can induce crystalline to amorphous phase transition in $Ge_2Sb_2Te_5$, $Ge_1Sb_2Te_4$ and $Ag_5In_5Sb_{30}Te_{60}$ films. This may be due to that the irradiation by femtosecond pulse is quite different from that by conventional laser. When the conventional laser irradiates on a sample, the heating time is rather long and the excitation process includes the heat diffusion in the layers. The irradiation by conventional laser has three stages: laser spot exposure and energy deposition, heat diffusion outside the laser spot, cooling after the laser exposure. The

thermal diffusion process which is the fundamental limitation of conventional laser recording because it will not only make the mark size wider than laser spot size but also deform the disk appears in the second and third process.

While at femtosecond laser irradiation on a sample, the energy is deposited within a very short time in a thin surface layer, leading to heating or melting. The so generated steep temperature gradient is subsequently smoothed by the heat diffusion towards the substrate. The characteristic diffusion length L_{th} during the pulse duration t depends on the thermal diffusivities D of the films according to $L_{th} \approx (Dt)^{1/2}$. The diffusion length during the fs pulse is negligible [$L_{th} \approx 0.2$ nm for $t = 100$ fs and $D(Ge_2Sb_2Te_5) = 0.0045$ cm^2/s] [114], whereas it might exceed 20 nm when using ns laser pulse as commonly done in optical disk. Furthermore, femtosecond pulse has much higher peak power compared to the conventional laser pulse. It can create a large number of highly excited electrons and holes before energy transfers from the excited carriers to the lattice. The free carriers reach extreme high energy while the lattice of atoms is still cold, which gives rise to novel and unusually phase transition.

Simulations [115] at the University of Arizona revealed that sub-nanosecond pulse could enhance the cooling rate by more than an order of magnitude higher than that of nanosecond pulse. Rapid cooling favors the formation of amorphous mark with smooth boundary. And Te-based chalcogenide glasses have the characteristic of long-chain structure which gives the medium small mobility in the liquid state. They tend to solidify while keeping the atomic distribution of the liquid state. Since the atoms keep the positions of the liquid state, they easily convert into the amorphous state when

cooled rapidly. Given the rapid cooling rate of femtosecond pulse, amorphization is possible after femtosecond pulse shines on phase change media.

Our results also show that single femtosecond pulse can induce crystalline to amorphous and amorphous to crystalline phase transitions in 100 nm $Ge_2Sb_2Te_5$ and $Ge_1Sb_2Te_4$ films. Intense femtosecond laser pulse may induce an ultrafast nonthermal phase transition in GeSbTe films. However, once the energy has been transferred from the free carriers to the lattice, the structural transformation path is thermal in nature. The following scenario was proposed to describe the principal processes that take place after femtosecond pulse shines on the sample. Femtosecond pulse first excites a thin layer of highly excited carriers on the surface of the 100 nm sample. Below the excited layer there is an intact layer of phase change films. The phase change taking place is mainly defined by the heat flow conditions. The cooling speed will determine the final state. Rapid cooling will promote amorphization, while slow cooling will catalyze crystallization. The cooling speed in the center of Gaussin beam is lower than that in the fringe. Furthermore, initial solidification will release enthalpy that will lower the supercooling to frustrate amorphization process and promote the nucleation and growth of the crystalline phase. The amount of latent heat released unpon solidification is related to amount of phase transition material. For 100 nm films, the enthalpy released during the solidification process may be large enough to reduce supercooling, thus promoting the nucleation and growth of the crystalline material. This recalescence frustrated amorphization process has been reported to occur on bulk solidification of Ge films [116] and GeSb films [21] upon picosecond laser irradiation.

Although ultrafast crystallization is observed in 100 nm $Ge_2Sb_2Te_5$ and $Ge_1Sb_2Te_4$ films, femtosecond pulse cannot induce amorphous to crystalline phase transition in 100 nm $Ag_5In_5Sb_{30}Te_{60}$ films. This may be due to the different crystalline mechanism of AgInSbTe and GeSbTe films.

Nevertheless, a more precision analysis cannot be given here. Intense femtosecond laser pulse may induce an ultrafast nonthermal phase transition in phase change media. The ultrafast dynamics in phase change media, to our knowledge, has never been investigated. Whether the mechanism of phase transitions in phase change media triggered by single femtosecond laser pulse is thermal or nonthermal is not clear yet. It needs to be further clarified with pump-probe setup, which is the focus of chapter 5: ultrafast dynamics in phase-change media excited by intense femtosecond laser pulse.

4.3.3 Conclusions

Our static experiments clear show that single femtosecond pulse can induce only crystalline to amorphous phase transition in 20 nm $Ge_2Sb_2Te_5$, $Ge_1Sb_2Te_4$ and $Ag_5In_5Sb_{30}Te_{60}$ films. Crystalline to amorphous and amorphous to crystalline phase transitions triggered by single femtosecond pulse have been observed in 100 nm $Ge_2Sb_2Te_5$ and $Ge_1Sb_2Te_4$ films. For $Ge_2Sb_2Te_5$ films with thickness no more than 60 nm, the results are similar to those of 20 nm films that single femtosecond pulse can induce only crystalline to amorphous phase transition and amorphous to crystalline phase transition could not be triggered by single femtosecond pulse. If the thickness of $Ge_2Sb_2Te_5$ films is no less than 65 nm, the results are similar to those in 100 nm films

that single femtosecond pulse can induce both crystalline to amorphous and amorphous to crystalline phase transitions.

4.4 Chapter Summary

In this chapter, the refractive indexes of phase change media were measured with Steag Etaoptic ETA-RT quality control system. The optical energy band gap of phase change media were calculated with the measured refractive index. The sample structures were designed with our in-house developed PCODD software and the measured refractive index of phase change media. Our the static experiments showed that single femtosecond pulse can induce crystalline to amorphous phase transition in 20 nm $Ge_2Sb_2Te_5$, $Ge_1Sb_2Te_4$ and $Ag_5In_5Sb_{30}Te_{60}$ films. Both crystalline to amorphous and amorphous to crystalline phase transitions triggered by single femtosecond pulse have been achieved only in 100 nm GeSbTe films. These ultrafast phase transitions were investigated by refractive measurement, XRD measurement and AFM measurement.

Chapter 5 Dynamics in phase change media following femtosecond laser excitation

Femtosecond laser-induced phase transitions in semiconductors have been the subject of interests ever since the development of femtosecond laser. The earlist experiments on femtosecond laser-excited semiconductors measured transient reflectivity [5][6], transmission [7], and provided evidence of phase changes in the materials within a few hundred femtoseconds after excitation. More recently, time-resolved visible-pump, x-ray diffraction probe experiments [98][98][101][102][103][104][105][105] provide direct evidences of milli-angstrom changes in lattice spacing after excitation by intense femtosecond pulse.

Several theoretical studies have addressed the electronic and structural transitions of semiconductors after irradiation by intense ultrafast. Many studies [113][109][110][111][112] shows that the breaking of covalent bonds by the electronic excitation causes rapid softening of the phonon modes. This softening leads to lattice instability within subpicosecond after excitation by femtosecond laser when approximately 10% of the valence electrons are excited.

It’s now clear that intense femtosecond laser excites the materials in extremely nonequalibrium conditions, which may give rise to novel phase transitions. Femtosecond laser inducing nonthermal phase transitions have been demonstrated in many

semiconductors, such as Si [5][6], GaAs [10][11]. Our static experiments in previous chapter clearly show that single femtosecond pulse can induce crystalline to amorphous and amorphous to crystalline phase transitions in 100 nm $Ge_2Sb_2Te_5$ and $Ge_1Sb_2Te_4$ films, while amorphous to crystalline phase transition cannot be induced by single femtosecond pulse in 100 nm $Ag_5In_5Sb_{30}Te_{60}$ films. The pump-probe setup described in chapter 3 could be employed to investigate the ultrafast dynamics in 100 nm amorphous $Ge_2Sb_2Te_5$ and $Ag_5In_5Sb_{30}Te_{60}$ films after irradiation by femtosecond pulse.

In this chapter, time-resolved measurement of reflective intensity change of 100 nm amorphous $Ge_2Sb_2Te_5$ and $Ag_5In_5Sb_{30}Te_{60}$ films after excitation by single femtosecond pulse will be presented. Our results clarify the nature of phase transitions in 100 nm amorphous $Ge_2Sb_2Te_5$ and $Ag_5In_5Sb_{30}Te_{60}$ films induced by femtosecond pulse.

5.1 Experiment in 100 nm amorphous $Ge_2Sb_2Te_5$ films

Our previous experiments clearly show that single femtosecond pulse can induce amorphous to crystalline phase transitions in 100 nm $Ge_2Sb_2Te_5$ films. Ultrafast time-resolved microscopy with both femtosecond time and micrometer spatial resolution [26], as described in chapter 3, was employed to monitor the evolution of the reflective intensity of 100 nm amorphous $Ge_2Sb_2Te_5$ surface after irradiated by single femtosecond laser in order to gain insight into the phase transition induced by femtosecond pulse.

The sample structure was: 0.6 mm polycarbonate substrate/ $(ZnS)_{80}(SiO_2)_{20}$ 120 nm/ $Ge_2Sb_2Te_5$ 100 nm/ $(ZnS)_{80}(SiO_2)_{20}$ 92 nm/ air

The sample was fabricated by a Balzers Cube sputtering system, which was guided by windows-based software. The 100 nm $Ge_2Sb_2Te_5$ films were sputtered using the DC magnetron sputtering method. The $(ZnS)_{80}(SiO_2)_{20}$ dielectric layers were sputtered by the RF sputtering method. The as-deposited sample was at amorphous background.

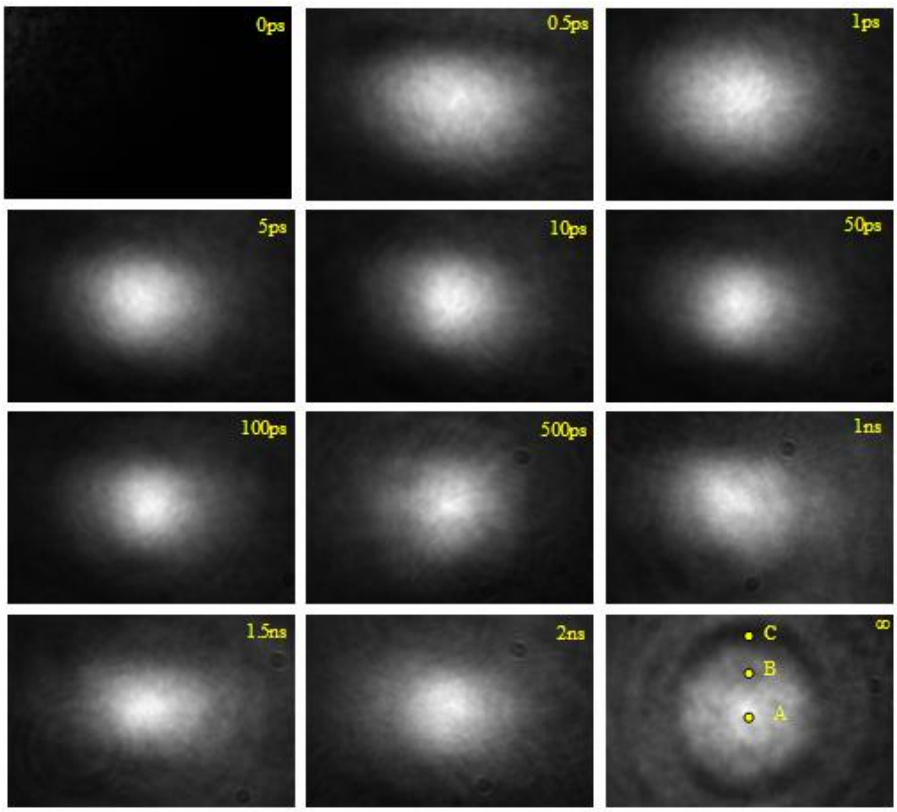

Figure 5.1 Pictures of 100 nm $Ge_2Sb_2Te_5$ surface at amorphous background at different time delay after exposure to the pump pulse at the energy of 14 μJ.

A sequence of micrographs of 100 nm $Ge_2Sb_2Te_5$ films at amorphous background, covering the entire period from initial deposition of laser energy to the appearance of final structural modifications, is shown in Figure 5.1. The contrast of the images in Figure 5.1 has not been enhanced and thus Figure 5.1 does provide a quantitative measurement of the evolution of the reflective intensity. Due to the large angle of 45°

between the pump beam and the probe beam, the actual delay depends on the spatial coordinate along the horizontal axis of the image (100 fs /42 μm). But the delay is constant in the vertical direction (Zero delay in Figure 5.1 is referred to the center of the spot). In the first frame ((Δt=0 ps), There is no bright spot in the center of the probe spot because the pump beam and the probe beam took an equal amount of time to reach the sample. In the next two frames (0.5 ps, 1 ps), the reflective intensity of the region irradiated by whole pump beam increased, giving rise to the appearance of an elliptical bright area without a sharply defined boundary. The bright region diminished in size at later delay (5 ps, 10 ps), then enlarged at even later delay (500 ps). The bright region in the surface area irradiated by pump beam remained nearly unchanged for approximately 2 ns delay. The bright region in the center of the probe spot in the last frame (Δt=∞), corresponding to a delay of several seconds, indicating that crystalline mark was formed in 100 nm amorphous $Ge_2Sb_2Te_5$ films after irradiation by single pump beam. The subsequent morphology examination of the final state after the irradiation by the single femtosecond pump pulse is shown in Figure 5.2. It indicated the formation of crystalline mark in 100 nm amorphous $Ge_2Sb_2Te_5$ films. This amorphous to crystalline phase transition induced by single femtosecond pulse had been further corroborated by X-ray diffractometer measurement in Chapter 4. Our result obtained from 100 nm amorphous $Ge_2Sb_2Te_5$ films is consistent with that of earlier experiments [22] using α-GeSb films. Electron diffraction in earlier experiments corroborated that intense femtosecond pulse can permanently induce a stable crystalline phase in α-GeSb films.

To quantitatively follow the evolution of the reflectivity intensity change of 100 nm amorphous $Ge_2Sb_2Te_5$ films after irradiation by single femtosecond pulse, the

reflectivity intensity change as a function of delay time is shown in Figure 5.3. Due to the Gaussian intensity profile of the focused pump beam, different spatial locations on the sample represent the behavior of the reflective intensity for different pump fluence. Three fluences were chosen, marked A, B and C in Figure 5.1, corresponding to excitation fluence of 60, 45 and 20 mJ/cm^2, respectively. Figure 5.3 shows that the reflective intensity change increased immediately after femtosecond pulse irradiation for all three fluences. It is likely that femtosecond pulse can induce non-thermal phase transition. Figure 5.3 also shows that the maximum reflective intensity for high and low fluence was different. The maximum reflective intensity was higher for high fluence (A) than that for low fluence (C). Our result that different fluence reached different maximum reflective intensity change in $Ge_2Sb_2Te_5$ films is different from that in GeSb [20] which reached the same maximum reflectivity for high and medium fluence. It may be that the carrier density excited by femtosecond pulse is higher for high fluence than that for low fluence. Figure 5.3 indicates that high and medium fluence triggered a transition from amorphous phase to crystalline and partial crystalline phase transitions, respectively, while low fluence may not induced phase transition. For high fluence (A), the reflective intensity continuously increased until 10 ps (Figure 5.3). However, the reflective intensity began to fluctuate after 1 ps delay for low fluence (C) (Figure 5.3). This may be one reason accounting for that high fluence triggered a transition from amorphous phase to crystalline phase transitions, while low fluence may not induced phase transition. Our result in $Ge_2Sb_2Te_5$ films is consistent with that of earlier experiments [22] using GeSb films that high fluence can induce amorphous to crystalline phase transition.

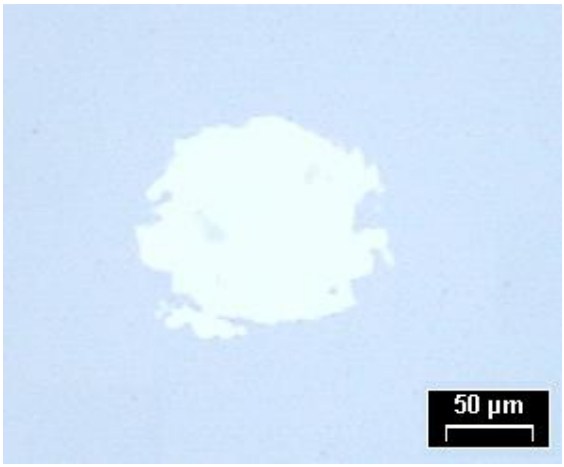

Figure 5.2 OM image of 100 nm amorphous $Ge_2Sb_2Te_5$ films after single femtosecond pump pulse irradiation at the energy of 14 μJ.

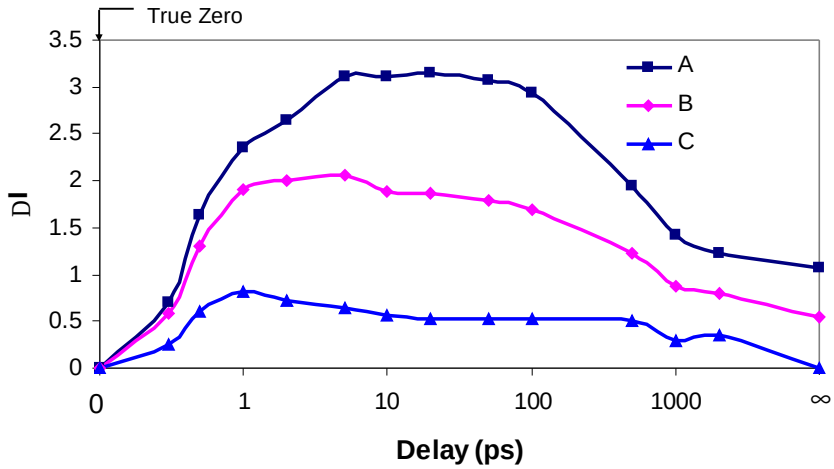

Figure 5.3 Reflectivity as a function of delay time measured at three different locations (marked as *A*, *B*, and *C* in the last frame of Figure 5.1), corresponding to excitation fluence of 60, 45 and 20 mJ/cm^2, respectively. Note the logarithmic time axis; the true zero delay (see text) is marked by an arrow. $\Delta I=[I(t)-I_a]/I_a$ and I_a is the reflective intensity of 100 nm amorphous $Ge_2Sb_2Te_5$ films.

5.2 Experiment in 100 nm amorphous $Ag_5In_5Sb_{30}Te_{60}$ films

Our previous experiments show that single femtosecond pulse cannot induce amorphous

phase to crystalline phase transition in 100 nm $Ag_5In_5Sb_{30}Te_{60}$ films. Ultrafast time-resolved microscopy [26] was employed to monitor the evolution of the reflective intensity of 100 nm amorphous $Ag_5In_5Sb_{30}Te_{60}$ surface after irradiation by single femtosecond pulse in order to gain insight into the ultrafast dynamics in 100 nm amorphous $Ag_5In_5Sb_{30}Te_{60}$ films following femtosecond laser excitation.

The sample structure was: 0.6mm polycarbonate substrate/ $(ZnS)_{80}(SiO_2)_{20}$ 120 nm/ $Ag_5In_5Sb_{30}Te_{60}$ 100 nm/ $(ZnS)_{80}(SiO_2)_{20}$ 92 nm/ air, which is similar to previous experiment in 100 nm $Ge_2Sb_2Te_5$ for comparison.

The sample was fabricated by a Balzers Cube sputtering system, which was guided by windows-based software. The 100 nm $Ag_5In_5Sb_{30}Te_{60}$ films were sputtered using the DC magnetron sputtering method. The $(ZnS)_{80}(SiO_2)_{20}$ dielectric layers were sputtered by the RF sputtering method. The as-deposited samples were at amorphous background.

First the right energy for the pump-probe experiment should be chosen. The same energy was tried in 100 nm amorphous $Ag_5In_5Sb_{30}Te_{60}$ films as that in $Ge_2Sb_2Te_5$ films (14 μJ). The OM image did not show any phase transition in 100 nm amorphous $Ag_5In_5Sb_{30}Te_{60}$ films after irradiation by single femtosecond pulse. Then the energy was slightly increased to 15 μJ. After femtosecond laser irradiation on 100 nm amorphous $Ag_5In_5Sb_{30}Te_{60}$ films and $Ge_2Sb_2Te_5$ films, the sample was observed with the OM, as shown in Figure 5.4 and Figure 5.5, respectively. After exposure to single femtosecond pulse at the energy of 15 μJ, an over burn mark without surrounding crystalline phase is formed in 100 nm amorphous $Ag_5In_5Sb_{30}Te_{60}$ films (Figure 5.4), while an over burn mark with surrounding crystalline phase is observed in 100 nm amorphous $Ge_2Sb_2Te_5$

films (Figure 5.5). Figure 5.4 indicates that the energy of 15 μJ was too high for experiment. So it was changed back to 14 μJ to perform the pump-probe experiment in 100 nm amorphous $Ag_5In_5Sb_{30}Te_{60}$ films.

Figure 5.4 OM image of 100 nm amorphous $Ag_5In_5Sb_{30}Te_{60}$ films after exposure to single femtosecond pulse at the energy of 15 μJ.

Figure 5.5 OM image of 100 nm amorphous $Ge_2Sb_2Te_5$ films after exposure to single femtosecond pulse at the energy of 15 μJ.

Figure 5.6 is a sequence of micrographs of 100 nm amorphous $Ag_5In_5Sb_{30}Te_{60}$ films, covering the entire period from initial deposition of laser energy to the appearance of the final structural modifications. The micrographs in 100 nm amorphous $Ag_5In_5Sb_{30}Te_{60}$ films (Figure 5.6) are almost similar to those in 100 nm $Ge_2Sb_2Te_5$ films (Figure 5.1) except the last frame ($\Delta t=\infty$). After exposure to femtosecond pulse, there is no bright spot

in the last frame of 100 nm amorphous $Ag_5In_5Sb_{30}Te_{60}$ films (Figure 5.6), while a bright spot is observed in the last frame of 100 nm amorphous $Ge_2Sb_2Te_5$ films (Figure 5.1).

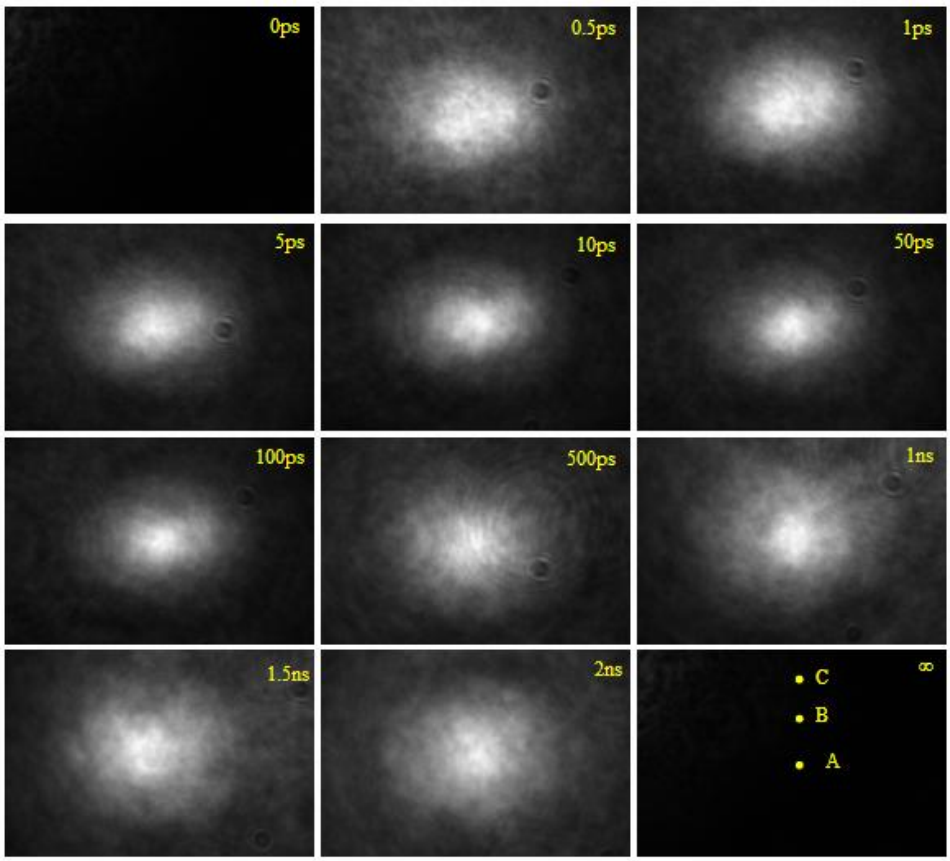

Figure 5.6 Pictures of 100 nm amorphous $Ag_5In_5Sb_{30}Te_{60}$ surface at different time delay after exposure to the pump pulse at the energy of 14 μJ.

Figure 5.6 shows that the reflective intensity of the area illuminated by pump-probe was almost the same as that irradiated by probe beam in the first frame ((Δt=0 ps) because the probe beam and the pump beam spend eaqual time to reach the sample. In the next two frames (0.5 ps and 1 ps), the reflective intensity of the region irradiated by whole pump beam increased, which gave rise to the appearance of an elliptical bright area without a sharply defined boundary. The appearance of the bright region in the surface area irradiated by pump beam remained nearly unchanged for approximately 2 ns delay.

However, the bright region disappeared in the last frame ($\Delta t=\infty$), corresponding to a delay of several seconds, indicating that re-amorphization took place in 100nm amorphous $Ag_5In_5Sb_{30}Te_{60}$ films after irradiation by single pump beam.

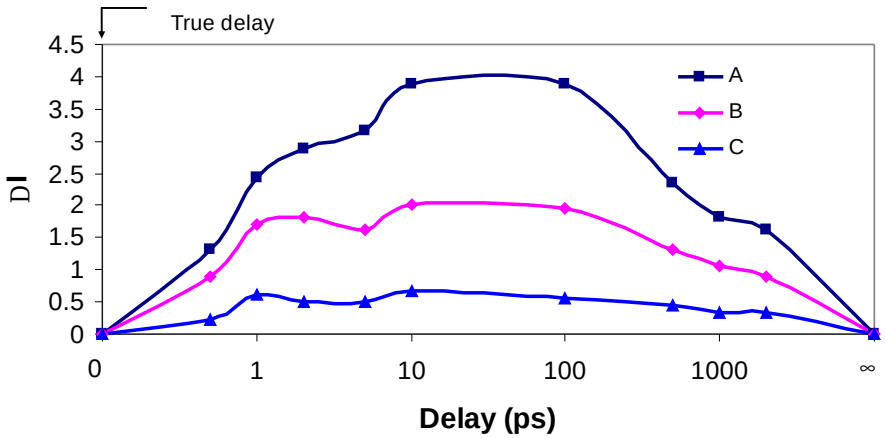

Figure 5.7 Reflectivity as a function of delay time measured at three different locations (marked as *A*, *B*, and *C* in the last frame of Figure 5.6), corresponding to excitation fluence of 60, 45 and 20 mJ/cm^2, respectively.. Note the logarithmic time axis; the true zero delay (see text) is marked by an arrow. $\Delta I=[I(t)-I_a]/I_a$ and I_a is the reflective intensity of 100 nm amorphous $Ag_5In_5Sb_{30}Te_{60}$ films.

To quantitatively follow the evolution of the reflectivity intensity change of 100 nm amorphous $Ag_5In_5Sb_{30}Te_{60}$ films after irradiation by single femtosecond pulse, the reflectivity intensity change as a function of delay time measured at three different fluences (marked in the last frame of Figure 5.6) is shown in Figure 5.7. The change in reflectivity intensity of 100 nm amorphous $Ag_5In_5Sb_{30}Te_{60}$ films shows similar behavior to that of 100 nm amorphous $Ge_2Sb_2Te_5$ films except for the final state. Re-amorphization on solidification in 100 nm amorphous $Ag_5In_5Sb_{30}Te_{60}$ films might occur for all three fluence, while high fluence induced crystallization in 100 nm amorphous $Ge_2Sb_2Te_5$ films. Figure 5.7 shows that the reflective intensity change increased immediately after femtosecond pulse irradiation for all three fluences. It is possible

because non-thermal phase transitions induced by femtosecond pulse have been found in many materials. Figure 5.7 also shows that the maximum reflective intensity for high and low fluence was different. The maximum reflective intensity was higher for high fluence (A) than that for low fluence (C). One possible reason is that the excited carrier density may be proportional to the laser fluence.

5.3 Analysis and discussion

5.3.1 Carrier excitation

The carrier dynamics after irradiation by intense femtosecond pulse begins with the excitation of themselves. The carrier relaxation begins during the excitation pulse. The lattice can also be changed as a direct result of electrons being excited from bonding state to anti-bonding states. So it is very important to know the excitation mechanism in $Ge_2Sb_2Te_5$ films and $Ag_5In_5Sb_{30}Te_{60}$ films after irradiation by femtosecond pulse.

Figure 5.8 illustrates different excitation mechanisms in semiconductors after irradiation by light. When photon energy is higher than the smallest band gap between conduction and valence states, single photon absorption occurs. Figure 5.8 (a) and (b) schematically show single photon absorption in direct band gap and in indirect band gap, respectively. Because single photon absorption in indirect band gap needs phonon assistance to conserve the momentum, direct vertical transition dominates the indirect one when both are allowed. When the minimum band gap is larger than photon energy, multiphoton absorption (Figure 5.8 (c)) occurs. These three processes increase both the energy and the

carrier density. Free carriers can also absorb photons and move to higher energy level, as shown in Figure 5.8 (d). Free carriers absorption increases only the energy, not the density of free carriers. When some carriers have excess energy above the bottom of the conduction band which is higher than the band gap, they may give their excess energy to the holes in the valence band. Then impact ionization occurs. In this process, a high energy electron loses energy and falls lower in the conduction band. Meanwhile a hole in the valence band gains energy and moves to higher energy level, as shown in Figure 5.8 (e). Therefore, impact ionization increases only the density of free carriers, not the total energy. Because no photon absorption is involved in impact ionization, it may begin during laser excitation and will continue after laser pulse duration.

As calculated in chapter 4, the as-deposited $Ge_2Sb_2Te_5$ films and $Ag_5In_5Sb_{30}Te_{60}$ films have an allowed indirect band gap at approximately 0.7 eV and 0.6 eV, respectively. The wavelength of the incident optical pulse is 800 nm, which is 1.55 eV. Therefore, single photon indirect absorption will be the dominant excitation process during pulse duration. This process needs phonon assistance to conserve the momentums as the transition is indirect. In addition, free carriers will also absorb photon to promote carriers from low energy level to high energy level. And nonlinear absorption processes, such as two-photon absorption process, which are intensity-dependent, may begin to play an important role at high fluence. Furthermore, the high density of free carriers will decrease the absorption depth of the pump pulse. Carriers excited by the front part of the pump pulse may change the refractive index of $Ge_2Sb_2Te_5$ and $Ag_5In_5Sb_{30}Te_{60}$ films and affect the photon absorption of the rear part of the pulse. It is possible that both nonlinear absorption processes and change in refractive index by the front part of pulse contribute

to the excitation process. All these processes take place during pulse duration.

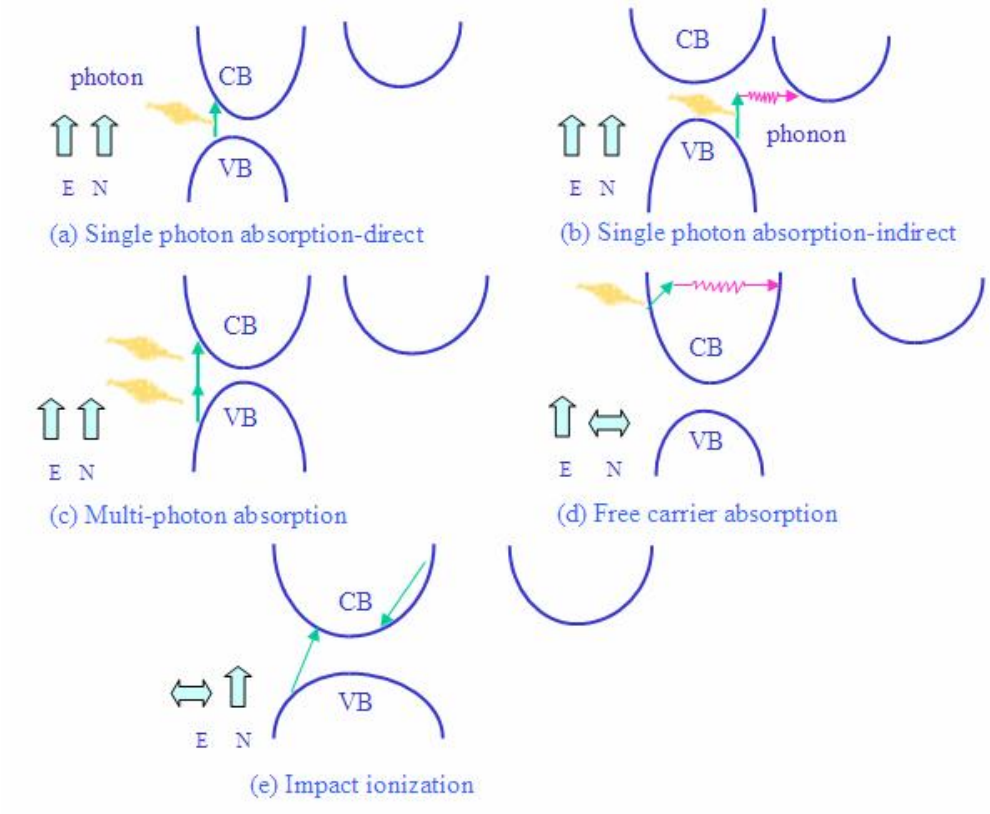

Figure 5.8 Carriers excitation mechanisms in semiconductors.

The intense femtosecond pulse creates a large amount of free carriers with high excess energy. Since the excess energy of the excited carriers via single photon absorption in 100 nm amorphous $Ge_2Sb_2Te_5$ and $Ag_5In_5Sb_{30}Te_{60}$ films is higher than their optical energy bandgaps, impact ionization will occur. It may begin during the pulse duration and will continue to increase carrier density after laser pulse duration. Impact ionization is the dominant carrier excitation process after the deposition of laser energy, which may accounts for the high reflectivity intensity lasting after laser pulse duration in Figure 5.3 and Figure 5.7.

The large amount of free carriers with high excess energy created by femtosecond pulse in 100 nm $Ge_2Sb_2Te_5$ and $Ag_5In_5Sb_{30}Te_{60}$ films will quickly redistribute and thermalize between themselves and lattice via carrier-carrier scattering and carrier phonon scattering [117].

5.3.2 Carrier and lattice dynamics

After carrier excitation, carrier and lattice will relax to reduce carrier density and energy. Carrier and lattice dynamics are modeled following S. K. Sundaram and E. Mazur [118]. The incident optical energy couples into the material by exciting electrons from the valance band (bonging state) to the conduction band (anti-bonding state). The sudden change of inter-atomic potential induced by intense femtosecond pulse immediately excites optical phonons. The time scale for excited carriers to transfer energy to longitudinal optical (LO) phonon is expected in several hundred femtoseconds [119][120]. Nevertheless, transfer energy from excited carriers to thermal motion of lattice is supposed to take many picoseconds. Because the emitted phonons carry little energy, LO phonon may take many scattering processes, and therefore several picoseconds are needed for carrier energy relaxation. Then the non-equilibrium high population LO photons decay into acoustic photons [99]. Thus phase transition in the time scale less than several picoseconds cannot be related to thermal model. The reflective intensity increase in our experiment (Figure 5.3 and Figure 5.7) was within picosecond time scale. It could not be interpreted with conventional thermal phase transition. A non-thermal phase transformation induced by a softening of the lattice structure due to the generation of a high density electron-hole population was suggested

to be the mechanism of the picosecond intensity increase in 100 nm amorphous $Ge_2Sb_2Te_5$ and $Ag_5In_5Sb_{30}Te_{60}$ films after excitation by single femtosecond pulse, as shown in Figure 5.9. In the frame of the theoretical models [109][110][111][112][113], nonthermal phase transformation is due to lattice destabilization in the presence of a dense electron-hole plasma. If the plasma density exceeds a critical value (approximately 10^{22} cm^{-3}, about 10% of the whole valence population), the transition to a disordered state is possible within a few vibrational periods. This process occurs homogeneously wherever the stability limit is exceeded.

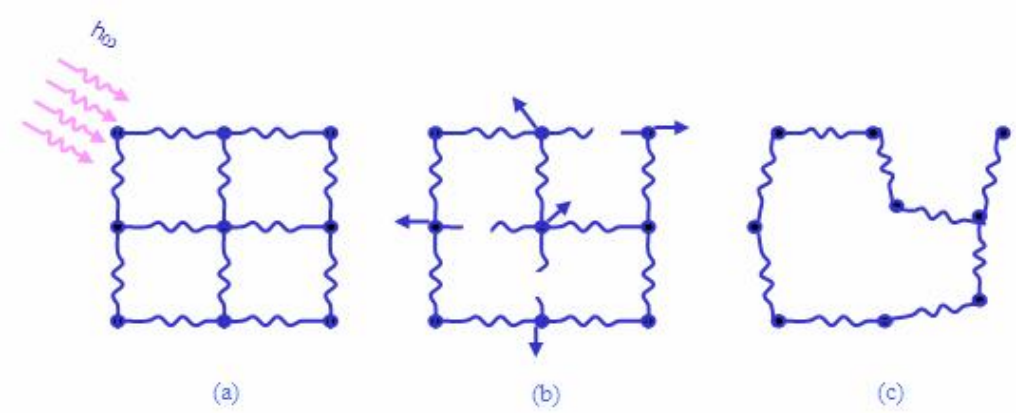

Figure 5.9 Schematically shown the mechanism for non-thermal lattice disordering: (a) bonding electrons absorb photons, (b) these electrons are excited to anti-bonding states, bonds break between atoms and (c) the atoms move to new equilibrium states, resulting in a disordered structure.

Figure 5.3 and Figure 5.7 also showed that the maximum reflective intensity for high and low fluence was different. The maximum reflective intensity was higher for high fluence (A) than that for low fluence (C). Our result that different fluence reached different maximum reflective intensity change in $Ge_2Sb_2Te_5$ and $Ag_5In_5Sb_{30}Te_{60}$ films is different from that using GeSb [20] which reached the same maximum reflectivity for high and medium fluence. It may be that the carrier density excited by femtosecond pulse is higher

for high fluence than that for low fluence.

Figure 5.3 clearly shows that high fluence induced crystalline phase transition, while low fluence cannot triggered phase transition. One possible reason is that high fluence may ensure that there are enough carriers to be excited from bonding state to antibonding state for the lattice to displace and change from a disordered state to an ordered state, while low fluence may mean that the excitation carrier density is not high enough for lattice ordering.

Figure 5.3 indicates that the final phases for high and medium fluence are different. High fluence induce crystalline phase, while probably partial crystalline phase is triggered by medium fluence. This may be due to the fact that intermediate states exist between the amorphous and polycrystalline structures in GeSbTe material [121], as shown in Figure 5.10. When femtosecond pulse with medium fluence shines on $Ge_2Sb_2Te_5$ material, the energy is not sufficient to excite enough carriers from bonding state to anti-bonding state, which may not allow all the bonding of neighbor atoms to break and realign. Instead, only parts of atoms are allowed to align, leading to an increase of the limited long-range periodic order of the amorphous state. Our result that different fluences induce different reflectivive intensity may be used for multilevel recording to increase recording density.

Although Femtosecond laser can induce ultrafast nonthermal phase transitions in both 100 nm amorphous $Ge_2Sb_2Te_5$ and $Ag_5In_5Sb_{30}Te_{60}$ films, the final states in these two materials on solidification after femtosecond laser irradiation are different. Crystallization takes place after solidification in 100 nm amorphous $Ge_2Sb_2Te_5$ films, while re-amorphization occurs in 100 nm amorphous $Ag_5In_5Sb_{30}Te_{60}$ films. One possible

reason may be due to different crystallization mechanisms of these two materials.

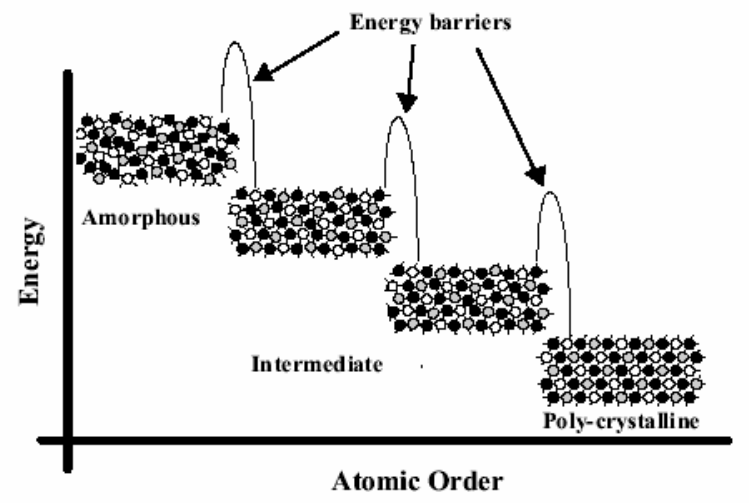

Figure 5.10 Structural state in phase materials.

5.3.3 Crystallization mechanism

The conventional crystallization process is described as nucleation of crystalline grains followed by the growth of these crystalline grains. Both the nucleation rate and growth rate are functions of temperature. If the nucleation rate of a material is higher than its growth rate, this material is called nucleation-dominant materials. If the nucleation rate of a material is lower than its growth rate, this material is called growth-dominant materials.

According to the crystallization mechanism, rewritable phase change materials, GeSbTe and AgInSbTe, are divided in two categories: "nucleation-dominant materials" and "growth-dominant materials" [122][122]. GeSbTe belongs to the former, nucleation-dominant materials, because it crystallizes through the formation of many crystalline seeds, or nuclei, that then grow to form small crystallites. While AgInSbTe belongs to

latter, growth-dominant materials, because nucleation is difficult and takes long time to occur in this material, but growth of a crystalline area, once a seed or nuclei is present, is very quick.

Crystallization temperature of phase change media is in the range of 150~250 °C when heating slowly. It increases with increasing heating rate. For femtosecond laser irradiation, the energy deposition time is very short, which may be too short for crystalline nuclei to grow in AgInSbTe materials. While the material will reach high temperature after thermal equilibrium, which may greatly increase the nucleation rate in GeSbTe materials. After femtosecond laser shines on samples, nucleation rate may be high in $Ge_2Sb_2Te_5$ films due to the high temperature. While for $Ag_5In_5Sb_{30}Te_{60}$ films, nucleation may not even take place in so short time, although the temperature is very high. This may be the reason that account for the crystallization induced by single femtosecond pulse in 100 nm amorphous $Ge_2Sb_2Te_5$ films, while re-amorphization occurring in 100 nm amorphous $Ag_5In_5Sb_{30}Te_{60}$ films after irradiation by single femtosecond pulse.

5.4 Conclusions

From the pump-probe experiment in 100 nm amorphous $Ge_2Sb_2Te_5$ films and $Ag_5In_5Sb_{30}Te_{60}$ films, following conclusions can be obtained:

1) Ultrafast time-resolved microscope with both femtosecond time and micrometer spatial resolution was employed to investigate the ultrafast dynamics in 100 nm

amorphous $Ge_2Sb_2Te_5$ films and $Ag_5In_5Sb_{30}Te_{60}$ films. The entire process of the phase transitions in 100 nm amorphous $Ge_2Sb_2Te_5$ films and $Ag_5In_5Sb_{30}Te_{60}$ films induced by single femtosecond pulse was revealed.

2) An intensity increase within picosecond delay in 100 nm amorphous $Ge_2Sb_2Te_5$ and $Ag_5In_5Sb_{30}Te_{60}$ films was observed. It cannot be interpreted with conventional thermal phase change. Non-thermal phase transition model is suggested as the mechanism of the picosecond intensity increase in $Ge_2Sb_2Te_5$ and $Ag_5In_5Sb_{30}Te_{60}$ films after irradiation by femtosecond pulse.
3) Single photon indirect absorption is the dominant excitation process during pulse duration, while impact ionization continues to increase carrier density after femtosecond pulse excitation, which may account for the high reflective intensity lasting for long time after pulse duration.
4) Femtosecond laser can induce amorphous to crystalline in 100nm $Ge_2Sb_2Te_5$ films, while crystallization cannot be triggered in 100 nm $Ag_5In_5Sb_{30}Te_{60}$ films. One possible reason is due to the different crystallization mechanisms of GeSbTe and AgInSbTe films.

Chapter 6 Phase transitions in super-lattice-like phase change media triggered by femtosecond pulse

Phase change optical data storage is one of the most popular technologies for the production of removable and rewritable storage media. In the last decade, significant progress has been made in the development of phase change optical disk with high data transfer rate. One approach is to develop phase change materials with fast crystallization speed. Other approach is to use complicated disk structure with additional interface layers to enhance the formation of nucleation sites.

Superlattice-like phase change optical disks, in which the recording layer consists of alternating thin layers with two different phase change materials, was first proposed by Chong *et al*,. [124] They found Superlattice-like phase change optical disks have faster crystallization speed [124][125][126], compared to conventional phase change optical disks.

Our previous experiments show that single femtosecond pulse can induce amorphous to crystalline and crystalline to amorphous phase transitions in 100 nm $Ge_2Sb_2Te_5$ films. The mechanism is nonthermal. However, whether femtosecond laser can induce any phase transitions in super-lattice-like phase change media or not is not clear yet.

In this chapter, the general concept of superlattice structure is introduced, followed by superlattice-like phase change optical disks. Then the static experimental results in superlattice-like phase change media will be presented. Finally the pump-probe setup will be used to investigate the ultrafast dynamics in superlattice-like phase change media following femtosecond pulse irradiation.

6.1 General concept of superlattice

As first introduced by Slater [127] in 1940s, the concept of superlattic is semiconductor structure consisting of several ultra-thin layers (atomic layers) in order to obtain specific electronic and photonic properties because slight modifications of chemical composition of each layer result in slight variations of energy bandgap from layer to layer. There are two kinds of superlattice structures, as proposed by Esaki and Tsu [127] in 1969. One type of superlattice is an artificial periodic potential in a semiconductor crystal using periodic *n*-type and *p*-type doped layers. This type of superlattice, resulted from modulation of the impurity in a semiconductor, is now termed as doping superlattice or n-i-p-i doping superlattice, as shown in Figure 6.1 (a). Another type of superlattice is based on a periodic structure of alternating layers of semiconductor materials with wide and narrow band gaps. This type of superlattice is called compositional superlattice, as shown in Figure 6.1 (b).

Scince then, the research on superlattices, the artificially structured materials was initiated. The earliest attentions were focused on crystalline superlattices which require lattice matching. Later, people found that superlattices could be extended to amorphous

semiconductor multilayers without lattice matching. Amorphous semiconductors have a short range order of random network that the nearest neighbor distance or bond length is essentially equal to that of the corresponding crystalline phase though the bond angle may fluctuate to some extent. Indeed, amorphous semiconductor multilayers could be regarded as a new class of superlattice structure when the potential well width is less than the quantum mechanical coherence length of carriers. Recent discovery [128][129][130] shows that well-defined periodic potential structure can be designed and fabricated by amorphous semiconductor heterojunction multilayer.

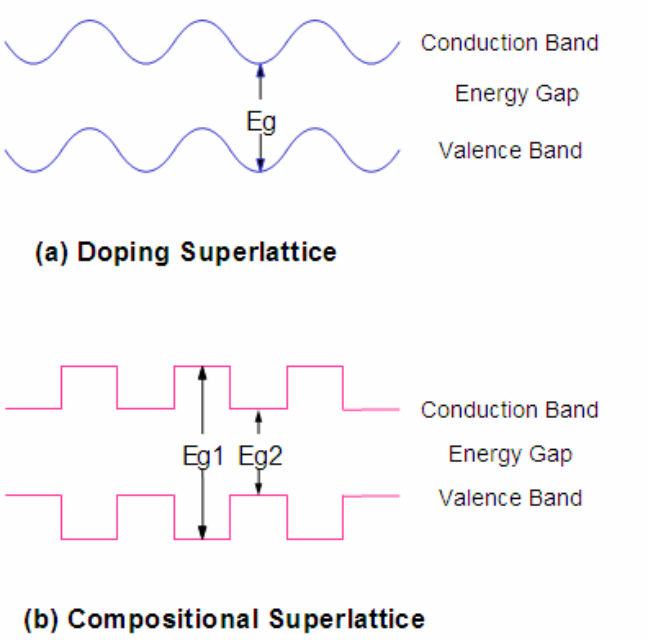

Figure 6.1 Schematically shows the two type of superlattice structures (a) doping superlattice and (b) compositional superlattice.

In this thesis, the so called superlattice-like phase change structure is based on the concept of compositional superlattice structure. In the next section, the novel properties of superlattice will be presented.

6.2 Properties of superlattice

Superlattice structure consists of a periodical repetition of alternating layers of two materials. It has novel physical properties as compared to their corresponding bulk materials. Experimental and theoretical studies [131][132][132][134] have revealed that the thermal conductivities in both in-plane and cross-plane of superlattice have been significantly decreased, as compared to their corresponding bulk materials. Many experiments [132][134] show that the thermal conductivity of superlattice structures are generally lower than the values calculated from the thermal conductivity of their corresponding materials according to the Fourier heat conduction theory. Ren and Dow [131] modeled the thermal conductivity of ideal superlattice structures by combining Callaway's model with a quantum mechanical treatment of the scattering rate. They predicted that mini-umklapp three-photon scattering siginificantly reduce the lattice thermal conductivity of a superlattice. The reduction is most significant in large samples with small superlattice periods and with large difference the superlattice layers. The predicted reduction in thermal conductivity from their model, however, is too low to explain the orders of magnitude reduction in the measured thermal conductivity of some superlattice structures. Chen and Neagu [132] established models on the in-plane and cross-plane thermal conductivity of superlattices based on the Boltzmann transport equation and proposed that below the critical thickness, thermal conductivity is strongly influenced by interface scattering of phonons. Above the critical thickness, dislocations are the dominant scattering centers in superlattice.

The recrystallization characteristics of the superlattice are also different from those of the

bulk materials [135]. Electron-hole pairs were created in superlattice after light irradiation. The lifetime of an electron-hole pair might range from several picoseconds up to nanoseconds. Prior to recombination of the photo-excited electron-hole pair, the chemical bond between neighboring atoms may become weak, which tends to encourage nucleation and rapid crystal growth. After recombination, the local bonding configurations may not be the same as those before photo-excitation. The rearrangement of bonds may be helpful in forming nuclei and increasing the speed of crystal growth. In addition, the non-radioactive dissipation of the large recombination energy raises the local temperature of the film, further accelerating the crystallization process.

It is clear that the band structure of superlattice will be different from those of the constituents if the thin layers consist of only a few layers of atoms. The bandgap change may decrease activation energy of phase-change media, leading to increase the crystallization speed of phase-change materials. Thus, change in the periods and thickness of superlattice may change the optical properties and crystallization speed of superlattice.

The optical properties of superlattice may also be strongly modified by localization and quantum-confinement effects. When the layers in the superlattice are sufficiently thin, it can be described as “ordinary” uniaxial material and its optical properties could be quite different from the constituents. Experiment [124] shows that the superlattice can greatly improve the nonlinear optical properties of materials. Optical absorption coefficient and refractive index of superlattice are strongly dependent on the optical intensity pass though the superlattice.

Superlattice structure has different physical properties, as compared to their corresponding bulk materials. The optical and thermal properties, and crystallization behaviors can be tailored via adjusting the superlattice structure, which is the idea used in superlattice-like phase change optical disk.

6.3 Superlattice-like phase change structure

In this thesis, the superlattice-like phase-change structure consists of alternate ultrathin layers of two different phase-change materials, i.e., PC-1 and PC-2, as shown in Figure 6.2 (a). Usually one material has a high crystallization speed, a low activation energy for crystallization and a low stability, whereas another material has a high activation energy and a high stability.

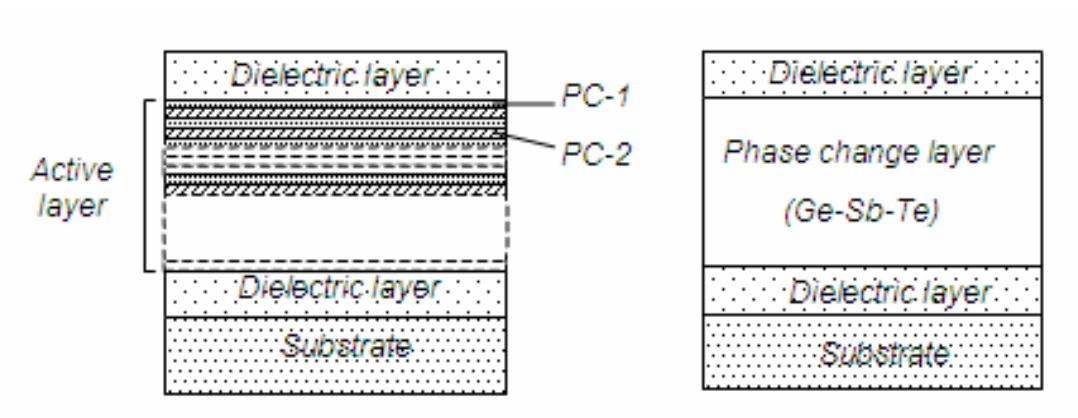

(a) (b)

Figure 6.2 Cross-sectional view of (a) superlattice-like sample and (b) conventional sample.

The ternary GeSbTe compounds can be considered as pseudobinary GeTe and Sb_2Te_3 alloys with different combinations. They have tetradymite-like structures, because

Sb_2Te_3 tetradymite-type units (TeSbTeSbTe) are the important constituent of their mixed-layered crystal structures [136]. The Sb_2Te_3 compound has a rhombohedral lattice of the tetradymite (Bi_2Te_2S) type (space group $R3m$) with the following lattice parameters in the hexagonal configuration: a=50.4264 nm, c=53.0458 nm [137]. The hexagonal unit cell contains three five-layer packs (N=15). The atomic layers are alternated in the Te1SbTe2SbTe1 sequence perpendicular to the c axis. The five-layer packets are bonded to each other by weak Van der Waals forces [136]. While GeTe compound has two polymorphic phases. The high-temperature β phase (T>700 K) has a cubic rocksalt structure (space group $Fm3m$) [138]. The low-temperature α-phase (T<700 K) has a rhombohedral structure of the α-As type (space group $R3m$) with lattice parameters: a=50.5986 nm and α=88.35° [138][139]. The α-phase is characterized by the displacement of the Ge and Te sublattices relative to each other along the [111] direction [140]. As a result, the Ge-Te double-layer packs of bismuth-type are formed.

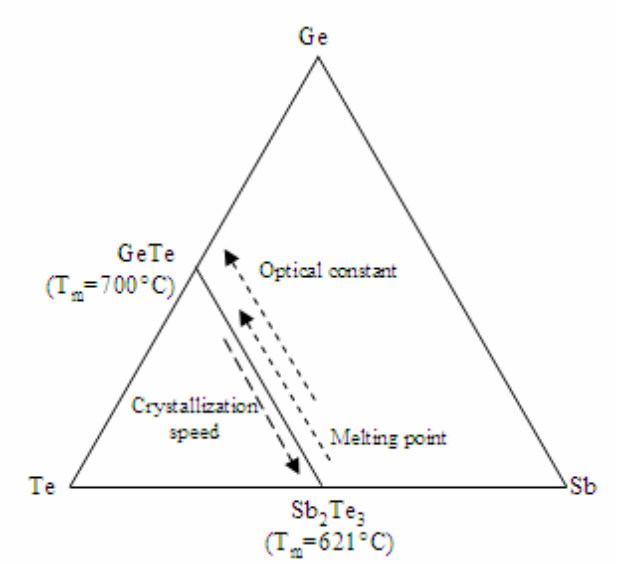

Figure 6.3 Schematically show the composition dependence of the crystallization speed and melting point in the phase diagram of the tenary GeSbTe system.

Figure 6.3 shows the composition dependence of the crystallization speed and melting point in the phase diagram of the tenary GeSbTe system. GeTe has a large difference in the optical constant between the amorphous and crystallize phase, which makes it suitable for applications in optical disk where both high reflection and high signal modulation are required. However, GeTe has a high crystallization temperature (189 °C) and a high melting point (~700 °C), making it difficult to be erased completely when the energy deposition time is very short. While Sb_2Te_3 has a low crystallization temperature between 90 and 100 °C and a melting point of 621 °C. It has a fast crystallization speed and a small difference in the optical constant between the amorphous and crystallize phase.

Binary compounds of GeTe and Sb_2Te_3 were selected as the two compositional materials of the SLL structure because of the following consideration:

1) The phase-change point and the melting point of GeTe (189 ℃ and ~700 ℃, respectively) are quite different from those of Sb_2Te_3 (partially crystallized when deposited, 621 ℃ for melting point). When being melt-quenched and annealed within tens of nanoseconds, it is less possible for any confusion or chemical reaction to take place between layers of the different compositional materials, which was confirmed by XPS measurement [126];
2) Adhesion between the alternative layers of these two materials is very strong;
3) The band gap discrepancy is large enough for GeTe and Sb_2Te_3 (the band gap is 0.73~0.95 eV for GeTe and 0.21 eV for Sb_2Te_3 at 300 K).

After the introduction of general concept of superlattice-like phase change optical disk, whether femtosecond pulse can induce any phase transition in superlattice-like phase change media or not will be investigated.

6.4 Phase transitions in superlattice-like phase change media triggered by femtosecond laser

The sample structure was 0.6mm polycarbonate substrate/ $(ZnS)_{80}(SiO_2)_{20}$ 120 nm/ superlattice-like phase change media / $(ZnS)_{80}(SiO_2)_{20}$ 92 nm/ air. The superlattice-like phase change media consists of alternate 2 nm GeTe films and 3 nm Sb_2Te_3 films. For example, 100 nm superlattice-like phase change media includes alternate 10 layers of GeTe and 10 layers of Sb_2Te_3. The total layers are 20. The as-deposited samples were in amorphous background. They could be changed to crystallize phase by the initializer.

The static experiment setup described in chapter 4 is used to investigate whether single femtosecond pulse can induce any phase transition in superlattice-like phase change media or not. Figure 6.4 and Figure 6.5 are OM images of 100 nm superlattice-like sample after single femtosecond pulse irradiation at amorphous and crystalline background, respectively. They indicate that single femtosecond pulse can induce crystalline mark at amorphous background and amorphous mark at crystalline background in 100 nm superlattice-like phase change media, similar to the results in 100 nm amorphous $Ge_2Sb_2Te_5$ films. The amorphous to crystalline phase transition triggered by single femtosecond pulse in 100 nm amorphous superlattice-like phase change media

is corroborated by X-ray diffractometer (XRD) measurement (Figure 6.6). Figure 6.6 also indicates that there is no confusion or chemical reaction to take place between GeTe and Sb_2Te_3 layers after initiazation and single femtosecond pulse irradiation, consistent with Shi's XPS measurement [126] which shows that after many time of high power irradiation,the SLL structure is still exist although there are slight diffusion between layers.

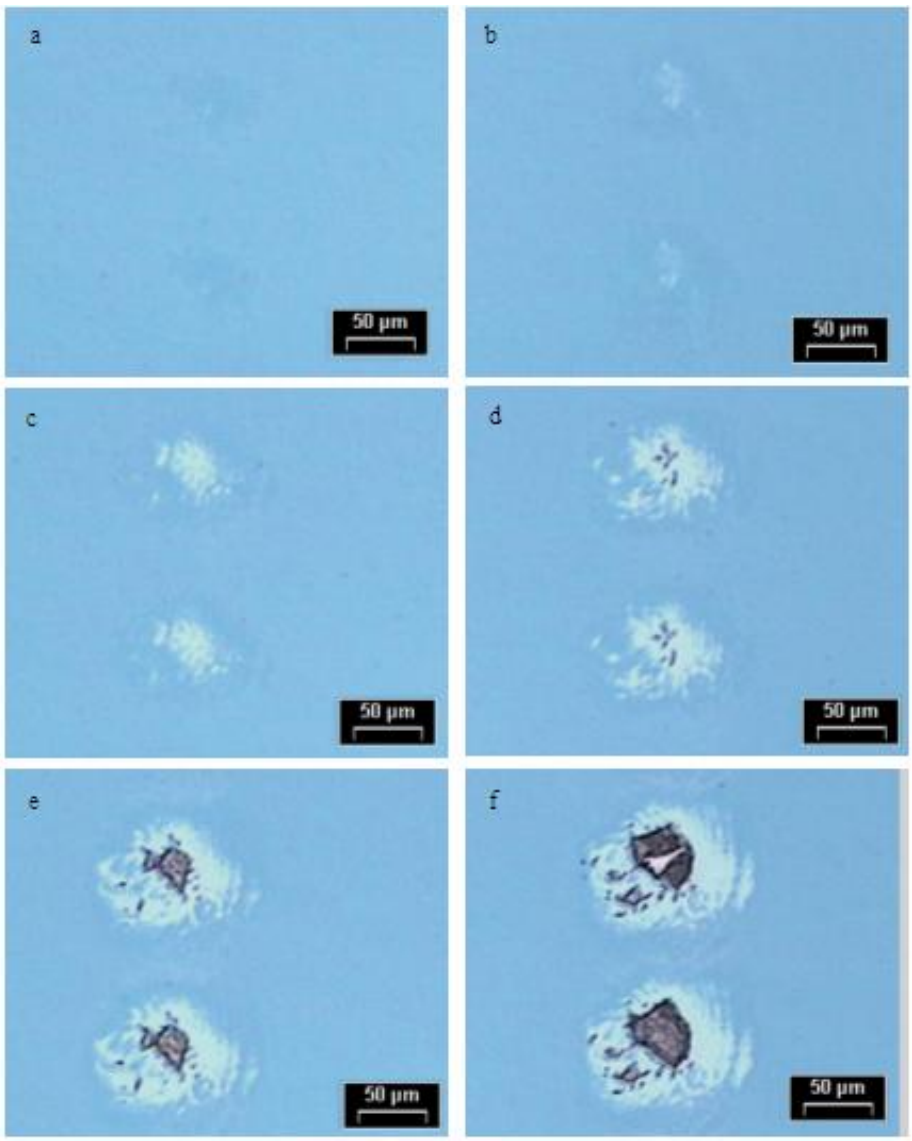

Figure 6.4 OM images of 100 nm amorphous superlattice-like phase change media after single femtosecond pulse irradiation. Pulse energy (a) 5 μJ; (b) 6 μJ; (c) 7 μJ; (d) 9 μJ; (e) 11 μJ and (f) 13 μJ.

With the increase of laser fluence, the size of crystalline marks and amorphous marks increases until the over-burn point appear in the center, as shown in Figure 6.4 and Figure 6.5, respectively. However, the amorphous over-burn marks induced by single femtosecond pulse are quite different from those of crystalline over-burn marks. Figure 6.4 (d), (e) and (f) show that the crystalline phase in the crystalline overburm marks is adjacent to the the over-burn point, whereas Figure 6.5 (d), (e) and (f) show that the amorphous phase in the the amorphous over-burn marks is separated from the over-burn point by a crystalline ring, indicating that the central high fluence triggers crystallinzation. One possible reason is that the cooling speed may be low enough in the center part of laser spot to promote the crystallization, although the laser fluence is high. While in the fringe part of laser spot, the cooling speed may be fast enough to induce amorphization.

However, the results in 20 nm superlattice-like phase change media, as shown in Figure 6.7 and Figure 6.8, are quite different from that in 100 nm superlattice-like phase change media. Single femtosecond pulse could only induce crystalline to amorphous phase transition in 20 nm superlattice-like phase change media, while amorphous to crystalline phase transition could not be triggered by single femtosecond pulse, as only over-burn marks were observed in Figure 6.7.

The same method as that for $Ge_2Sb_2Te_5$ films in Chapter 4 was employed to investigate the phase transitions induced by single femtosecond pulse in superlattice-like phase change media with the thickness between 20 nm and 100 nm. Our results (Figure 6.9, Figure 6.10, Figure 6.11 and Figure 6.12) show that when the films thickness of superlattice-like phase change media was no less than 55 nm, the results are similar

to those in 100 nm superlattice-like phase change media that single femtosecond pulse could induce both amorphous and crystalline phase transitions. While when the films thickness of superlattice-like phase change media was no more than 50 nm, the results are similar to those in 20 nm superlattice-like phase change media that single femtosecond pulse could only induce crystalline to amorphous phase transition.

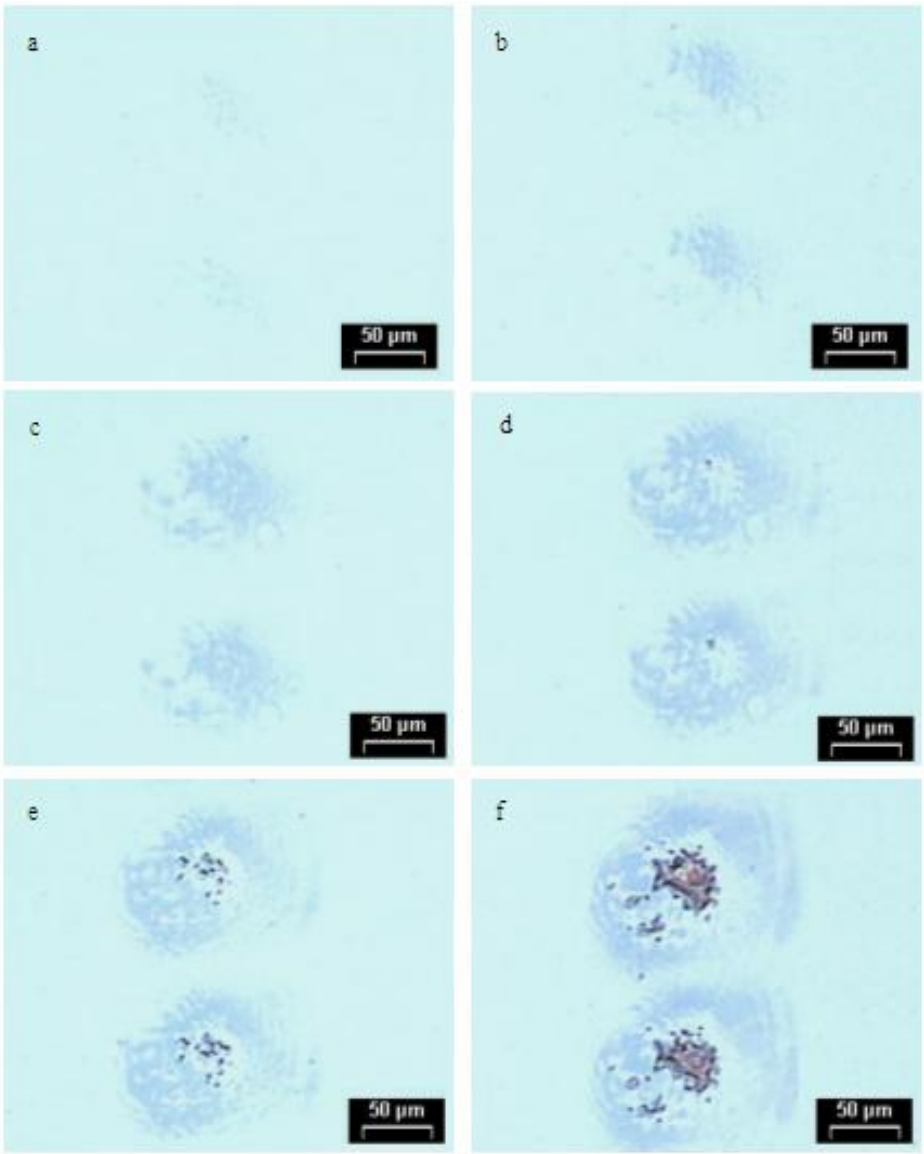

Figure 6.5 OM images of 100 nm crystalline superlattice-like phase change media after single femtosecond pulse irradiation. Pulse energy (a) 5 μJ; (b) 6 μJ; (c) 7 μJ; (d) 9 μJ; (e) 11 μJ and (f) 13 μJ.

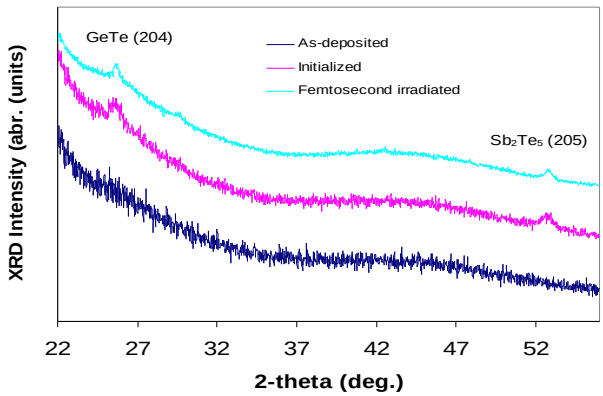

Figure 6.6 XRD patterns of 100 nm superlattice-like phase change media at as-deposited phase and after initialization and single femtoseond laser irradiation.

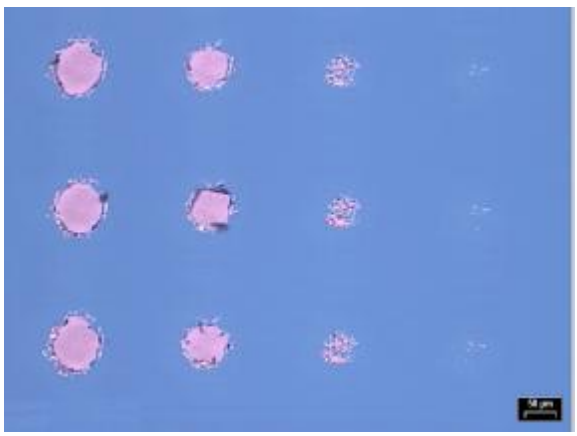

Figure 6.7 OM image of 20 nm superlattice-like phase change media at amorphous background after single femtosecond pulse irradiation. Pulse energy from left to right: 12 μJ, 10 μJ, 8 μJ, and 6 μJ.

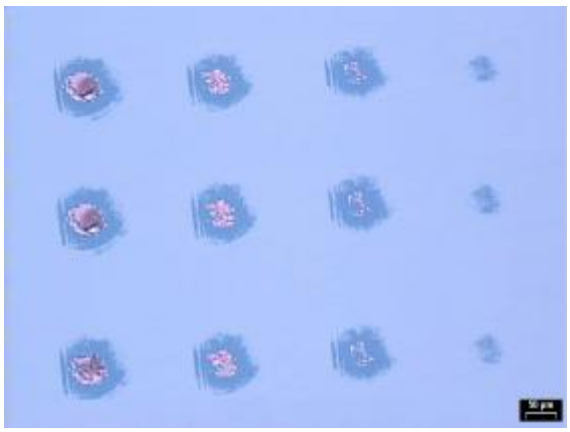

Figure 6.8 OM image of 20 nm superlattice-like phase change media at crystalline background after single femtosecond pulse irradiation. Pulse energy from left to right: 10 μJ, 8 μJ, 6 μJ and 4 μJ.

Our static experiments clearly show that the film thickness of superlattice-like phase change media which could achieve both amorphous and crystalline phase transition after single femtosecond pulse irradiation is thinner than that of $Ge_2Sb_2Te_5$ films. One possible reason is that the alternate thin layers of superlattice-like phase change media consist of only a few layers of atoms which may change the band gap and decrease activation energy, leading to increase the crystallization speed.

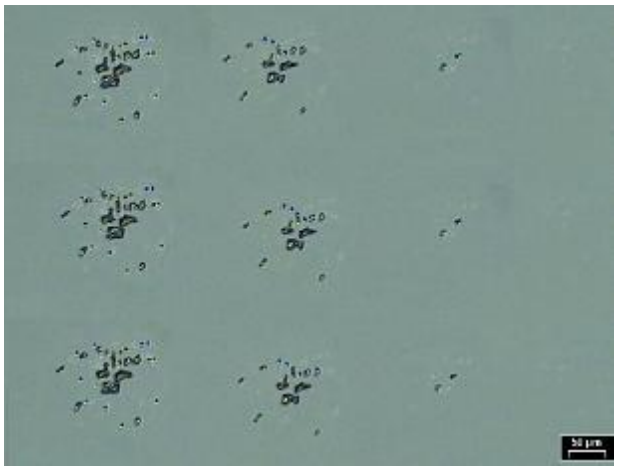

Figure 6.9 OM image of 55 nm superlattice-like phase change media at amorphous background after single femtosecond pulse irradiation. Pulse energy from left to right: 14 μJ, 13 μJ, 12 μJ and 10 μJ.

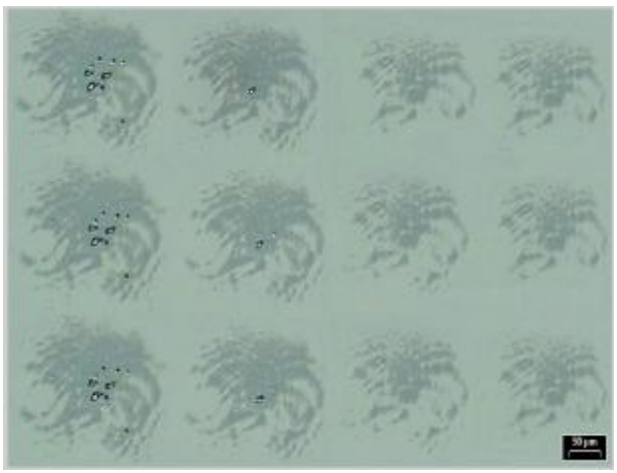

Figure 6.10 OM image of 55 nm superlattice-like phase change media at crystalline background after single femtosecond pulse irradiation. Pulse energy from left to right: 12 μJ, 10 μJ, 9 μJ and 8 μJ.

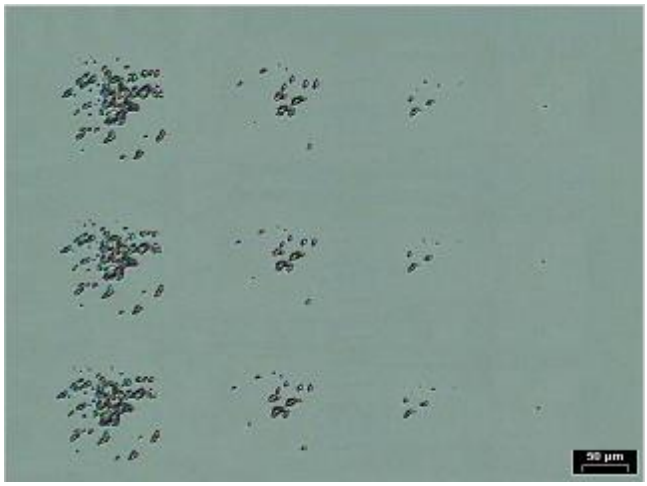

Figure 6.11 OM image of 50 nm superlattice-like phase change media at amorphous background after single femtosecond pulse irradiation. Pulse energy from left to right: 13 μJ, 12 μJ, 10 μJ, and 9 μJ.

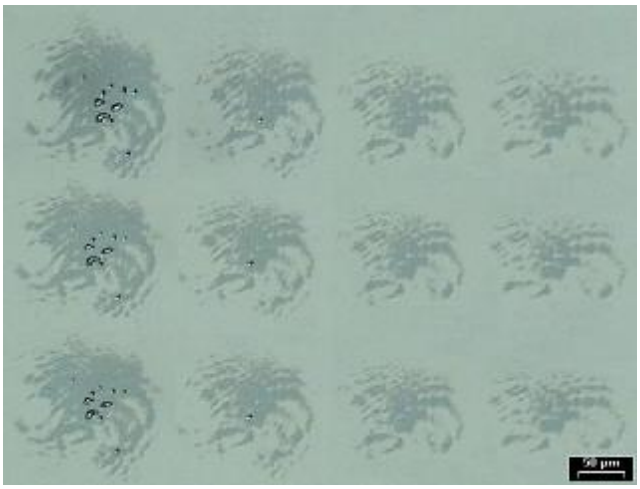

Figure 6.12 OM image of 50 nm superlattice-like phase change media at crystalline background after single femtosecond pulse irradiation. Pulse energy from left to right: 10 μJ, 9 μJ, 8 μJ, and 7 μJ.

However, a more detailed explaination could not be given here. The pump-probe setup should be employed to investigate the ultrafast dynastics in superlattice-like phase change media after irradiation by single femtosecond pulse in order to gain insight into the mechanism of these ultrafast phase transitions.

6.5 Ultrafast dynamics in superlattice-like phase change media

The pump-probe experiment setup described in chapter 3 is employed to investigate the ultrafast dynastics in 100 nm amorphous superlattice-like phase change media after irradiation by single femtosecond pulse. The sample structure was the same as previous experiments. The sample was in as-deposited background.

6.5.1 Results

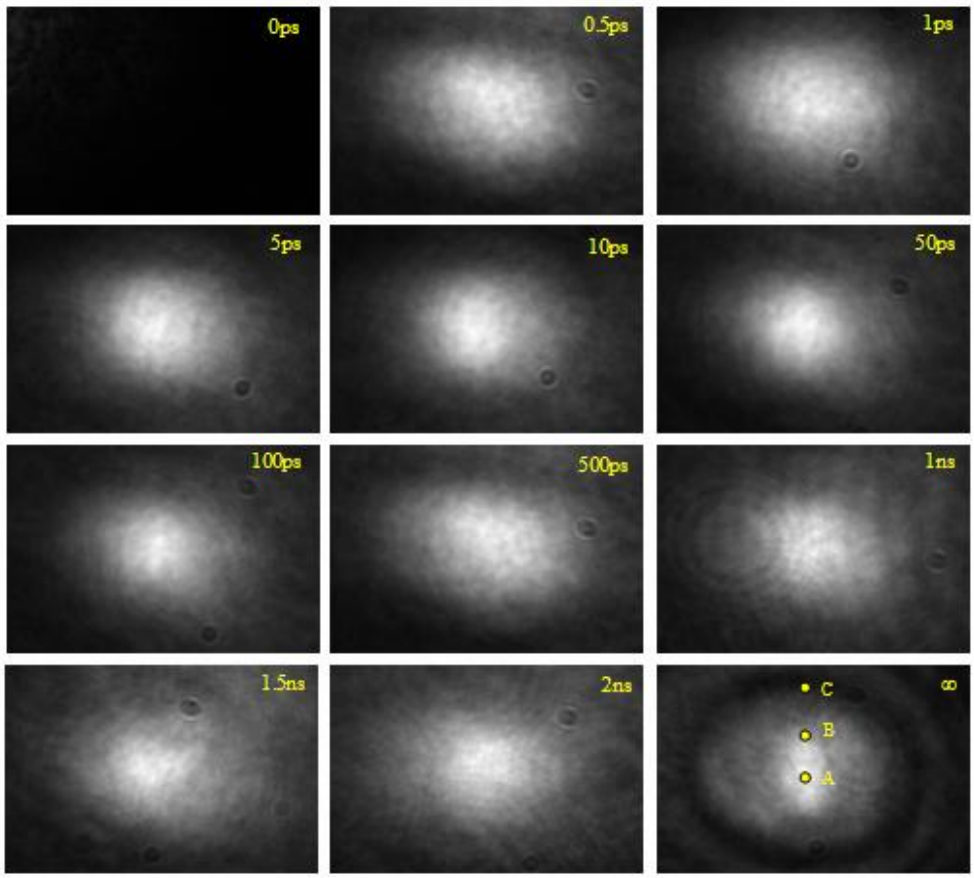

Figure 6.13 Pictures of 100 nm amorphous superlattice-like phase change media after single femtosecond pump pulse irradiation at the energy of 14 μJ.

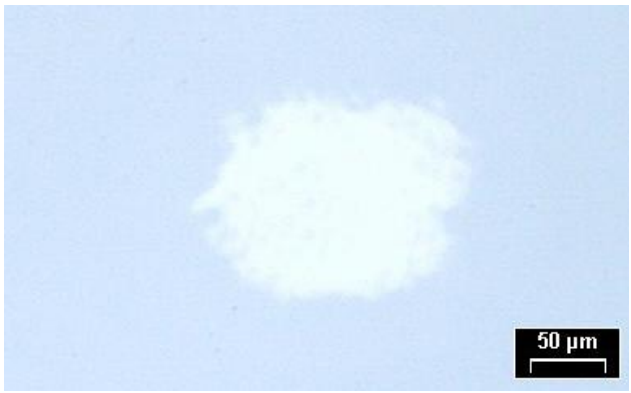

Figure 6.14 OM image of 100 nm amorphous superlattice-like phase change media after irradiation by single femtosecond at the energy of 14 μJ.

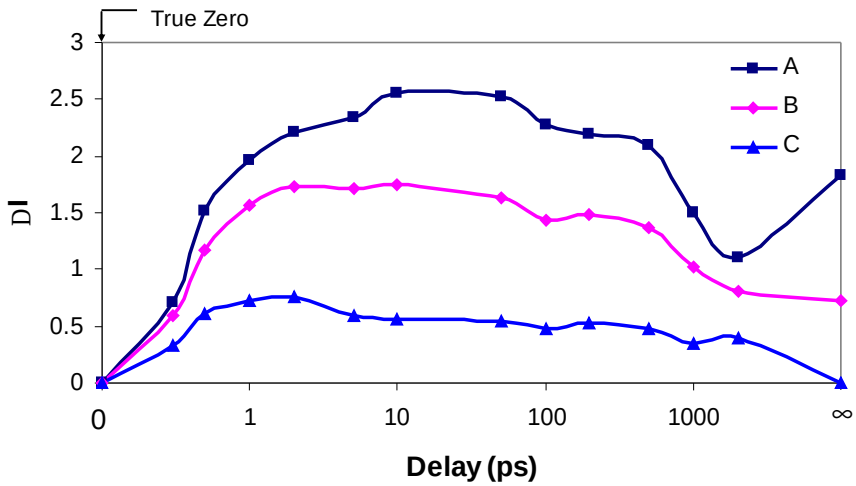

Figure 6.15 Reflective intensity change as a function of delay time measured at three different fluences (marked A, B and C in the last frame of Figure 6.13), corresponding to excitation fluence of 60, 45, 20 mJ/cm^2, respectively. $\Delta I=[I(t)-I_a]/I_a$ and I_a is the reflective intensity of 100 nm amorphous superlattice-like phase change media .

A sequence of micrographs, covering the entire period from initial deposition of laser energy to appearance of the final structural modifications in 100 nm amorphous superlattice-like phase change media, is shown in Figure 6.13. In the first frame ((Δt=0ps), the reflective intensity of the area illuminated by pump-probe was almost the same as that of the area irradiated by probe beam because the pump beam and the probe beam took an equal amount of time to reach the sample. In the next two frames (0.5

ps, 1 ps), the reflective intensity of the region irradiated by whole pump beam increased which gave rise to the appearance of a bright area without a sharply defined boundary. The appearance of the bright region in the surface area irradiated by pump beam remained nearly unchanged for approximately 2 ns delay except that the size of the bright region diminished at later delay (50 ps, 100 ps) and enlarged at even later delay (1 ns). The bright region in the center of the probe spot in the last frame ($\Delta t=\infty$), corresponding to a delay of several seconds, suggested that crystalline mark was formed in 100 nm superlattice-like phase change media at amorphous background after single pump beam irradiation.

The subsequent morphology examination of the final state after the irradiation of the single femtosecond pump pulse is shown in Figure 6.14. It indicated the formation of crystalline mark in 100 nm superlattice-like phase change media at as-deposited background after excitation by single 100 fs pulse.

To quantitatively follow the evolution of the reflectivity intensity change after femtosecond pulse irradiation, the reflectivity intensity change as a function of delay time is shown in Figure 6.15. Three fluences were chosen, marked A, B and C in Figure 6.13, corresponding to excitation fluence of 60, 45, 20 mJ/cm^2, respectively. Figure 6.15 shows that the result in 100 nm amorphous superlattice-like phase change media is similar to that in 100 nm amorphous $Ge_2Sb_2Te_5$ films. The reflective intensity change increased immediately after femtosecond pulse irradiation for all three fluences (Figure 6.15). It is possible because femtosecond laser can induce nonthermal phase transition. Figure 6.15 shows that there is a big drop of reflective intensity at high fluence at

approximately 2 ns and the maximum reflective intensity for high, medium and low fluence was different. The maximum reflective intensity was higher for high fluence (A) than that for low fluence (C). One possible reason is that the excited carrier density is different for different fluence. The excited carrier density may be proportional to fluence than that for low fluence. Figure 6.15 also shows that high and medium fluence triggered a transition from as-deposited phase to crystalline phase and partial crystalline phase, respectively, whereas low fluence cannot induce crystallization. High fluence may induce more carriers to be excited from bonding state to antibonding, compared to medium fluence, which may favor the lattice ordering. While for low fluence, the carrier density may be not high enough for lattice ordering to occur.

6.5.2 Discussions

Similar to 100 nm amorphous $Ge_2Sb_2Te_5$ films and $Ag_5In_5Sb_{30}Te_{60}$ films, single photon absorption is the dominant excitation process in 100 nm amorphous superlattice-like phase change media during pulse duration since both GeTe and Sb_2Te_3 have band gap lower than single photon energy of 1.55 eV at the wavelength of 800 nm. After carrier excitation, free carriers have excess energy higher than the band gap of Sb_2Te_3 which is 0.21 eV at 300 K. Impact ionization takes place. Because no photon absorption is involved, impact ionization begins during pulse duration and will continue to increase carrier density after the deposition of laser energy. Impact ionization may be the reason that accounts for the high reflectivity intensity lasting after pulse duration in Figure 6.15.

After carrier excitation, carriers with high density and energy will redistribute and thermalize between themselves and lattice via carrier-carrier scattering and carrier

phonon scattering [117]. Figure 6.15 shows that the reflective intensity in 100 nm amorphous superlattice-like phase change media increases in sub-picosecond time scale after irradiation by single femtosecond pulse. Similar to 100 nm amorphous $Ge_2Sb_2Te_5$ and $Ag_5In_5Sb_{30}Te_{60}$ films, the sub-picosecond reflective intensity increase in 100 nm amorphous superlattice-like phase change media (Figure 6.15) could not be interpreted with conventional thermal phase transition. The non-thermal phase transformations induced by a softening of the lattice structure due to generation of a high density electron-hole population was suggested to be the mechanism of the sub-picosecond reflective intensity increase in 100 nm amorphous superlattice-like phase change media.

Figure 6.15 also shows that the maximum reflective intensity for high and low fluence is different in 100 nm amorphous superlattice-like phase change media. This may be due to different carrier density excited by different fluence. The carrier density excited by femtosecond pulse may be higher for high fluence than that for low fluence. Thus high fluence may ensure that there are enough excitation carriers for lattice to displace and change from a disordered structure to an ordered structure, while low fluence may mean that the excitation carrier density is not high enough for lattice ordering to occur.

Figure 6.15 clearly shows that the final phases for high and medium fluence are different in 100 nm amorphous superlattice-like phase change media. High fluence may induce crystalline phase, while partial crystalline phase may be triggered by medium fluence. Superlattice-like phase change media may also have intermediate states exist between the amorphous and polycrystalline structures, just like GeSbTe material. When femtosecond pulse with medium fluence shines on superlattice-like phase change media, the energy is not sufficient to excite high carrier density from bonding state to anti-bonding state.

It cannot allow all the bonding of neighbor atoms to break and realign. Instead, only parts of atoms are allowed to align, leading to an increase of the limited long-range periodic order of the amorphous state.

There is a big drop of reflective intensity at high fluence at approximately 2 ns in Figure 6.15. It may be that once the energy of the excited carriers has been transferred from the free carriers to the lattice, the structural transformation will take place. Due to the large cooling rate and high supercooling after 100 fs pulse irradiation, amorphization will occur, which decreases the reflective intensity. However, initial solidification will release enthalpy which will lower the supercooling to frustrate amorphization process and promote the nucleation and growth of the crystalline phase. For 100 nm superlattice-like phase change media, the enthalpy released during initial solidification may be large enough to reduce supercooling and to promote the nucleation and growth of the crystalline material, which increases the reflective intensity.

Figure 6.16 is the normalized reflective intensity change as a function of delay time of 100 nm amorphous superlattice-like phase change media and $Ge_2Sb_2Te_5$ films after excitation by single femtosecond pulse at the maximum fluence. The maximum reflective intensity change was set to 1 in order to compare between them. Figure 6.16 shows that the change is almost similar between these two media after 100 fs pulse irradiation until 100 ps. Superlattice-like phase change media has a less drop of reflective intensity than $Ge_2Sb_2Te_5$ films between 100 ps to 2 ns. One possible reason is that superlattice-like phase change media has lower thermal conductivity, compared to their bulk materials. The high energy free carriers in superlattice-like phase change media may

not so quick to transfer energy to the lattice as that in $Ge_2Sb_2Te_5$ films. They will remain in high energy until even later delay, which may promote crystallization.

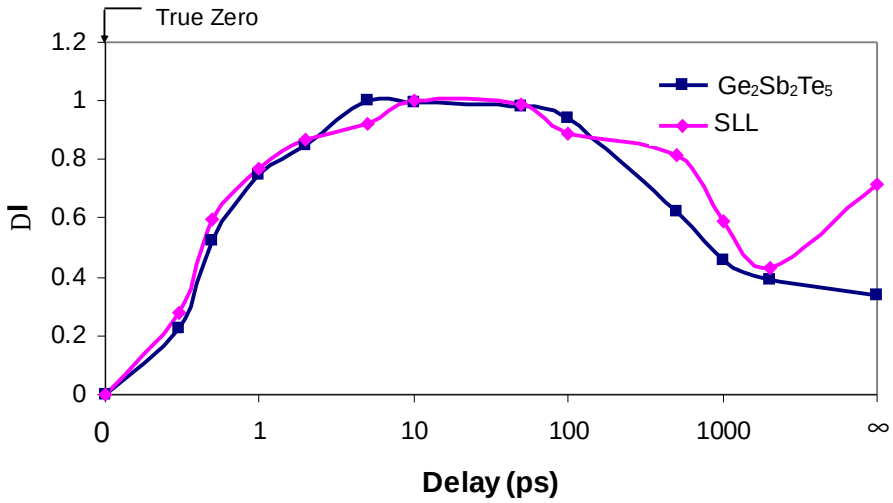

Figure 6.16 Normalized reflective intensity change as a function of delay time between 100 nm amorphous superlattice-like phase change media and $Ge_2Sb_2Te_5$ films measured at the fluence of 60 mJ/cm^2. $\Delta I=[I(t)-I_a]/I_a$ and I_a is the reflective intensity of amorphous phase. The maximun ΔI is set to 1 for comparision.

6.6 Conclusions

From the experiments on 100 nm amorphous superlattice-like phase change media, following conclusions can be obtained:

1) Single femtosecond laser can induce both amorphous to crystalline and crystalline to amorphous phase transitions in superlattice-like phase change media when the film thickness is no less than 55 nm. While for film thickness no more than 50 nm, Single femtosecond pulse can induce only crystalline to amorphous phase transition.
2) Ultrafast time-resolved microscopy with both femtosecond time and micrometer spatial resolution was employed to investigate the ultrafast dynamics in 100nm

amorphous superlattice-like media. The entire process of phase transitions in 100 nm superlattice-like phase change media induced by single femtosecond pulse was revealed.

3) An intensity increase within picosecond delay in superlattice-like media after femtosecond laser excitation was observed. It cannot be interpreted with conventional thermal phase change. Non-thermal phase transition model is suggested as the mechanism of the picosecond intensity increase in superlattice-like media after excitation by single femtosecond pulse.

4) Single photon indirect absorption is the dominant excitation process during pulse duration, while impact ionization continues to increase carrier density after femtosecond pulse excitation, which may account for the high reflective intensity lasting for long time after pulse duration.

Chapter 7 Conclusions and future work

Femtosecond laser can create extreme non-equilibrium conditions in materials that give rise to novel and unusual phase transitions. It is believed that femtosecond laser is very promising for phase change optical data storage. This thesis focused the interaction of femtosecond laser with phase change media and superlattice-like phase change media in order to gain insight into the phase transitions in phase change media and superlattice-like phase change media triggered by femtosecond laser.

Our experiments show that crystalline and amorphous phase transformations triggered by femtosecond laser pulse in $Ge_2Sb_2Te_5$ films could be achieved by proper control of the heat flow conditions imposed by the film thickness. For thin films, femtosecond pulse can only induce crystalline to amorphous phase transition. While for thick films, such as 100 nm, amorphous to crystalline and crystalline to amorphous phase transitions were triggered by femtosecond pulse. Those phase transitions can also be observed in 100 nm superlattice-like phase change media. However, crystallization could not be triggered by single femtosecond pulse although single femtosecond pulse can induce amorphous mark in 100 nm $Ag_5In_5Sb_{30}Te_{60}$ films. One possible reason is due to the different crystallization mechanisms between AgInSbTe and GeSbTe films.

Our experiments in 100 nm $Ge_2Sb_2Te_5$ films and superlattice-like phase change media show that high fluence could induce amorphous to crystalline phase transition, while low fluence may not triggered phase transition . One possible reason is that high fluence may

ensure that there is enough carriers to be excited from bonding state to anti-bonding state for lattice to displace from a disordered structure to an ordered structure, while low fluence may mean that the excited carriers is not enough for lattice ordering.

Our results in 100 nm $Ge_2Sb_2Te_5$ films and superlattice-like phase change media also show that different fluence induce different reflectivity intensity, and different phase upon solidification. The possible reason is that GeSbTe has many intermediate phases between amorphous phase and crystalline phase. Different fluence creates different carrier density, which induces different lattice displacement and results in different phases. That different reflective intensity induces by different fluence may be used in multilevel recording to increase recording density.

For all the materials studied in this thesis, single photon indirect absorption is the dominant excitation mechanism duration laser pulse duration when irradiation by femtosecond pulse at the wavelength of 800 nm. Because the excited carriers have excess energy higher than the optical band gap, impact ionization, which begins during the deposition of laser energy and continues after pulse duration due to no photon absorption involved, may be the dorminant excitation mechanism after pulse duration.

Our experiments show that an instantaneous increase in reflective intensity shortly after irradiation of femtosecond laser for all fluence in all the materials studied in this thesis. It cannot be accounted for the thermal processes. The ultrafast nonthermal phase transition was suggested to be the most plausible explanation for our observation.

Our results show that even a single femtosecond pulse can induce amorphous to

crystalline and crystalline to amorphous phase transitions in GeSbTe films and may provide the means to achieve more than 1 TBit/s data transfer rate capability.

Although much can be learnt from our experiments, further study is still needed. Theoretical simulation, for example, simulation the relationship between carrier densitty and reflective intensity is needed to understand more clearly the carrier and lattice dynamics after femtosecond laser irradiation. More experiments such as X-ray diffraction need to be conducted to identify the non-thermal phase to which the materials transform.

In addition to general pump-probe experiments that measured reflective intensity to probe ultrafast dynamics in this study, future experiments could measure the broadband dielectic function to gain more information about the phase transitions induced by femtosecond laser, because dielectric function is the intrinsic property of a material, and concentrate on individual process such as carrier excitation process to identify which is the dominant process.

We used 800 nm light to probe the dynamics of the phase transitions in phase change media triggered by femtosecond laser. Nevertheless, 800 nm light interacts predominately with valence and free electrons and not with the core electrons and nuclei that most directly indicate structure. Time-resolved optical pump ultrafast x-ray diffraction probe experiments offer hope to “observe” directly the structure of the transient phases triggered by femtosecond pulse and the structural dynamics that cause the transition. In the future, time-resolved x-ray diffraction and dielectric function measurements could be used to study both structural and electronic dynamics on ultrashot timescales.

References

[1] P. Lee. CD-R/DVD: Disc Recording Demystified. pp.1-10, New York: McGraw-Hill, 2000.

[2] G. Bouwhuis. Principles of optical disc systems. pp.7-10, Adam Hilger Publisher, USA, 1985.

[3] M. Mansuripur. The physical Principles of Magneto-Optical Recording. pp. 1-18, New York: Cambridge University Press. 1995.

[4] E. W. Willams. The CD-RAM and Optical Disc Recording System. pp. 80-138, Oxford: Oxford University Press. 1994.

[5] C. V. Shank, R. Yen, and C. Hirlimann. Time-Resolved Reflectivity Measurements of Femtosecond-Optical-Pulse-Induced Phase Transitions in Silicon, Phys. Rev. Lett. 50, pp. 454-457. 1983.

[6] C. V. Shank, R. Yen, and C. Hirlimann. Femtosecond-Time-Resolved Surface Structural Dynamics of Optically Excited Silicon, Phys. Rev. Lett. 51, pp. 900-902. 1983.

[7] H. W. K. Tom, G. D. Aumiller, and C. H. Brito-Cruz. Time-resolved study of laser-induced disorder of Si surfaces, Phys. Rev. Lett. 60, pp. 1438-1441. 1988.

[8] K. Sokolowski–Tinten, J. Bialkowski, and D. von der Linde. Ultrafast laser-induced order-disorder transitions in semiconductors, Phys. Rev. B, Vol. 51, pp. 14186–14198. 1995.

[9] S. V. Govorkov, T. Schröder, I. L. Shumay, and P. Heist. Transient gratings and second-harmonic probing of the phase transformation of a GaAs surface under

femtosecond laser irradiation, Phys. Rev. B, Vol. 46, pp. 6864-6868. 1992.

[10] P. Saeta, J.-K. Wang, Y. Siegal, N. Bloembergen, and E. Mazur. Ultrafast electronic disordering during femtosecond laser melting of GaAs, Phys. Rev. Lett. 67, pp. 1023-1026. 1991.

[11] E. N. Glezer, Y. Siegal, L. Huang, and E. Mazur. Behavior of *chi* $^{(2)}$ during a laser-induced phase transition in GaAs, Phys. Rev. B, Vol. 51, pp. 9589-9596. 1995.

[12] L. Huang, J. P. Callan, E. N. Glezer, and E. Mazur. GaAs under Intense Ultrafast Excitation: Response of the Dielectric Function, Phys. Rev. Lett. 80, pp. 185-188. 1998.

[13] J. P. Callan, A. M.-T. Kim, C. A. D. Roeser, and E. Mazur. Universal dynamics during and after ultrafast laser-induced semiconductor-to-metal transitions, Phys. Rev. B, Vol. 64, pp. 073201-073203. 2001.

[14] J. P. Callan, A. M. T Kim, C. A. D Roeser, et al., Ultrafast Laser-Induced Phase Transitions in Amorphous GeSb Films, Phys. Rev. Lett. 86, pp. 3650-3653. 2001.

[15] L. Shumay and U. Höfer. Phase transformations of an InSb surface induced by strong femtosecond laser pulses, Phys. Rev. B, Vol. 53, pp. 15878–15884. 1996.

[16] C. N Afonso, J Solis, F Catalina, et al., Ultrafast reversible phase-change in GeSb films for erasable optical storage, Appl. Phys. Lett. 60, pp. 3123-3125. 1992.

[17] C. N Afonso, M. C. Morilla, J Solis, et al., Fast-crystallizing Sb-based thin-films under picosecond and nanosecond laser-pulses, Mat. Sci. Eng. A, 173, pp. 343-346. 1993.

[18] J Solis, C. N Afonso, S. C. W Hyde, et al. Existence of electronic excitation

enhanced crystallization in GeSb amorphous thin films upon ultrashort laser pulse irradiation, Phys. Rev. Lett. 76, pp. 2519-2522. 1996.

[19] J Solis, M. C Morilla, C. N Afonso. Laser-induced structural relaxation and crystallization phenomena in the picosecond time scale in GeSbO thin films, J. Appl. Phys. 84, pp. 5543-5546. 1998.

[20] K. Sokolowski-Tinten, J. Solis, J. Bialkowski, J. Siegel, C. N. Afonso and D. von der Linde. Dynamics of Ultrafast Phase Changes in Amorphous GeSb Films, Phys. Rev. Lett. 81, pp. 3679-3682. 1998.

[21] J. Siegel, C. N. Afonso, and J. Solis. Dynamics of ultrafast reversible phase transitions in GeSb films triggered by picosecond laser pulses, Appl. Phys. Lett. 75, pp. 3102-3104. 1999.

[22] J. Solis and C. N. Afonso. Ultrashort-laser-pulse-driven rewritable phase-change optical recording in Sb-based films, Appl. Phys. A, Vol. 76, pp. 331-338. 2003.

[23] J. Siegel, A. Schropp, J. Solis, C. N. Afonso and M. Wuttig**.** Rewritable phase-change optical recording in $Ge_2Sb_2Te_5$ films induced by picosecond laser pulses, Appl. Phys. Lett. 84**,** pp. 2250-2253. 2004.

[24] T Ohta, M Birukawa, N. Yamada, K. Hirao. Optical recording; phase-change and magneto-optical recording, J. Magnetism and Magnetic Materials, 242 –245, pp. 108 –115. 2002.

[25] R. Zhao, K. G. Lim, Z. R. Li, J. F. Liu, J. J Ho, T. C. Chong, Z. J. Liu, B. X. Xu and L. P. Shi. Computer-Aided Design and Analysis of Rewritable Phase-Change Optical Disk, Jpn. J. Appl. Phys. Vol.39, pp. 3458-3462. 2000.

[26] M. C. Downer, R. L. Fork, and C. V. Shank. Femtosecond imaging of melting

and evaporation at a photo-excited silicon surface, J. Opt. Soc. Am. B 2, pp. 595-599. 1985.

[27] K. K. Schwartz. The Physics of Optical Recording. Berlin, New York: Springer-Verlag, 1993, pp 18-25.

[28] Tetsuya Nishida, MotoTetsuya Nishidayasu Terao, Yasushi Miyauchi, Shinkichi Horigome, Toshimitsu Kaku, and Norio Ohta. Single-beam overwrite experiment using In-Se based phase-change optical media, Appl. Phys. Lett. Vol. 50, pp. 667-669. 1987.

[29] J. Tauc. Amorphous and liquid semiconductors. London , New York , Plenum, 1974.

[30] S. R. Ovshinsky. Reversible Electrical Switching Phenomena in Disordered Structures, Phys. Rev. Lett. 21. pp. 1450-1453. 1968.

[31] J. Feinleib, S. C. Moss and S. R. Ovshinsky. Rapid Reversible light-induced Crystallization of Amorphous Semiconductors, Appl. Phys. Lett. Vol. 18, pp. 254-257. 1971.

[32] J. Feinleib and S. R. Ovshinsky. Reflectivity studies of the Te(Ge, As)-based amorphous semiconductor in the conducting and insulating states, J. Non-Cryst. Solids, Vol.4, pp. 564-572. 1970.

[33] R. J. von Gutfeld and P. Chaudhari. Laser writing and erasing on chalcogenide films, J. Appl. Phys. Vol. 43, pp. 4688-4693. 1972.

[34] W. Smith. Injection laser writing on chalcogenide films, Appl. Opt. Vol. 13, pp. 795-798. 1974.

[35] E. Bell and F. W. Spong. Reversible optical recording in trilayer structures, Appl. Phys. Lett. Vol. 38, pp. 920-922. 1981.

[36] P. C. Clemens. Reversible optical storage on a low-doped Te-based chalcogenide film with a capping layer, Appl. Opt. Vol. 22, pp. 3165-3168. 1983.

[37] M. Takenaga, N. Yamada, K. Nishiuchi, N. Akahira, T. Ohta, S. Nakamura and T. Yamashita. TeOx thin films for an optical disc memory, J. Appl. Phys. Vol. 54, pp. 5376-5380. 1983.

[38] W. Y. Lee, H. Coufal, C. R. Davis, V. Jipson, G. Lim, W. Parrish, F. Sequeda, and R. E. Davis. Nanosecond pulsed laser-induced segregation of Te in TeOx films, J. Vac. Sci. Technol. A, Vol. 4, pp. 2988 -2992. 1986.

[39] M. Chen, K. A. Rubin, V. Marrello, U. G. Gerber, and V. B. Jipson. Reversibility and stability of tellurium alloys for optical data storage applications, Appl. Phys. Lett. Vol 46, pp. 734-736. 1985.

[40] M. Chen, K. A. Rubin, and R. W. Barton. Compound materials for reversible, phase-change optical data storage, Appl. Phys. Lett. Vol 49, pp. 502-504. 1986.

[41] N. Yamada, E. Ohno, K. Nishiuchi, N. Akahira and M. Takao. Rapid-phase transitions of GeTe-Sb_2Te_3 pseubobinary amorphous thin films of an optical disk memory, J. Appl. Phys. 69, pp. 2849-2856. 1991.

[42] Z. L. Mao and H. Chen and A. Jung. The structure and crystallization characteristic of phase-change optical material $GeSb_2Te_4$, J. Appl. Phys. Vol. 78, pp. 2338-2342. 1995.

[43] Y Maeda, H Andoh, I Ikuta, and H Minemura. Reve T. Matsunaga et al., Structural investigation of $GeSb_2Te_4$: A high-speed phase-change material, Phys. Rev. B, Vol. 69, pp. 104111 1-8. 2004.

[44] M. Naito et al., Local structure analysis of Ge-Sb-Te phase change materials

using high-resolution electron microscopy and nanobeam diffraction, J. Appl. Phys. Vol. 95, pp. 8130-8135. 2004.

[45] H. Iwasaki, Y. Ide, M. Harigaya, Y. Kageyama and I. Fujimura. Completely erasable phase change optical disk, Jpn. J. Appl. Phys. Vol. 31. pp. 461-465. 1992.

[46] M. Shinotsuka, T. Shibaguchi, M. Abe and Y. Ide. Potentiality of the Ag-In-Sb-Te Phase Change Recording Material for High Density Erasable Optical Discs, Jpn. J. Appl. Phys. Vol. 36, pp. 536-538. 1993.

[47] T Nishida, M Terao, Y Miyauchi, S Horigome, T Kaku, and N Ohta. Single-beam overwrite experiment using In-Se based phase-change optical media, Appl. Phys. Lett. Vol. 50, pp. 667-669. 1987.

[48] Y Maeda, H Andoh, I Ikuta and H Minemura. Reversible phase-change optical data storage in InSbTe alloy films, J. Appl. Phys. Vol. 64, pp. 1715-1719. 1988.

[49] Michiaki Shinotsuka, Takashi Shibaguchi, Michiharu Abe and Yukio Ide. Potentiality of the Ag-In-Sb-Te Phase Change Recording Material for High Density Erasable Optical Discs, Jpn. J. Appl. Phys., Vol. *36*, pp. 536-538. 1997.

[50] A. V. Kolobov, P. Fons, A. I. Frenkel, A. Ankudinov, J. Tominaga and T. Uruga. Understanding the phase-change mechanism of rewritable optical media, Nature Materials. Vol. **3**, pp. 703-708. 2004.

[51] E. W. Willams. The CD-RAM and Optical Disc Recording System, pp. 80-138, Oxford: Oxford University Press. 1994.

[52] Yem-Yeu Chang and Lih-Hsin Chou. Erasing Mechanisms of Ag-In-Sb-Te Compact Disk (CD)-Rewritable, Jpn. J. Appl. Phys. Vol.39, pp. 294-296. 2000.

[53] Lih-Hsin Chou and Yem-Yeu Chang. Erasing and Jitter Variation Mechanisms of

Ag-In-Sb-Te Compact Disk-Rewritable at Double and Quadruple Compact Disk Velocities, Jpn. J. Appl. Phys. Vol. 40, pp. 1272-1278. 2001.

[54] Chao-An Jong, Weileung Fang, Chain-Ming Lee and Tsung-Shune Chin. Mechanical Properties of Phase-change Recording Media: GeSbTe Films, Jpn. J. Appl. Phys., Vol. 40, pp. 3320-3325. 2001.

[55] Takeo Ohta, Kenichi Nishiuchi, Kenji Narumi, Yasuo Kitaoka, Hiromichi Ishibashi, Noboru Yamada and Takashi Kozaki. Overview and the Future of Phase-Change Optical Disk Technology, Jpn. J. Appl. Phys. Vol. 39, pp. 770-774. 2000.

[56] Bernardus A. J. Jacobs and Johan P. W. B. Duchateau. Improved High-Density Phase-Change Recording, Jpn. J. Appl. Phys. Vol. 36, pp. 491-494. 1997.

[57] Naoyasu Miyagawa, Eiji Ohno, Kenichi Nishiuchi and Nobuo Akahira. Phase Change Optical Disk Using Land and Groove Method Applicable to Proposed Super Density Rewritable Disc Specifications. Jpn. J. Appl. Phys. Vol.35, pp. 502-503. 1996.

[58] Masataka Yamaguchi, Takahiro Togashi, Satoshi Jinno, Hideo Kudo, Eiji Muramatsu, Shoji Taniguchi and Akiyoshi Inoue. 4.7 GB Phase Change Optical Disc with In-Groove Recording, Jpn. J. Appl. Phys. Vol. *38*, pp. 1806-1810. 1999.

[59] Moonkyo Chung, Kyung Min Chung, Taek Sung Lee, Byung-ki Cheong, Won Mok Kim, Ki-Bong Song, Young Dong Kim and Soon Gwang Kim. Analysis of Read-out Signals in Land/Groove Recording of a Phase-Change Optical Disc, Jpn. J. Appl. Phys. Vol. 39, pp. 3453-3457. 2000.

[60] Roel van Woudenberg. Short Wavelength Phase-Change Recording, Jpn. J. Appl. Phys., Vol. 37, pp. 2159-2162. 1998.

[61] Fumihiko Yokogawa, Seiichi Ohsawa, Tetsuya Iida, Yoshitsugu Araki, Kaoru Yamamoto and Yoshiaki Moriyama. The Path from a Digital Versatile Disc (DVD) using a Red Laser to a DVD using a Blue Laser, Jpn. J. Appl. Phys., Vol. 37, pp. 2176-2178. 1998.

[62] Isao Ichimura, Fumisada Maeda, Kiyoshi Osato, Kenji Yamamoto and Yutaka Kasami. Optical Disk Recording Using a GaN Blue-Violet Laser Diode, Jpn. J. Appl. Phys., Vol. 39, pp. 937-942. 2000.

[63] B.D. Terris, H.J. Mamin, and D. Rugar. Near-Field Optical Data Storage, Appl. Phys. Lett., Vol. 68, pp. 141-143. 1996.

[64] B. D. Terris, H. J. Mamin, D. Rugar, W. R. Studenmund, and G. S. Kino. Near-field optical data storage using a solid immersion lens. Appl. Phys. Lett. Vol.65 pp.388-390. 1994.

[65] J. Tominaga, T. Nakano, and N. Atoda. An approach for recording and readout beyond the diffraction limit with an Sb thin film, Appl. Phys. Lett. Vol. 73 pp. 2078-2080. 1998.

[66] L. P. Shi, T. C. Chong, X. S. Miao, P. K. Tan and J. M. Li. A New Structure of Super-Resolution Near-Field Phase-Change Optical Disk with a Sb_2Te_3 Mask Layer. Jpn. J. Appl. Phys., Vol. 40, pp. 1649-1650. 2001.

[67] Takashi Nakano, Akira Sato, Hiroshi Fuji, Junji Tominaga, and Nobufumi Atoda. Transmitted signal detection of optical disks with a superresolution near-field structure, Appl. Phys. Lett. Vol. 75, pp. 151-153. 1999.

[68] T. Kikukawa, T. Nakano, T. Shima, and J. Tominag. A Rigid bubble pit formation and huge signal enhancement in super-resolution near-field structure

disk with platinum-oxide layer. Appl. Phys. Lett. Vol. 81, pp. 4697-4699. 2002.

[69] J. Kim, I. Hwanf, H. Kim, I park and J. Tominaga. Singal characteristics of Super-RENS disk for 100 GB capacity, In Technical Digest ISOM 2004, pp140-141.

[70] L. P. Shi, T. C. Chong, H. B. Yao, P. K. Tan and X. S. Miao. Super-resolution near-field optical disk with an additional localized surface plasmon coupling layer, J. Appl. Phys. Vol. 91, pp. 10209-10211. 2002.

[71] L. P. Shi, T. C. Chong, P. K. Tan, J. M. Li, X. Hu and X. S. Miao. Investigation on Super-resolution Near-field phase change blue-ray optical disk with a Sb_2Te_3 mask layer, In Technical Digest ISOM 2004, pp146-147.

[72] L. P. Shi, T. C. Chong, P. K. Tan, X. S. Miao, J. J. Ho and Y. J. Wu. Study of the Multi-Level Reflection Modulation Recording for Phase Change Optical Disks, Jpn. J. Appl. Phys. Vol.39, pp. 733-736. 2000.

[73] M. O'Neill and T. Wong. Multi-level Data Storage System using Phase-change Optical Discs, In Technical Digest ODS 2000, Whistler, BC, May 2000.

[74] K. Balasubramanian et al, Multilevel-Enabled Double-Density DVD (Re)writable, In Technical Digest ISOM/ODS 2002.

[75] S. McLaughlin et al, MultiLevel DVD: Coding beyond 3 bits/data-cell, In Technical Digest ISOM/ODS 2002.

[76] K. Balasubramanian et al, Rewritable Multi-level Recording using Blue Laser and Growth-Dominant Phase-Change Optical Discs, Proc. SPIE, Vol. 4342, pp. 160-163, 2001.

[77] M. Horie et al, Material Characterization and Application of Eutectic SbTe-based

Phase-change Optical Recording Media, Proc. SPIE. Vol. 4342, pp. 76-87. 2001.

[78] Henry Hieslmair, Jason Stinebaugh, Terrence Wong, and Michael O'Neill. 34GB Multilevel-enabled Rewritable System using Blue Laser and High-NA Optics, In Tech. Dig. Symp. Optical Memory & Optical Data Storage (2002) PD3.

[79] M. Mansuripur. DNA, Human Memory, and the Storage Technology of the 21st Century, Optical Data Storage Conference, Santa Fe, New Mexico, April 2001.

[80] M. Mansuripur et al, Information storage and retrieval using Macromolecules as storage media. Optical Data Storage Conference, Vancouver, Canada, May 2003

[81] M. Mansuripur and P. Khulbe. Macromolecular data storage with petabyte/cm3 density, highly parallel read/write operations, and genuine 3D storage capability, Optical Data Storage Conference, Monterey, California, April 2004.

[82] Isao Ichimura, Koichiro Kishima, Kiyoshi Osato, Kenji Yamamoto, Yuji Kuroda and Kimihiro Saito. Near-field phase-change optical recording of 1.36 numerical aperture, Jpn. J. Appl. Phys. Vol. 39, pp. 962-967. 2000.

[83] E. P. Ippen and C. V. Shank. Dynamic spectroscopy and subpicosecond pulse compression, Appl.Phys.Lett. Vol. 27, pp.488-490. 1975.

[84] J. P Zhou, G Taft, C-P Huang, M M. Murnane, H. C. Kapteyn and I. P. Christov. Pulse evolution in a broad-bandwidth Ti:sapphire laser, Opt. Lett. Vol. 19, pp. 1149-1151. 1994.

[85] M. L. M. Balistreri, H. Gersen, J. P. Korterik, L. Kuipers, N. F. van Hulst. Tracking Femtosecond Laser Pulses in Space and Time, Science 295, pp. 1080-1082. 2001.

[86] P. Corkum. Attosecond pulses at last, Nature 403, pp. 845 – 846. 2000.

[87] P. M. Paul, E. S. Toma, P. Breger, G. Mullot, F. Auge, P. Balcou, H. G. Muller, P. Agostini. Observation of a train of attosecond pulses from high harmonic generation, Science 292, pp. 1689-1692. 2001.

[88] M. Drescher, M. Hentschel, R. Kienberger, G. Tempea, C. Spielmann, G. A. Reider, P. B. Corkum and F. Krausz. X-ray pulses approaching the attosecond frontier, Science 291, pp. 1923-1927. 2001.

[89] Y Silberberg. Physics at the attosecond frontier, Nature 414, pp. 494 – 495. 2001.

[90] M. Hentschel, R. Kienberger, C. Spielmann, G. A. Reider, N. Milosevic, T. Brabec, P. Corkum, U. Heinzmann, M. Drescher and F. Krausz. Attosecond metrology, Nature 414, pp. 509-513, 2001.

[91] N. A. Papadogiannis, B. Witzel, C. Kalpouzos, and D. Charalambidis. Observation of Attosecond Light Localization in Higher Order Harmonic Generation, Phys. Rev. Lett. 83, pp. 4289–4292. 1999.

[92] S. V. Govorkov, I. L. Shumay, Wolfgang Rudolph and T. Schroder. Time-resolved second-harmonic study of femtosecond laser-induced disordering of GaAs surfaces, Optics Lett., Vol. 16, pp. 1013. 1991.

[93] R. Trebino,K. W. DeLong, D. N. Fittingho, J. N. Sweetser, M. A. Krumbugel, B. A. Rich-man and D. Kane. Measuring ultrashort laser pulses in the time-frequency domain using frequency-resolved optical gating, Rev. Sci. Instrum. Vol. 68, pp. 3277-3295. 1997.

[94] M. M. Murnane, H. C. Kapteyn, M. D. Rosen and R. W. Falcone, Ultrafast X-ray pulses from laser-produced plasmas, Science 251, pp. 531-536. 1991.

[95] C. Rischel, A. Rousse, I. Uschmann, P. A. Albouy, J. P. Geindre, P. Audebert, J. C. Gauthier, E. Forster, J. L. Martin and A. Antonetti. Femtosecond time-

resolved x-ray diffraction from laser-heated organic films, Nature 390, pp. 490-492. 1997.

[96] R. W. Schoenlein, W. P. Leemans, A. H. Chin, P. Volfbeyn, T. E. Glover, P. Balling, M. Zolotorev, K.-J. Kim, S. Chattopadhyay, and C. V. Shank. Femtosecond X-ray Pulses at 0.4 Å Generated by 90° Thomson Scattering: A Tool for Probing the Structural Dynamics of Materials, Science 274, pp. 236-238. 1996.

[97] H. Schwoerer, P. Gibbon, S. Düsterer, R. Behrens, C. Ziener, C. Reich and R. Sauerbrey. MeV X-rays and photoneutrons from femtosecond laser-produced plasmas, Phys. Rev. Lett., 86, pp. 2317–2320, 2001.

[98] A. Rousse, C. Rischel, S. Fourmaux, I. Uschmann, S. Sebban, G. Grillon, P. Balcou, E. Forster, J. P. Geindre, P. Audebert, J. C. Gauthier, D. Hulin. Non-thermal melting in semiconductors measured at femtosecond resolution, Nature, Vol. 410, pp. 65-68. 2001.

[99] A. H. Chin, R. W. Schoenlein, T. E. Glover, P. Balling, W. P. Leemans, and C. V. Shank, Ultrafast Structural Dynamics in InSb Probed by Time-Resolved X-Ray Diffraction, Phys. Rev Lett. 83, pp. 336-339. 1999.

[100] J. Larsson ***et al.***, Ultrafast structural changes measured by time-resolved X-ray diffraction. Appl. Phys. A 66, pp. 587-591. 1998.

[101] C. Rose-Petruck, R. Jimenez, T. Guo, A. Cavalleri, C. W. Siders, F. Ráksi, J. Squier, B. Walker, K. R. Wilson and C. P. J. Barty. Picosecond-milliangstrom lattice dynamics measured by ultrafast X-ray diffraction, Nature 398, pp. 310-312. 1999.

[102] C. W. Siders, A. Cavalleri, K. Sokolowski-Tinten, Cs. Tóth, T. Guo, M. Kammler, M. Horn von Hoegen, K. R. Wilson, D. von der Linde, C. P. J. Barty. Detection of non-thermal melting by ultrafast x-ray diffraction, Science 286, pp. 1340-1342. 1999.

[103] A. M. Lindenberg, I. Kang, S. L. Johnson, T. Missalla, P. A. Heimann, Z. Chang, J. Larsson, P. H. Bucksbaum, H. C. Kapteyn, H. A. Padmore, R.W. Lee, J. S. Wark, and R.W. Falcone. Time-resolved X-ray diffraction from coherent phonons during a laserinduced phase transition, Phys. Rev. Lett. 84, pp. 111-114. 2000.

[104] D. Von Der Linde and K. Sokolowski-Tinten. "X-ray diffraction experiments with femtosecond time resolution, J. Modern Optics, Vol. 50, pp. 683-694. 2003.

[105] K. Sokolowski-Tinten, C. Blome, J. Blums, A. Cavalleri, C. Dietrich, A. Tarasevitch, I. Uschmann, E. Förster, M. Horn-von-Hoegen, and D. von der Linde. Femtosecond X-ray measurement of coherent lattice vibrations near the Lindemann stability limit, Nature 422, pp. 287-289. 2003.

[106] N. F. Mott and E. A. Davis. Electronic Processes in Non-Crystalline Materials. Oxford, U.K.: Clarendon, 1967.

[107] A. Pirovano, A. L. Lacaita, A. Benvenuti, F. Pellizzer, R. Bez. Electronic switching in phase-change memories, Electron Devices, IEEE Transactions on electron devices, Vol 51, p452-459. 2004.

[108] J. I. Pankove. Optical processes in semiconductors. pp 256-280. New York: Dover Publications, 1971.

[109] P. Stampfli and K. H. Bennemann. Time dependence of the laser-induced

femtosecond lattice instability of Si and GaAs: Role of longitudinal optical distortions, Phys. Rev. B, Vol. 49, pp. 7299-7305. 1994.

[110] P. Stampfli and K. H. Bennemann. Dynamical theory of the laser-induced lattice instability of silicon, Phys. Rev. B, Vol. 46, pp. 10686-10692. 1992.

[111] P. Stampfli and K. H. Bennemann. Theory for the instability of the diamond structure of Si, Ge, and C induced by a dense electron-hole plasma, Phys. Rev. B, Vol. 42, pp. 7163-7173. 1990.

[112] P. L. Silvestrelli, A. Alavi, M. Parrinello, and D. Frenkel. Ab initio Molecular Dynamics Simulation of Laser Melting of Silicon, Phys. Rev. Lett. Vol. **77**, pp. 3149-3152. 1996.

[113] R. Biswas and V. Ambegoakar. Phonon spectrum of a model of electronically excited silicon, Phys. Rev. B, Vol. 26, pp. 1980-1988. 1982.

[114] T. Ohta, N. Yamada, H. Yamamoto, T. Mitsuyu, T. Kozaki, J. Qiu, and K. Hirao. Progress of the phase-change optical disk memory, Mater. Res. Soc. Symp. Proc. Vol 674, pp. V1.1.1-12. 2001.

[115] M. Mansuripur, C. B. Peng, J. Erwin, B. Kevin, and L. Warren. Optical, Thermal, and Materials Aspects of Short Laser Pulses for Optical Data Storage, In Technical Digest: International Symposium on Optical Memory and Optical Data Storage, pp. 123-125. 2002.

[116] J. Solis, J. Siegel, and C. N. Afonso. Recalescence after solidification in Ge films melted by picosecond laser pulses, Appl. Phys. Lett. **7**5, pp. 1071-1073. 1999.

[117] T. Elsaesser, J. Shah, L. Rota and P. Lugli. Initial thermalization of photoexcited carriers in GaAs studied by femtosecond luminescence spectroscopy. Phys. Rev. Lett. 66, pp. 1757–1760. 1991.

[118] S. K. Sundaram and E. Mazur. Inducing and probing non-thermal transitions in semiconductors using femtosecond laser pulses, Nature, Vol. 1, pp. 1-8. 2002.

[119] J. A. Kash, J. C. Tsang, and J. M. Hvam. Subpicosecond Time-Resolved Raman Spectroscopy of LO Phonons in GaAs, Phys. Rev. Lett. 54, pp. 2151–2154. 1985.

[120] A. Leitenstorfer, C. Fürst, A. Laubereau, W. Kaiser, G. Tränkle and G. Weimann. Femtosecond Carrier Dynamics in GaAs Far from Equilibrium, Phys. Rev. Lett. 76, pp. 1545–1548. 1996.

[121] T. Lowery. Ovonic Unified Memory, ECD presentation, http://ovonic.com/website_OUM. Pdf

[122] G. F. Zhou, H. J. Borg, J. C. N. Rijpers, M. H. R. Lankhorst and J. J. L. Horikx. Crystallization Behavior of Phase Change Materials: Comparison between Nucleation- and Growth-dominated Crystallization, Proc. SPIE, Vol 4090, pp. 108-115. 2000.

[123] G. F Zhou. Materials aspects in phase change optical recording, Mat. Sci. Eng. A, Vol. 304-306, pp. 73-80. 2001.

[124] T. C. Chong, L. P. Shi, X. S. Miao, P. K. Tan, R. Zhao and Z. P. Cai. Study of the Superlattice-Like Phase Change Optical Recording Disks, Jpn. J. Appl. Phys. Vol. 39 pp. 737-740. 2000.

[125] T. C. Chong, L. P. Shi, P. K. Tan, X. Hu, W. Qiang, J. M. Li and X. S. Miao. Superlattice-Like Structure for High Recording Speed Phase Change Optical Discs, Jpn. J. Appl. Phys. Vol. 41, pp. 1623-1627. 2002.

[126] T. C. Chong, L. P. Shi, W. Qiang, P. K. Tan, X. S. Miao and X. Hu. Superlattice-Like Structure for Phase Change Optical recording, J. Appl. Phys. Vol. 91, pp. 3981-3987. 2002.

[127] Ming-Fu Li. Modern Semiconductor Quantum Physics. pp. 403-406, Singapore: World Scientific. 1994.

[128] H. W. Deckman, J. H. Dunsmuir, B. Abeles. Microfabricated TEM sections of amorphous superlattices, J. Vac. Sci. Technol. A, Vol 3, pp. 950-954. 1985.

[129] H. W. Deckman, J. H. Dunsmuir and B. Abeles. Transmission electron microscopy of hydrogenated amorphous semiconductor, Appl. Phys. Lett., *46*, pp.171-173. 1985.

[130] M. Zacharias and P. Streitenberger. Crystallization of amorphous superlattices in the limit of ultrathin films with oxide interfaces, Phys. Rev. B, Vol. 62, pp. 8391-8396. 200.

[131] S. Y. Ren and J. D. Dow. Thermal Conductivity of Superlattices, Phys. Rev. B, Vol. 25, pp. 3750-3755. 1982.

[132] A. Balandin and K. L. Wang. Significant Decrease of the Lattice Thermal Conductivity due to Phonon Confinement in a Free-standing Semiconductor quantum Well. Physical Review B, *58(3)*, pp. 1544-1549. 1998.

[133] G. Chen and M. Neagu. Thermal Conductivity and Heat Transfer in Superlattice, Appl. Phys. Lett., Vol. 71, pp. 2761-2763. 1994.

[134] S. -M. Lee, David G. Cahill and R. Venkatasubramanian. Thermal Conductivity of Si-Ge Superlattices. Appl. Phys. Lett., *70(22)*, pp. 2957-2959. 1997.

[135] L. E. Shelimova, O. G. Karpinsky, M. A. Kretova and E. S. Avilov. Phase Equilibra in the Ge-Bi-Te Ternary System at 570-770K Temperature Range, J. Alloys and Comps, Vol. 243, pp. 194-201. 1996.

[136] F. Hulliger, in: Physics and Chemistry of Materials with Layered Structures, Vol. 5, p. 195. Reidel, Dordrecht, 1976.

[137] T. L. Anderson and H. B. Krause. Refinement of the Sb_2Te_3 and Sb_2Te_2Se structures and their relationship to nonstoichiometric $Sb_2Te_{3-y}Se_y$ compounds, Acta Cryst. B30, pp. 1307-1310. 1974.

[138] O. G. Karpinsky, L. E. Shelimova, M. A. Kretova and J. -P. Fleurial. An X-ray study of the mixed-layered compounds of (GeTe)n (Sb_2Te_3)m homologous series, J. Alloys and Comps, Vol. 268, pp. 112-117. 1998.

[139] N.Kh. Abrikosov, L.E. Shelimova, Semiconducting Materials Based on A B Compounds, Nauka, Moscow, 1975.

[140] J. Goldak, C.S. Barret, D. Innes, W. Youdelis, Structure of Alpha GeTe, J. Chem. Phys. Vol. 44, pp. 3323-3325. 1966.

Publications

Journal papers

1. **Q. F. Wang**, L. P. Shi, S. M. Huang, X. S. Miao, K. P. Wong and T. C. Chong. Dynamics of Ultrafast Crystallization in As-deposited $Ge_2Sb_2Te_5$ Films，Jpn. J. Appl. Phys, Vol. 43, pp. 5006-5008. 2004.
2. Z. B. Wang, M. H. Hong, B. S. Luky'anchuk, S. M. Huang, **Q. F. Wang**, L. P. Shi, and T. C. Chong. Parallel nanostructuring of GeSbTe film with particle-mask, Appl. Phys. A, 79, pp.1603-1606. 2004.
3. Z. B. Wang, M. H. Hong, B. S. Luky'anchuk, Y.Lin, **Q. F. Wang**, and T. C. Chong. Angle effect in laser nanopatterning with particlemask, J. Appl. Phys., Vol. 96 pp.6845-6850. 2004.

Conference proceedings

1. **Q. F. Wang**, L. P. Shi, S. M. Huang, X. S. Miao and T. C. Chong. Phase Transformation of $Ge_1Sb_4Te_7$ Films Induced by SingleFemtosecond Pulse, Proceedings of SPIE, Vol. 5380 pp. 403-410, 2004
2. **Q.F. Wang**, L.P. Shi, S.M. Huang, X.S. Miao, K.P. Wong and T.C. Chong. Femtosecond Laser-induced Crystallization in As-deposited $Ge_1Sb_2Te_4$ Films, Material Research Society Symposium Proceeding, Vol. 803 HH5.7. 2004.
3. **Q.F. Wang**, L.P.Shi, Z.B. Wang, B. Lan, K.J. Yi, M.H. Hong and T.C.Chong. Ultrafast phase transitions in $Ge_1Sb_2Te_4$ films induced by femtosecond laser beam,

Proceedings of SPIE, Vol. 5069 (2003) 165

Conference papers with abstracts only

1. **Q. F. Wang**, L. P. Shi, S. M. Huang, X. S. Miao, K. P. Wong and T. C. Chong. Phase Transformation of $Ge_1Sb_4Te_7$ Films Induced by Single Femtosecond Pulse, Technique Digest, Optical Data Storage Topical Meeting, 5380-58. 2004.
2. **Q. F. Wang**, L. P. Shi, K. J. Yi and T. C. Chong. Dynamics of Ultrafast Phase Transitions in GeSbTe Films, Technique Digest, Materials Research Society Fall Meeting, HH5.7. 2003.
3. **Q.F. Wang**, L.P. Shi, K.J. Yi, X.S. Miao, M.H. Hong and T.C. Chong. Ultrafast Laser-induced Phase Transitions in Amorphous $Ge_1Sb_2Te_4$ Films, International Symposium on Optical Memory, We-F-06. 2003.
4. **Q. F. Wang**, L. P. Shi, Z. B. Wang, B. Lan, K. J. Yi, M. H. Hong, T. C. Chong. Ultrafast reversible phase transitions in GeSbTe films triggered by femtosecond laser pulse, Technique Digest, Optical Data Storage Topical Meeting, 96/TuE25. 2003.